Pergamon

Geochimica et Cosmochimica Acta, Vol. 61, No. 5, pp. 907–950, 1997
Copyright © 1997 Elsevier Science Ltd
Printed in the USA. All rights reserved
0016-7037/97 $17.00 + .00

PII S0016-7037(96)00339-0

Inorganic species in geologic fluids: Correlations among standard molal thermodynamic properties of aqueous ions and hydroxide complexes

EVERETT L. SHOCK,[1] DAVID C. SASSANI,[1,*] MARC WILLIS,[1,†] and DIMITRI A. SVERJENSKY[2]

[1]Department of Earth and Planetary Sciences, Washington University, St. Louis, Missouri 63130, USA
[2]Department of Earth and Planetary Sciences, The Johns Hopkins University, Baltimore, Maryland 21218, USA

(*Received March* 2, 1995; *accepted in revised form September* 29, 1996)

Abstract—Correlations among experimentally determined standard partial molal thermodynamic properties of inorganic aqueous species at 25°C and 1 bar allow estimates of these properties for numerous monatomic cations and anions, polyatomic anions, oxyanions, acid oxyanions, neutral oxy-acid species, dissolved gases, and hydroxide complexes of metal cations. Combined with correlations among parameters in the revised Helgeson-Kirkham-Flowers (HKF) equation of state (Shock et al., 1992), these estimates permit predictions of standard partial molal volumes ($\bar{V}^\circ$), heat capacities ($\bar{C}^\circ_P$), and entropies ($\bar{S}^\circ$), as well as apparent standard partial molal enthalpies ($\Delta\bar{H}^\circ_{P,T}$) and Gibbs free energies ($\Delta\bar{G}^\circ_{P,T}$) of formation to 1000°C and 5 kb for hundreds of inorganic aqueous species of interest in geochemistry. Data and parameters for more than 300 inorganic aqueous species are presented. Close agreement between calculated and experimentally determined equilibrium constants for acid dissociation reactions and cation hydrolysis reactions supports the generality and validity of these predictive methods. These data facilitate the calculation of the speciation of major, minor, and trace elements in hydrothermal and metamorphic fluids throughout most of the crust of the Earth. *Copyright © 1997 Elsevier Science Ltd*

1. INTRODUCTION

There are numerous equations of state which allow calculation of the thermodynamic properties of H_2O including the Haar-Gallagher-Kell (HGK) equation of state (Haar et al., 1984) which allows calculation to 2200°C and 30 kb, and the Hill equation of state (Hill, 1990) which allows calculation to 2000°C and 250 kb. Calculations in the critical region of H_2O are greatly improved with equations provided by Johnson and Norton (1991), who also address the electrostatic properties of H_2O in this region. The treatment of Johnson and Norton (1991) merges the nonclassical equation of state of Levelt Sengers et al. (1983) with the HGK equation of state, and is the basis for other theoretical developments which allow calculation of the properties of aqueous species to 1000°C and 5 kb (Shock et al., 1992). As emphasized by Johnson and Norton (1991) and Shock et al. (1992), the ranges of temperature and pressure over which thermodynamic data for aqueous species can be calculated with the revised Helgeson-Kirkham-Flowers (HKF) equation of state are largely a consequence of the availability of experimental data on dielectric properties of H_2O and conductance of aqueous electrolyte solutions. Although not as broad as the ranges of temperatures and pressure over which thermodynamic properties of minerals, gases, and H_2O can be evaluated, the present range of applicability of the revised-HKF equations includes temperatures up to 1000°C and pressures to 5 kb, encompassing many geologic processes in the upper crust. Recent advances in predicting the static dielectric constant of H_2O at pressures >5 kb (Franck et al., 1990; Archer and Wang, 1990; Wasserman et al., 1995) suggest that accurate calculations with the revised-HKF equations may be possible at pressures ≳20 kb.

Thermodynamic properties of very few aqueous species have been measured over the entire ranges of temperature and pressure where calculations are now possible for aqueous solutions. Nevertheless, there is considerable systematic behavior in the available high temperature/pressure data, much of which has been analyzed and regressed, or used to test predictions, in a series of publications over the past decade (Tanger and Helgeson, 1988; Shock and Helgeson, 1988, 1990; Oelkers and Helgeson, 1988; Shock et al., 1989, 1992; Shock, 1995; Sverjensky et al., 1997) which are based on extensions of the Helgeson-Kirkham-Flowers (HKF) equation of state for aqueous species (Helgeson and Kirkham, 1974a,b, 1976; Helgeson et al., 1981). Correlations which emphasize the considerable systematic behavior in the thermodynamic properties of aqueous ions (Shock and Helgeson, 1988; Sassani and Shock, 1992, 1994), dissolved gases (Shock et al., 1989), aqueous organic compounds (Shock and Helgeson, 1990; Shock, 1992, 1993, 1995; Helgeson, 1992; Schulte and Shock, 1993; Amend and Helgeson, 1997), and aqueous metal-ligand complexes (Shock and Koretsky, 1993, 1995; Sverjensky et al., 1997; Sassani and Shock, 1997b), allow estimates of parameters for the revised-HKF equations of state and calculation of thermodynamic properties for hundreds of aqueous species. It is the purpose of this paper to (1) build upon the data for inorganic ions presented by Shock and Helgeson (1988), (2) present correlations which allow estimation of data for aqueous species not currently available from experiments, and (3) extend the estimation procedure to include hydroxide complexes of metal cations. The correlation algorithms presented below can be used together with thermodynamic data for H_2O to

*Present address: INTERA Inc., 1261 Town Center Drive, Las Vegas, Nevada 89134, USA.
†Present address: Golder Associates Inc., 1809 North Mill Street, Suite C, Naperville, Illinois 60563, USA.

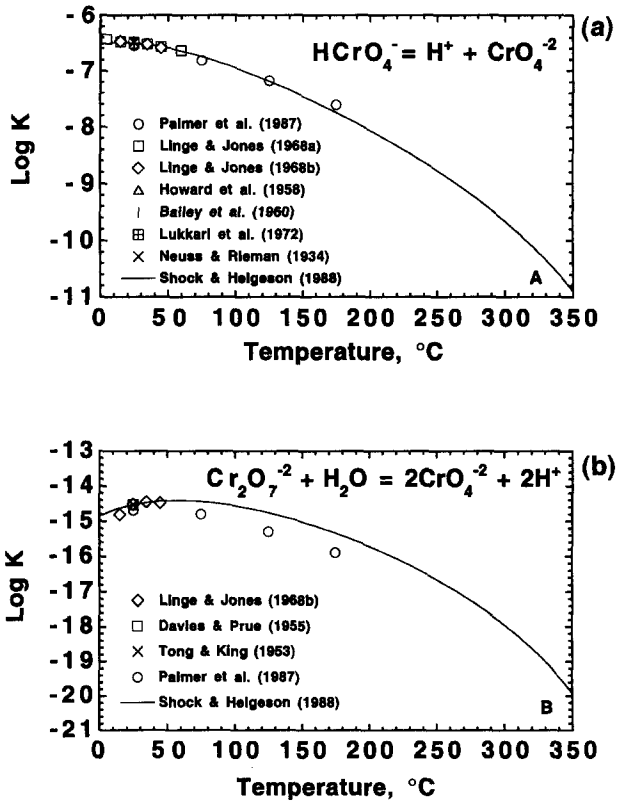

Fig. 1. Dissociation constants for chromate species as functions of temperature showing the divergence between experimental values and predictions made with data and parameters from Shock and Helgeson (1988). The divergence is larger in (b) than (a), but both predictions were improved in the present study.

evaluate standard partial molal properties for hundreds of inorganic aqueous species at high temperatures and pressures that can then be incorporated in geochemical modeling calculations.

Several advances have motivated the revisions described below. First, a number of experimental results have been reported since the construction of the correlations presented by Shock and Helgeson (1988). Many of these data are incorporated in the revised correlations and predictive methods. Second, values of the standard partial molal entropies ($\bar{S}^\circ$) of tetravalent cations predicted by Shock and Helgeson (1988) differ by many calories from the few experimental values. This issue is addressed more fully by Sassani and Shock (1992, 1994) who provide correlations that take explicit account of the coordination of aqueous cations in order to estimate effective electrostatic radii (r_e) and values of $\bar{S}^\circ$. As a result, correlations for other properties can now be extended to include tetravalent species with considerable confidence. Finally, it was discovered that in a few instances equilibrium constants predicted from data and parameters provided by Shock and Helgeson (1988) diverge from independent experimental values by as much as half a log unit at elevated temperatures. Examples of this divergence for reactions involving some aqueous chromium species are shown in Fig. 1. It was found that including these data in the regression process improved correlations among data and parameters, and influenced the construction of correlations for hydroxide complexes. It is hoped that these improvements lead to more accurate estimates for a wider variety of aqueous species. In addition, these new correlations provide part of the framework employed in related studies of the aqueous speciation of platinum-group elements (Sassani and Shock, 1997a), rare earth elements (Haas and Shock, 1994; Haas et al., 1995), actinide ions (Shock et al., 1997a), uranium (Sassani et al., 1993a,b; Shock et al., 1997b), and titanium (Willis and Shock, 1997) at high temperatures and pressures.

2. UPDATED DATA FOR AQUEOUS IONS

Many sets of experimental data for aqueous electrolytes have appeared in recent years and several of these provide an opportunity to revise standard partial molal thermodynamic properties (for standard states and other conventions, see Appendix) and equation-of-state parameters evaluated for aqueous ions by Shock and Helgeson (1988), and augment the 128 ions they considered. Additionally, Sassani and Shock (1992, 1994) showed that correlations between standard molal entropies ($\bar{S}^\circ$) of monatomic aqueous ions and their effective electrostatic radii, calculated from the radii of their crystallographic counterparts, could be extended to include tetravalent cations. The resulting estimates of $\bar{S}^\circ$ for tetravalent cations are considerably more accurate than the estimates of Shock and Helgeson (1988). These experimental and theoretical developments, together with the revised correlations among standard partial molal properties discussed below, make it possible to include a wider variety of aqueous ions in geochemical calculations. Data for ions from Shock and Helgeson (1988) which were not modified in the present study are listed in Table 1. The following discussion covers the data and parameters for aqueous ions which were revised in the present study based on regression of experimental data. Volumetric and calorimetric data are treated first, followed by regression of equilibrium constants at high temperatures and pressures.

2.1. Standard Partial Molal Volumes and Heat Capacities

Following the approach of Shock and Helgeson (1988), we used the model of Helgeson et al. (1981) to evaluate the concentration dependence of partial molal properties. This model, which is based on the Hückel equation, is summarized by Shock and Helgeson (1988) and described in considerable detail by Helgeson et al. (1981). In the nomenclature of this model, the Greek letter ρ is used to represent difference functions between measured apparent molal properties and those calculated with the Hückel equation. For the kth electrolyte, the volume and heat capacity difference functions are designated $\rho_{V,k}$ and $\rho_{J,k}$, respectively. Standard partial molal volumes ($\bar{V}^\circ_k$) and heat capacities ($\bar{C}^\circ_{P,k}$) are obtained from experimental data with the relations

$$\rho_{V,k} = \bar{V}^\circ_k + \frac{\upsilon_k b_{V,k} I}{4} \qquad (1)$$

Table 1. Summary of experimental standard partial molal thermodynamic properties of aqueous ions at 25°C and 1 bar and the parameters required to calculate the corresponding properties at high pressure and temperatures with the revised - HKF equation of state from Shock and Helgeson (1988) which were not revised in the present study.

Ion	ΔG_f°[a]	ΔH_f°[a]	S°[b]	$\bar{C}_p^{\circ}$[b,f]	$\bar{V}^{\circ}$[c]	a_1[d] x10	a_2[e] x 10^{-2}	a_3[e]	a_4[f] x 10^{-4}	c_1[b]	c_2[f] x 10^{-4}	ω° x 10^{-5}
H^+	0.	0.	0.	0.	0.	0.	0.	0.	0.	0.	0.	0.
Li^+	-69933.	-66552.	2.70	14.2	-0.87	-0.0237	-0.0690	11.5800	-2.7761	19.2	-0.24	0.4862
Na^+	-62591.	-57433.	13.96	9.06	-1.11	1.8390	-2.2850	3.2560	-2.726	18.18	-2.981	0.3306
K^+	-67510.	-60270.	24.15	1.98	9.06	3.5590	-1.4730	5.4350	-2.712	7.40	-1.791	0.1927
Rb^+	-67800.	-60020.	28.8	-3.0	14.26	4.2913	-0.9041	7.4070	-2.7416	5.7923	-3.6457	0.1502
Cs^+	-69710.	-61670.	31.75	-6.29	21.42	6.1475	-0.1309	4.2094	-2.7736	6.27	-5.736	0.0974
Mg^{+2}	-108505.	-111367.	-33.00	-5.34	-21.55	-0.8217	-8.5990	8.3900	-2.390	20.80	-5.892	1.5372
Ca^{+2}	-132120.	-129800.	-13.50	-7.53	-18.06	-0.1947	-7.2520	5.2966	-2.4792	9.00	-2.522	1.2366
Sr^{+2}	-134760.	-131670.	-7.53	-10.05	-17.41	0.7071	-10.1508	7.0027	-2.3594	10.7452	-5.0818	1.1363
Ba^{+2}	-134030.	-128500.	2.3	-12.30	-12.60	2.7383	-10.0565	-0.0470	-2.3633	3.80	-3.450	0.9850
BO_2^-	-162240.	-184600.	-8.9	-41.0	-14.5	-2.2428	-6.2065	-6.3216	-2.5224	-1.6521	-11.3863	1.7595
HCO_3^-	-140282.	-164898.	23.53	-8.46	24.6	7.5621	1.1505	1.2346	-2.8266	12.9395	-4.7579	1.2733
CO_3^{-2}	-126191.	-161385.	-11.95	-69.5	-5.02	2.8524	-3.9844	6.4142	-2.6143	-3.3206	-17.1917	3.3914
Pb^{+2}	-5710.	220.	4.2	-12.7	-15.6	-0.0051	-7.7939	8.8134	-2.4568	8.6624	-5.6216	1.0788
NO_3^-	-26507.	-49429.	35.12	-16.4	29.0	7.3161	6.7824	-4.6838	-3.0594	7.70	-6.725	1.0977
NO_2^-	-7700.	-25000.	29.4	-23.3	25.0	5.5864	5.8590	3.4472	-3.0212	3.4260	-7.7808	1.1847
NH_4^+	-18990.	-31850.	26.57	15.74	18.13	3.8763	2.3448	8.5605	-2.8759	17.45	-0.021	0.1502
$H_2PO_4^-$	-270140.	-309820.	21.6	-7.0	31.3	6.4875	8.0594	2.5823	-3.1122	14.0435	-4.4605	1.3003
HPO_4^{-2}	-260310.	-308815.	-8.0	-58.3	5.4	3.6315	1.0857	5.3233	-2.8239	2.7357	-14.9103	3.3363
OH^-	-37595.	-54977.	-2.56	-32.79	-4.18	1.2527	0.0738	1.8423	-2.7821	4.15	-10.346	1.7246
HS^-	2860.	-3850.	16.3	-22.17	20.65	5.0119	4.9799	3.4765	-2.9849	3.42	-6.27	1.4410
HSO_3^-	-126130.	-149670.	33.4	-1.4	33.3	6.7014	8.5816	2.3771	-3.1338	15.6949	-3.3198	1.1233
SO_4^{-2}	-177930.	-217400.	4.50	-64.38	13.88	8.3014	-1.9846	-6.2122	-2.6970	1.64	-17.998	3.1463
HSO_4^-	-180630.	-212500.	30.0	5.3	35.2	6.9788	9.2590	2.1108	-3.1618	20.0961	-1.9550	1.1748
$S_2O_3^{-2}$	-124900.	-155000.	16.0	-57.3	28.5	6.6685	12.4951	-7.7281	-3.2955	-0.0577	-14.7066	2.9694
$S_2O_8^{-2}$	-266500.	-321400.	58.4	-25.0	79.0	13.3622	24.8454	-4.0153	-3.8061	12.9632	-8.1271	2.3281
F^-	-67340.	-80150.	-3.15	-27.23	-1.32	0.6870	1.3588	7.6033	-2.8352	4.46	-7.488	1.7870
Cl^-	-31379.	-39933.	13.56	-29.44	17.79	4.0320	4.8010	5.5630	-2.847	-4.40	-5.714	1.4560
ClO_3^-	-1900.	-24850.	38.8	-12.3	36.9	7.1665	9.7172	1.9307	-3.1807	8.5561	-5.5401	1.0418
Br^-	-24870.	-29040.	19.80	-30.42	24.85	5.2690	6.5940	4.7450	-3.143	-3.80	-6.811	1.3858
BrO_3^-	4450.	-16030.	38.65	-20.6	35.4	6.9617	9.2173	2.1272	-3.1600	3.7059	-7.2308	1.0433
I^-	-12410.	-13600.	25.50	-28.25	36.31	7.7623	8.2762	1.4609	-3.1211	-6.27	-4.944	1.2934
IO_3^-	-30600.	-52900.	28.3	-16.2	25.9	5.7148	6.1725	3.3240	-3.0342	7.7293	-6.3345	1.2002
Ni^{+2}	-10900.	-12900.	-30.8	-11.7	-29.0	-1.6942	-11.9181	10.4344	-2.2863	13.1905	-5.4179	1.5067
Cu^{+2}	15675.	15700.	-23.2	-5.7	-24.6	-1.0121	-10.4726	9.8662	-2.3461	20.3	-4.39	1.4769
Ag^+	18427.	25275.	17.54	7.9	-0.8	1.7285	-3.5608	7.1496	-2.6318	12.7862	-1.4254	0.2160
Cd^{+2}	-18560.	-18140.	-17.4	-3.5	-15.6	0.0537	-10.7080	16.5176	-2.3363	15.6573	-3.7476	1.2528
La^{+3}	-164000.	-169600.	-52.0	-37.2	-38.6	-2.7880	-14.3824	10.9602	-2.1844	4.2394	-10.6122	2.1572
Nd^{+3}	-160600.	-166500.	-49.5	-43.2	-43.1	-3.3707	-14.5452	8.3211	-2.1777	1.6236	-11.8344	2.2550
Sm^{+3}	-159100.	-165200.	-50.7	-43.3	-42.0	-3.2065	-15.6108	11.8857	-2.1337	1.9385	-11.8548	2.2955
Eu^{+3}	-137300.	-144700.	-53.0	-36.6	-41.3	-3.1037	-15.3599	11.7871	-2.1440	6.0548	-10.4900	2.3161
Gd^{+3}	-158600.	-164200.	-49.2	-35.9	-40.4	-2.9771	-15.0506	11.6656	-2.1568	6.5606	-10.3474	2.3265
Dy^{+3}	-158700.	-166500.	-55.2	-31.7	-40.7	-3.0003	-15.1074	11.6879	-2.1545	9.5076	-9.9419	2.3792
Ho^{+3}	-161400.	-169000.	-54.3	-33.3	-41.6	-3.1198	-15.3992	11.8026	-2.1424	8.6686	-9.8178	2.3899
Er^{+3}	-159900.	-168500.	-58.3	-34.3	-43.0	-3.3041	-15.8492	11.9794	-2.1238	8.2815	-10.0215	2.4115
Tm^{+3}	-159900.	-168500.	-58.1	-34.3	-43.0	-3.2967	-15.8312	11.9724	-2.1245	8.4826	-10.0215	2.4333
Yb^{+3}	-153000.	-160300.	-56.9	-36.4	-44.5	-3.4983	-16.3233	12.1658	-2.1042	7.3533	-10.4493	2.4443
Lu^{+3}	-159400.	-167900.	-63.1	-32.0	-45.0	-3.5630	-16.4812	12.2279	-2.0977	9.5650	-9.7160	2.4554

a. cal mol^{-1}. b. cal $mol^{-1}K^{-1}$. c.cm^3mol^{-1}. d. cal $mol^{-1}bar^{-1}$. e. cal K mol^{-1} bar^{-1}. f. cal K mol^{-1}.

and

$$\rho_{J,k} = \bar{C}^{\circ}_{P,k} + \frac{\upsilon_k b_{J,k} \bar{I}}{4} \tag{2}$$

where $b_{V,k}$ and $b_{J,k}$ can be calculated from the appropriate derivatives of the extended term of the Hückel equation (see Helgeson et al., 1981; Shock and Helgeson, 1988), $\bar{I}$ stands for the effective ionic strength defined by

$$\bar{I} \equiv \tfrac{1}{2} \sum_j Z_j^2 m_j \tag{3}$$

where Z_j represents the charge of the jth ion, m_j designates the molality of the jth ion, and

$$\upsilon_k \equiv \sum_j \upsilon_{j,k} \tag{4}$$

where $\upsilon_{j,k}$ stands for the number of moles of the jth ion in the kth electrolyte. To the extent that $\bar{I}$ is equal to the stoichiometric ionic strength, I, defined by

$$I \equiv \tfrac{1}{2} \sum_j \upsilon_{j,k} Z_j^2 m_k \tag{5}$$

where m_k signifies the molality of the kth electrolyte, a plot of $\rho_{V,k}$ vs. I, or $\rho_{J,k}$ vs. I, will be linear, and the intercept will correspond to $\bar{V}^{\circ}$ or $\bar{C}^{\circ}_P$, respectively. Values of $b_{V,k}$ and $b_{J,k}$ are evaluated from the slopes of such plots, and departures from linearity with increasing concentration can be attributed to ion association (Helgeson et al., 1981). Values

Table 2. Standard partial molal volumes and heat capacities of aqueous electrolytes obtained in the present study from the indicated sources of experimental data and used to revise data and equation of state parameters for aqueous ions.

T,°C	$\bar{V}^{\circ}$[a]	$\bar{C}_P^{\circ}$[b]
	$HClO_4$	
10		-13.9[c]
15	42.4[d]	-9.8[d]
25		-6.0[e]
25	44.1[d]	-4.9[d]
25	44.2[f]	---
35	45.5[d]	-0.9[d]
35	45.4[f]	---
40		-2.1[c]
45	46.8[d]	1.7[d]
45	46.4[f]	---
55	47.8[d]	6.5[d]
55		-0.6[c]
55	47.3[f]	---
65	48.0[f]	---
75	49.0[f]	---
	$Zn(ClO_4)_2$	
10	58.6[p]	-40.7[p]
15	59.8[t]	---
25	64.1[p]	-17.3[p]
25	63.3[t]	-17.0[i]
25	60.0[k]	---
35	65.8[t]	---
40	68.0[p]	-8.0[p]
45	69.2[t]	---
55	70.3[p]	-4.8[p]
	$UO_2(ClO_4)_2$	
10	89.60[q]	-18.7[q]
25	94.13[q]	-1.8[q]
40	97.72[q]	3.8[q]
55	99.09[q]	3.7[q]

T,°C	$\bar{V}^{\circ}$[a]	$\bar{C}_P^{\circ}$[b]
	$NaReO_4$	
13.28	43.6[s]	---
15		-1.43[s]
15.87	42.8[s]	---
18		-0.8[s]
22.87	47.0[s]	---
25		6.1[s]
47.96	51.2[s]	---
50		14.5[s]
70		15.3[s]
72.96	54.2[s]	---
88.17	54.6[s]	---
90		13.7[s]
98.67	55.7[s]	---
100		12.91[s]
123.53	57.3[s]	---
	$NaTcO_4$	
14.28	44.4[s]	---
17.87	43.5[s]	---
22.87	45.8[s]	---
25		7.1[s]
47.95	50.4[s]	---
50		15.1[s]
72.95	52.0[s]	---
75		16.1[s]
98.67	54.4[s]	---
100		13.1[s]
123.52	55.5[s]	---

T,°C	$\bar{V}^{\circ}$[a]
	$Fe(ClO_4)_2$
15	62.7[g]
25	66.2[g,l]
35	68.5[g]
45	71.4[g]
	$Mn(ClO_4)_2$
15	68.5[g]
25	71.4[g]
25	71.3[i]
35	73.4[g]
45	76.4[g]
55	77.8[g]
	$MnCl_2$
15	17.6[g]
25	18.3[g]
25	18.2[m]
25	18.5[n]
25	19.5[j]
35	18.3[g]
35	19.5[j]
45	18.2[g]
45	19.2[j]
55	17.7[g]
55	18.7[j]
65	17.8[j]
75	17.1[j]
	$CoCl_2$
15	9.6[g]
25	10.3[g]
25	11.2[j]

T,°C	$\bar{V}^{\circ}$[a]
	$CoCl_2$
25	10.5[k]
35	10.5[g]
35	11.4[j]
45	10.5[g]
45	11.2[j]
55	10.3[g]
55	10.7[j]
65	9.9[j]
75	9.1[j]
	KCN
15	32.1[r]
25	33.0[r]
35	33.6[r]
45	33.8[r]
	$FeCl_2$
15	12.8[g]
25	13.4[g]
25	13.7[h]
35	13.7[g]
45	13.7[g]
	$Co(ClO_4)_2$
15	59.5[g]
25	62.9[g,l]
35	65.4[g]
45	68.0[g]
55	69.5[g]

Notes
a. $cm^3\ mol^{-1}$
b. $cal\ mol^{-1}\ K^{-1}$
c. Hovey & Hepler (1989)
d. Pogue & Atkinson (1988)
e. Hovey et al. (1988)
f. Herrington et al. (1985)
g. Pogue & Atkinson (1989a)
h. Karapet'yants et al. (1977)
i. Spitzer et al. (1978b)
j. Herrington et al. (1986)
k. Spitzer et al. (1978a)
l. Swaddle & Mak (1983)
m. Rard & Miller (1984)
n. Spitzer et al. (1979b)
p. Pan & Tremaine (1994)
q. Hovey et al. (1989)
r. Mathieson & Curthoys (1974)
s. Lemire et al. (1992)
t. Pogue & Atkinson (1989b)

of $\bar{V}^{\circ}$ or $\bar{C}_P^{\circ}$ obtained from plots of this type are listed in Table 2. Values of the solvation[‡] and nonsolvation contributions to each of these standard partial molal properties were calculated with Eqns. A10, A11, A14, and A15 or A16 from the summary of the revised-HKF equation of state in the Appendix.

As described by Shock and Helgeson (1988), plots of the nonsolvation contribution to the standard partial molal volume, $\Delta\bar{V}_n^{\circ}$, against $(1/T - \theta)$ and the nonsolvation contribution to the standard partial molal heat capacity, $\Delta\bar{C}_{P,n}^{\circ}$, against $(1/T - \theta)^2$ allow regression of experimental data for the species-dependent parameters σ, ξ, c_1, and c_2 (see Eqns. A11 and A16 in the Appendix). Plots of this type are shown in Figs. 2 and 3, and values of σ, ξ, c_1, and c_2 generated by this procedure are listed in Table 3. Values of σ and c_2 in Table 3 are consistent with correlations involving equation-of-state parameters for inorganic aqueous ions described by Shock and Helgeson (1988) and given by

$$\sigma = 1.11\Delta\bar{V}_n^{\circ} + 1.8 \qquad (6a)$$

and

$$c_2 \times 10^{-4} = 0.2037\bar{C}_P^{\circ} - 3.0346 \qquad (6b)$$

Values of σ, together with correlations for the a_1 and a_4 equation-of-state parameters given by (Shock and Helgeson, 1988)

$$a_1 = 1.3684 \times 10^{-2}\Delta\bar{V}_n^{\circ} + 0.1765 \qquad (6c)$$

and

$$a_4 = -4.134a_2 - 27790 \qquad (6d)$$

were used together with Eqns. A5, A11, A12, and A13 to evaluate the a_1, a_2, a_3, and a_4 equation-of-state parameters from the values of $\bar{V}^{\circ}$ given in Table 3. Comparison of calculated and experimental values of $\bar{V}_k^{\circ}$ and $\bar{C}_{P,k}^{\circ}$ can be made with the plots shown in Figs. 4 and 5. Values of $\bar{V}^{\circ}$, $\bar{C}_P^{\circ}$ and equation-of-state parameters obtained in the present study as a consequence of regressing new experimental measurements are listed in Table 4, together with standard partial molal entropies ($\bar{S}^{\circ}$), and standard partial molal enthalpies ($\Delta\bar{H}_f^{\circ}$) and Gibbs free energies of formation ($\Delta\bar{G}_f^{\circ}$) at 25°C and 1 bar. Data and parameters for ions updated as a consequence of revised correlations are described and tabulated below.

[‡] During the regression analysis, solvation contributions were calculated with values of the Born coefficient (ω_j) given in Table 4. The temperature and pressure dependence of ω_j was calculated with methods described by Shock et al. (1992), and values of the Born functions Q, X and Y from Johnson and Norton (1991) and/or Shock et al. (1992).

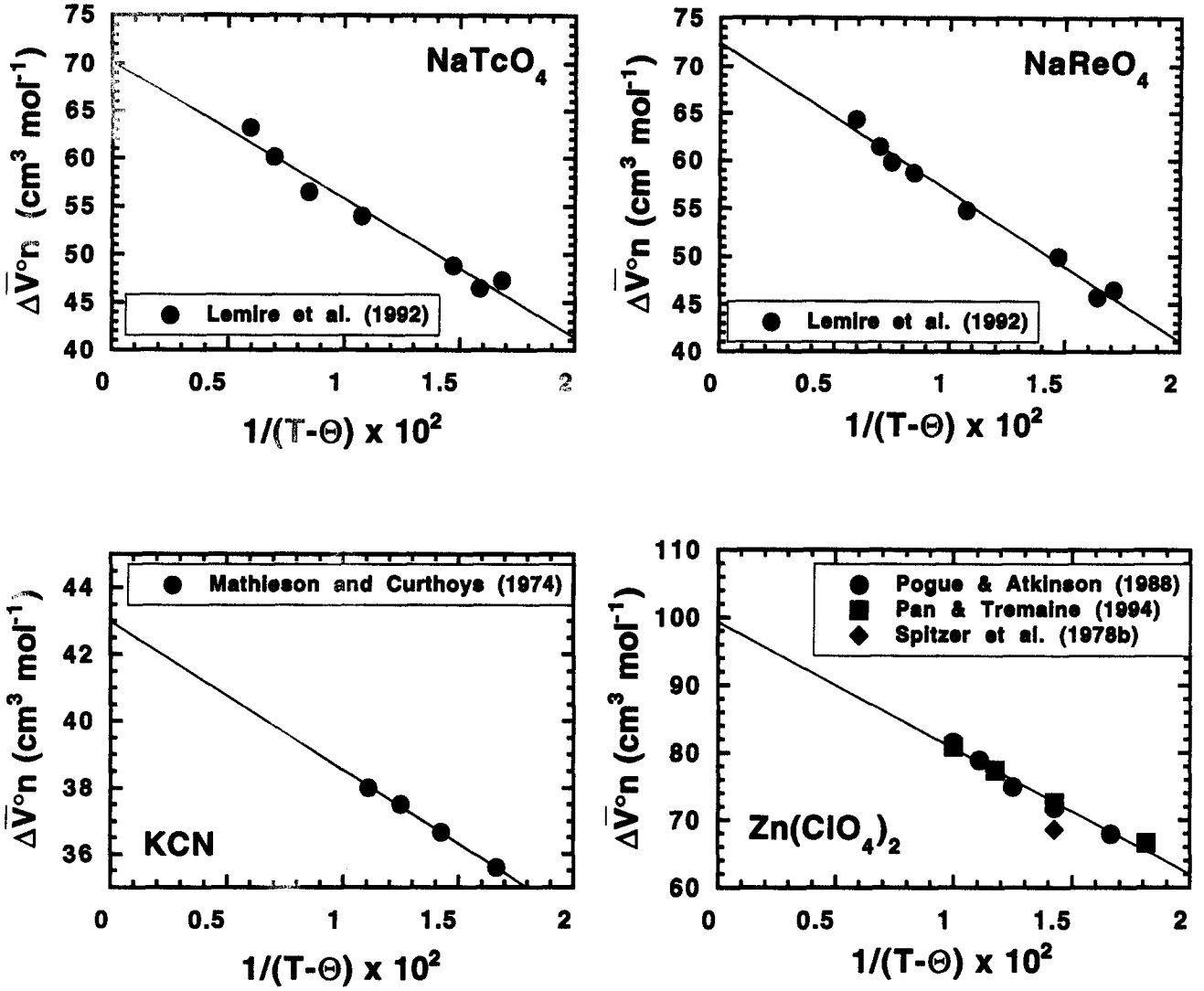

Fig. 2. Plots of the nonsolvation contributions to the standard partial molal volume of electrolytes against a temperature function that includes the temperature of singular behavior in supercooled water (Θ = 228 K). Symbols show experimental data and the lines are the result of regression in this study with Eqn. A11.

2.2. Comparison of Predicted and Experimental Equilibrium Constants

In some cases, the usefulness and accuracy of the revised parameters in Table 4 can be evaluated by comparing predicted equilibrium constants with their experimental counterparts as shown in Fig. 6 for reactions involving CrO_4^{-2}, $HCrO_4^-$, and $Cr_2O_7^{-2}$. In this figure, the solid curves correspond to values of the equilibrium constants calculated with the revised-HKF equation of state using parameters taken from Table 3. The symbols represent experimental data from the literature sources cited. It can be seen in Fig. 6 that *predictions* based on experimental standard partial molal data at 25°C and 1 bar, together with the correlation algorithms proposed by Shock and Helgeson (1988), are in fairly close agreement with the experimental data. Closer agreement is shown in Fig. 7 between values of the equilibrium constant for

$$HSO_4^- = SO_4^{-2} + H^+ \quad (7)$$

reported by Dickson et al. (1990) with those predicted *in advance* by Shock and Helgeson (1988). The agreement depicted in Figs. 6 and 7, along with that shown in many other comparisons between calculations and experimental data (see Shock and Helgeson, 1988, 1990; Shock et al., 1989, 1992; Shock, 1993, 1995; Shock and Koretsky, 1993, 1995; Sverjensky et al., 1997) indicates that the correlation algorithms proposed by Shock and Helgeson (1988, 1990) make it possible to regress equilibrium constant data with the revised-HKF equations to obtain equation-of-state parameters and standard state properties.

2.3. Regression of Equilibrium Constants at High Temperatures and Pressures

Regression of log K data at high temperatures and pressures has been used to obtain values of $\bar{S}°$, $\bar{V}°$, and $\bar{C}°_P$ at

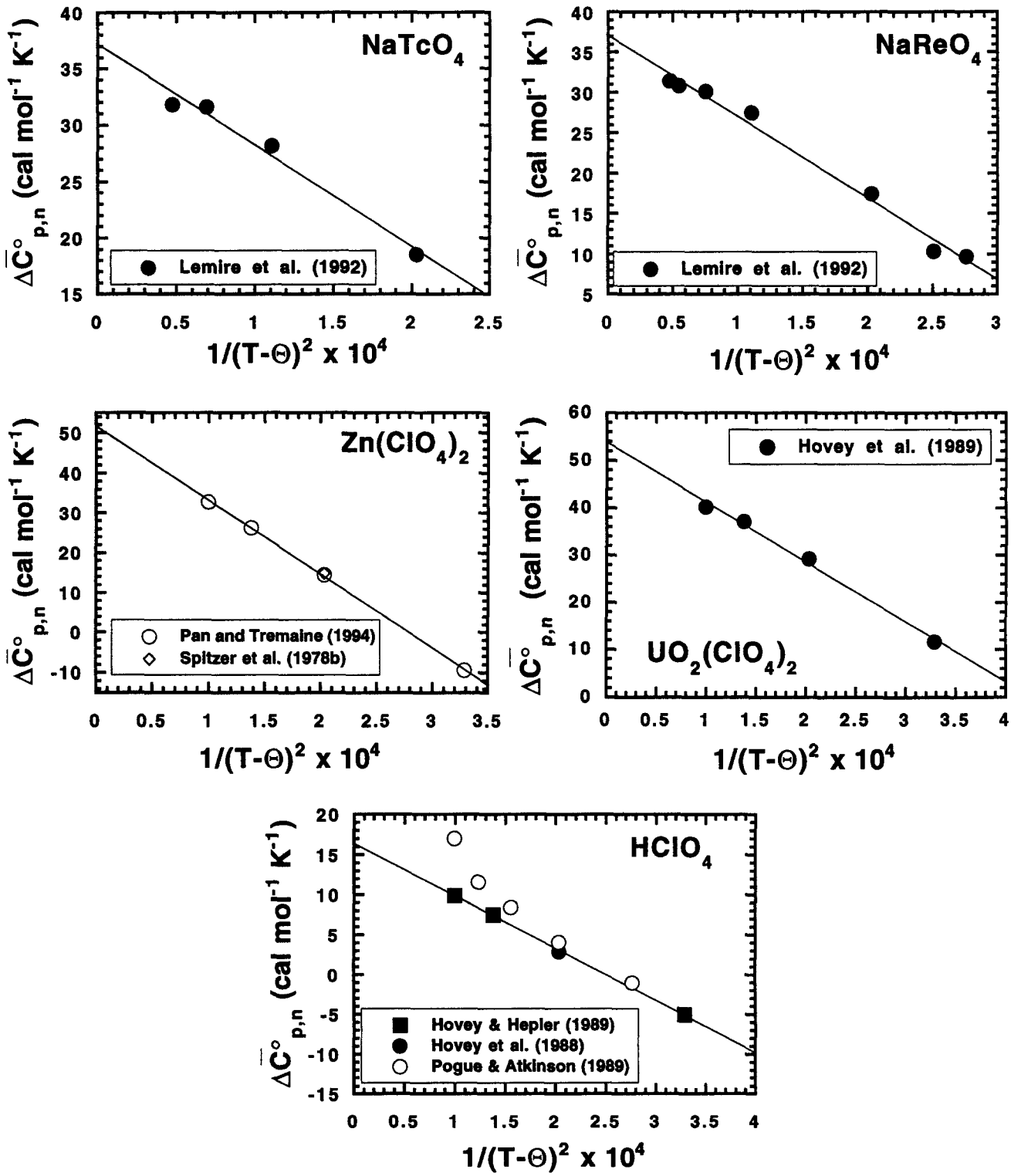

Fig. 3. Plots of the nonsolvation contributions to the standard partial molal heat capacity of electrolytes against a temperature function that includes the temperature of singular behavior in supercooled water (Θ = 228 K). Symbols show experimental data and the lines are the result of regression in this study with Eqn. A16.

25°C and 1 bar for dissolved gases (Shock et al., 1989), aqueous organic compounds (Shock and Helgeson, 1990; Shock, 1992, 1993, 1995), and metal-ligand complexes (Shock and Koretsky, 1993, 1995; Sverjensky et al., 1997; Sassani and Shock, 1997b; Willis and Shock, 1997). In the present study, this approach was used to obtain the standard partial molal properties for HWO_4^-, AlO_2^-, and Al^{+3} as described in this section, and corresponding prop-

Table 3. Values of $\bar{V}^\circ$ and $\bar{C}_p^\circ$ for aqueous ions at 25°C and 1 bar, together with equation of state parameters obtained by regression of experimental data as listed in Table 2 and as depicted in Figs. 2 and 3.

Ion	$\bar{V}^{\circ a}$	σ^a	$\xi^b \times 10^{-2}$	$\bar{C}_p^{\circ c}$	$c_1{}^c$	$c_2{}^d \times 10^{-4}$
ClO_4^-	44.2	59.1	-8.66	-6.0	16.45	-6.57
CN^-	23.9	30.43	-2.33	---	---	---
ReO_4^-	47.8	68.29	-12.62	-2.4	18.93	-7.08
TcO_4^-	47.8	66.16	-11.43	-2.3	18.95	-5.95
Mn^{+2}	-17.1	-13.3	-0.242	---	---	---
Fe^{+2}	-22.2	-17.5	-0.758	---	---	---
Co^{+2}	-25.5	-19.5	-1.311	---	---	---
Zn^{+2}	-24.3	-18.83	-1.37	-5.33	18.74	-5.37
UO_2^{+2}	5.73	6.05	2.36	10.2	21.07	0.43

a. $cm^3\ mol^{-1}$. b. $cm^3\ K\ mol^{-1}$. c. $cal\ mol^{-1}\ K^{-1}$. d. $cal\ K\ mol^{-1}$

erties for hydroxide complexes of metal cations discussed below.

Equilibrium constants are shown in Fig. 8a for

$$HWO_4^- = WO_4^{-2} + H^+ \quad (8)$$

as a function of temperature. The symbols in Fig. 8a represent the experimental values referenced in the figure, but the curve is the result of regression of these data with the revised-HKF equation of state for values of $\bar{S}^\circ$ and $\bar{C}_P^\circ$ at 25°C and 1 bar. The regression of these data produced the values tabulated in Table 4. Values of $\bar{V}^\circ$ cannot be obtained by regression of these temperature-dependent data, but can be estimated from one of the revised correlations described below.

Several recent experimental studies on gibbsite and boehmite solubility provide equilibrium constants for reactions involving Al^{+3} and its hydroxide complexes (Wesolowski, 1992; Palmer and Wesolowski, 1992, 1993; Castet et al., 1992, 1993; Bourcier et al., 1993; Wesolowski and Palmer, 1994). Although there is considerable disagreement at low pH values among these studies and between these studies and earlier experiments, there is considerable close agreement in measured solubilities at high pH where the predominant reaction is

$$\underset{\text{gibbsite}}{Al(OH)_3} + OH^- = Al(OH)_4^- \quad (9)$$

which is rewritten to be consistent with the conventions described below as

$$\underset{\text{gibbsite}}{Al(OH)_3} + OH^- = AlO_2^- + 2H_2O \quad (10)$$

Experimental values of $\bar{V}^\circ$ and $\bar{C}_P^\circ$ for $NaAl(OH)_4$ ($NaAlO_2$) at various temperatures were regressed by Shock and Helgeson (1988) to obtain revised-HKF equation-of-state parameters[§] for AlO_2^-. These parameters were used in the present study to regress the data shown in Fig. 8b to obtain the value of $\bar{S}^\circ$ for AlO_2^- at 25°C and 1 bar listed in Table 4. Data for gibbsite from Hemingway and Robie (1977) were also used in the regression procedure. The regression results are indicated by the curve in Fig. 8b. In order to avoid uncertainties which would attend the confusion in the literature concerning the solubility of gibbsite at low pH values, it was decided in this study to employ data from Couturier et al. (1984) for the reaction

$$Al^{+3} + 2H_2O = AlO_2^- + 4H^+ \quad (11)$$

which are independent of gibbsite solubility measurements. These data were regressed to obtain the value of $\bar{S}^\circ$ for Al^{+3} listed in Table 4 by using the revised-HKF equation-of-state parameters for Al^{+3} predicted from the correlation algorithm using $\bar{V}^\circ$ and $\bar{C}_P^\circ$ determinations for $AlCl_3$ and $Al(NO_3)_3$ solutions. The experimental data of Couturier et al. (1984) are shown in Fig. 8c, together with other experimental data and the results of the regression procedure. It should be emphasized that at temperatures above the range of the Couturier et al. (1984) values the curve in Fig. 8c represents predicted log K values which are in close agreement with the higher temperature data. The standard partial molal properties for aqueous ions updated in the present study allow revision and extension of correlations among standard state properties published by Shock and Helgeson (1988) as described in the next section.

3. CORRELATIONS AMONG STANDARD STATE PROPERTIES AT 25°C AND 1 BAR

Comparisons shown in Figs. 6 and 7 indicate that accurate predictions of equilibrium constants are possible with the revised-HKF equations of state and correlation algorithms. However, these correlation algorithms require values of $\bar{V}^\circ$ and $\bar{C}_P^\circ$ at 25°C and 1 bar. Although values of $\bar{V}^\circ$ and $\bar{C}_P^\circ$ have been determined experimentally for many aqueous ions, there are numerous ions and other aqueous species of geochemical interest for which such data are lacking. In an effort to overcome the absence of such data, Shock and Helgeson (1988) proposed correlations among standard state entropies, heat capacities, and volumes of aqueous ions at 25°C and 1 bar. Although these correlations regularly permit close approximations of equilibrium constants at high temperature and pressure, there was room for improvement for the reasons outlined in the introduction. The resulting set of

[§] Johnson et al. (1992) omitted this aqueous species from the SUPCRT92 files despite its inclusion in Shock and Helgeson (1988).

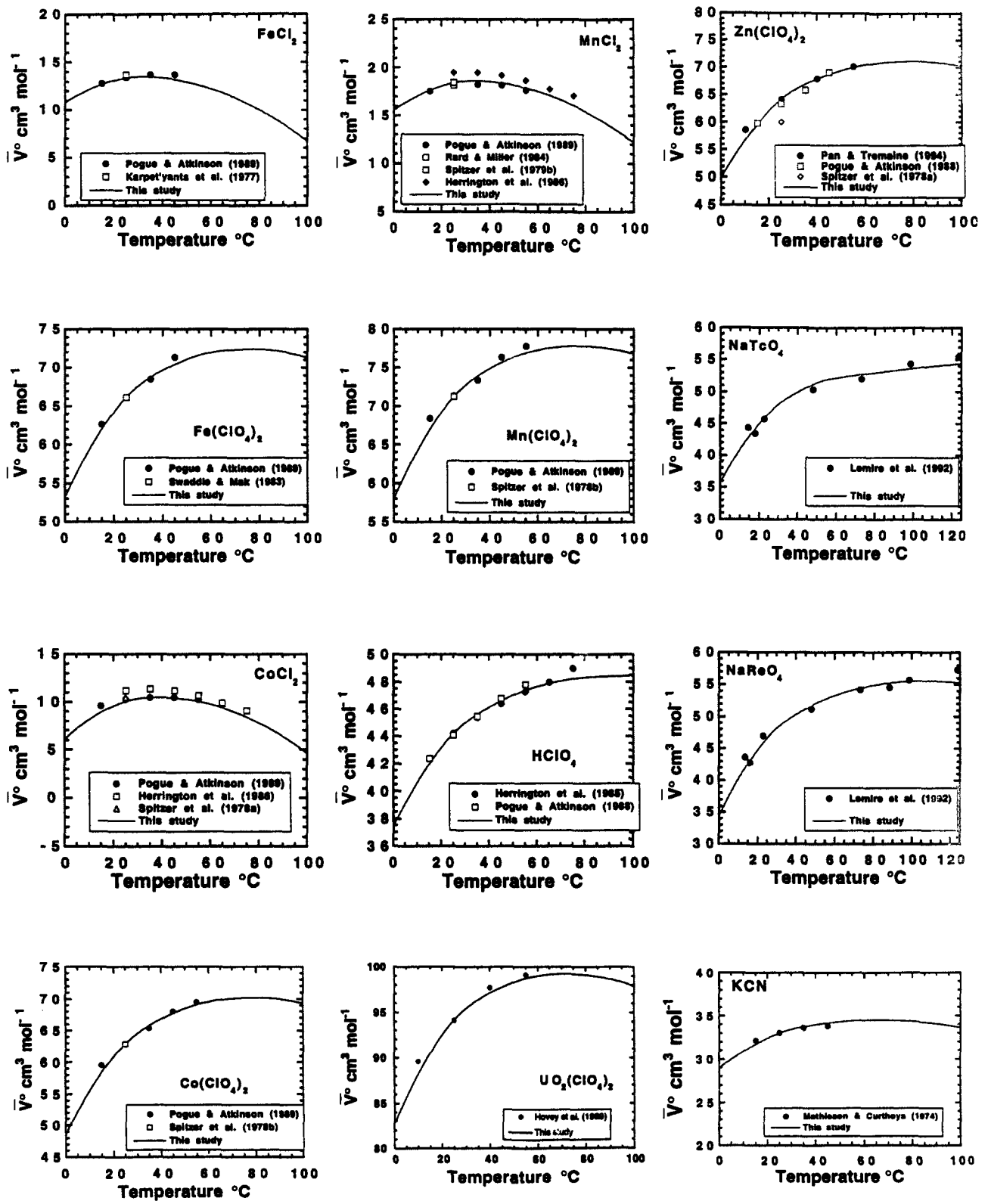

Fig. 4. Plots of the standard partial molal volumes of several electrolytes from experimental studies (symbols) and calculated (curves) with the revised-HKF equation of state using parameters from Tables 3 and 4.

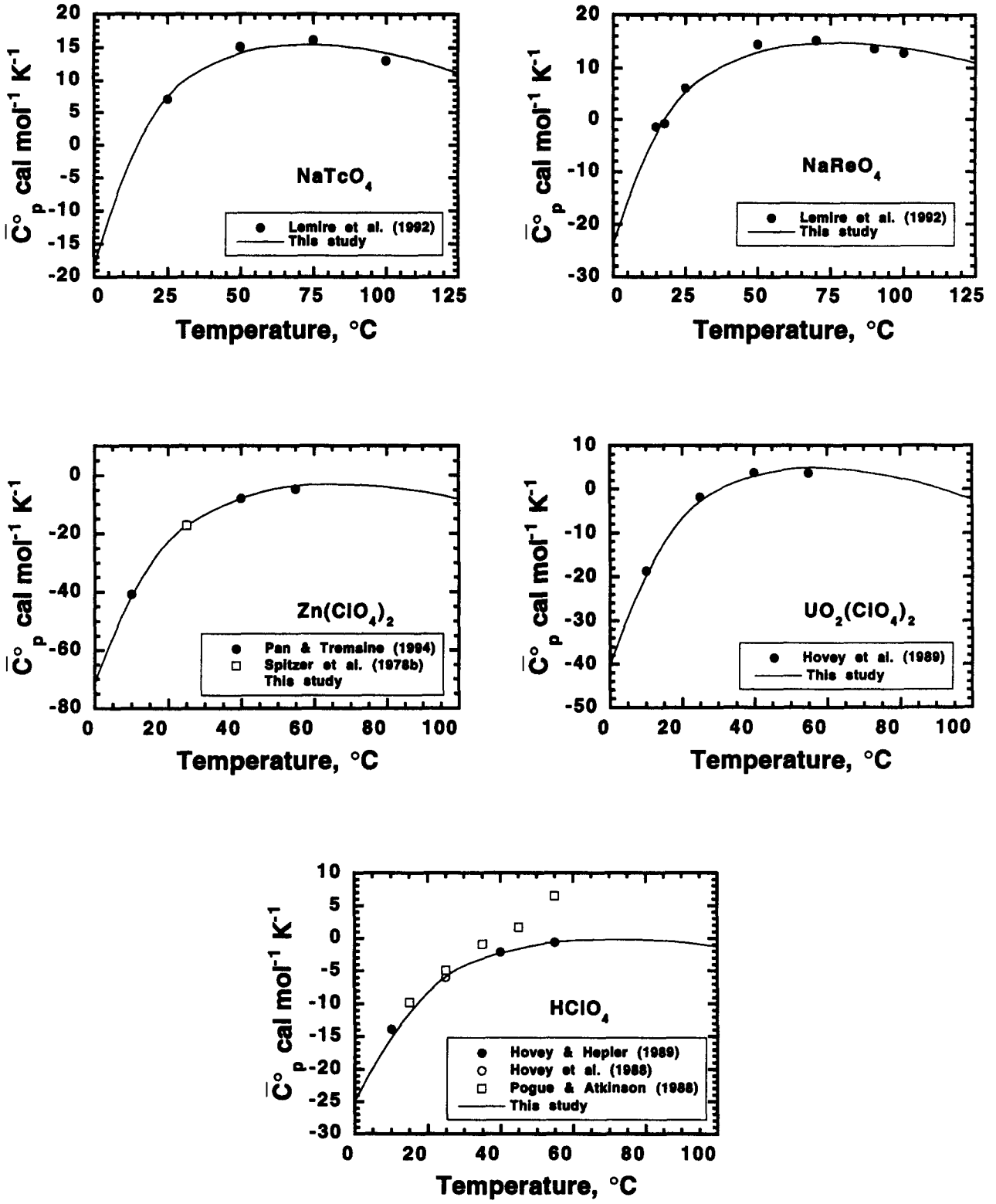

Fig. 5. Plots of the standard partial molal heat capacity of several electrolytes from experimental studies (symbols) and calculated (curves) with the revised-HKF equation of state using parameters from Tables 3 and 4.

correlations described in this section yield more accurate predictions than those proposed by Shock and Helgeson (1988). Combined with revised methods for estimating $\bar{S}^{\circ}$ described by Sassani and Shock (1992, 1994) these correlations allow improvements in the accuracy of predicted data at high temperatures and pressures.

Table 4. Summary of standard partial molal properties of aqueous ions at 25°c and 1 bar and equation of state parameters revised or added in the present study through regression of experimental data.

Ion	$\Delta\bar{G}_f^{\circ}$[a]	$\Delta\bar{H}_f^{\circ}$[a]	$\bar{S}^{\circ}$[b]	$\bar{C}_p^{\circ}$[b]	$\bar{V}^{\circ}$[c]	a^d_1x10	a^d_2x10^{-2}	a_3[e]	a_4[f] x 10^{-4}	c_1[b]	c_2[f] x 10^{-4}	ω^g x 10^{-5}
ClO_4^-	-2040.[m]	-30910.[m]	43.5[m]	-6.0[l]	44.2[l]	8.1411	15.5654	-7.8077	-3.4224	16.45[l]	-6.57[l]	0.9699
ReO_4^-	-166000.[w]	-188200.[w]	48.1[w]	-2.4[l]	47.8[l]	8.6103	20.0581	-16.7541	-3.6081	18.93[l]	-7.08[l]	0.9004
TcO_4^-	-151100.[h]	-173200.[g]	47.5[g]	-2.3[l]	47.8[l]	8.6135	18.7256	-13.3543	-3.5530	18.95[l]	-5.95[l]	0.9101
CrO_4^{-2}	-174800.[i]	-210930.[i]	13.8[i]	-62.6[r]	19.8[r]	5.4891	5.6223	3.5382	-3.0113	-2.8608	-15.7861	3.0024
$HCrO_4^-$	-183700.[i]	-210000.[i]	46.6[i]	1.5[r]	44.9[r]	8.2211	12.2925	0.9174	-3.2871	15.5492	-2.7290	0.9230
MnO_4^-	-107600.[y]	-129900.[y]	46.5[y]	-1.8[m]	42.0[m]	7.8248	11.3277	1.2912	-3.2472	13.6317	-3.4012	0.9248
$Cr_2O_7^{-2}$	-312970.[s]	-355370.[u]	72.[t]	-29.1[r]	72.7[r]	12.4303	22.5680	-3.1161	-3.7119	8.6580	-8.9622	2.1216
MoO_4^{-2}	-200400.[k]	-238300.[k]	9.[k]	-47.5[m]	30.4[m]	6.9651	2.7095	18.6617	-2.8909	6.6829	-12.7102	3.0777
WO_4^{-2}	-218500.[x]	-236500.[k]	9.7[x]	-44.5[m]	32.2[m]	7.2074	8.7933	4.4891	-3.1424	8.3308	-12.0991	3.0657
HWO_4^-	-223400.[v]	-255000.[u]	31.2[t]	30.6[t]	41.0[ae]	7.7661	11.1820	1.3532	-3.2412	34.7493	3.1986	1.1559
PO_4^{-3}	-243500.[m]	-305300.[m]	-53.0[m]	-124.6[ai]	-30.6[m]	-0.5258	-9.0576	9.2927	-2.4045	-15.1599	-28.4155	5.6114
AlO_2^-	-198693.[ab]	-222125.[u]	-7.22[t]	-11.9[m]	10.0[m]	3.7221	3.9954	-1.5879	-2.9441	15.2391	-5.4585	1.7418
Al^{+3}	-115609.[ac]	-126834.[u]	-77.7[t]	-32.5[m]	-44.4[m]	-3.3802	-17.0071	14.5185	-2.0758	10.7[m]	-8.06[m]	2.7530
Ga^{+3}	-38000.[m]	-50600.[m]	-79.[m]	-26.5[z]	-40.5[z]	-2.8378	-14.7065	11.5197	-2.1709	16.2356	-8.4326	2.7787
Pr^{+3}	-162600.[m]	-168800.[m]	-50.0[m]	-40.3[ah]	-42.8[ah]	-3.2061	-14.2894	8.5328	-2.1882	3.9607	-11.2844	2.3369
Tb^{+3}	-159500.[m]	-166900.[m]	-54.0[m]	-35.8[ah]	-40.9[ah]	-2.9245	-14.9162	11.5979	-2.1623	7.1853	-10.3677	2.4007
Mn^{+2}	-55100.[y]	-52900.[y]	-16.2[y]	-4.1[m]	-17.1[l]	-0.1015	-8.0040	8.8400	-2.4480	16.6672	-3.8697	1.4006
Co^{+2}	-13000.[m]	-13900.[m]	-27.0[m]	-7.8[m]	-25.5[l]	-1.2252	-8.9356	5.3191	-2.4095	15.2013	-4.6234	1.4769
Zn^{+2}	-35200.[m]	-36660.[m]	-26.2[m]	-5.33[l]	-24.3[l]	-1.0676	-8.9290	6.1282	-2.4098	18.74[l]	-5.37[l]	1.4574
Rh^{+3}	52450.[ad]	42830.[ad]	-71.6[j]	-30.2[ad]	-43.5[aa]	-3.2866	-15.8020	11.9492	-2.1256	13.0231	-9.1862	2.6654
Cr^{+3}	-49300.[h]	-60000.[k]	-77.[j]	-22.9[q]	-40.0[p]	-2.7824	-14.5709	11.4661	-2.1765	17.9914	-7.6992	2.7403
UO_2^{+2}	-227680.[n]	-243550.[n]	-23.5[n]	10.2[l]	5.73[l]	3.0256	-4.1084	15.3326	-2.6091	21.07[l]	0.43[l]	1.4099
Th^{+4}	-168500.[w]	-183800.[w]	-101.[w]	-0.2[af]	-53.40[ag]	-4.2886	-18.2500	12.9154	-2.0244	40.2222	-3.0752	3.7093

a. cal mol^{-1}. b. cal mol^{-1} K^{-1}. c. cm^3 mol^{-1}. d. cal mol^{-1} bar^{-1}. e. cal K mol^{-1} bar^{-1}. f. cal K mol^{-1}. g. Glushko (1965, 1966, 1968, 1970, 1971, 1972, 1973, 1974, 1978, 1979, 1981, 1982). h. Calculated from $\Delta\bar{H}_f^{\circ}$ and $\bar{S}^{\circ}$ in the table, together with S° of the elements from Cox et al. (1989) and/or ref. g. i. O'Hare and Boerio (1975). j. Sassani and Shock (1992; 1994). k. Dellien et al. (1976). l. Table 3. m. Shock and Helgeson (1988). n. Grenthe et al. (1992). p. From regression of data for $Cr(NO_3)_3$ reported by Spitzer et al. (1979c) and $Cr(ClO_4)_2$ from Swaddle and Mak (1983), together with data for NO_3^- for Table 1 and ClO_4^- from this table. q. From regression of data for $Cr(NO_3)_3$ reported by Spitzer et al. (1979c) r. Calculated from data given by Hovey and Hepler (1990) together with the corresponding value of K^+ from Table 1. s. Calculated from value of ΔG_f° for CrO_4^{-2} in Table and value of log K for $2CrO_4^{-2} + 2H^+ = Cr_2O_7^{-2} + H_2O$ reported by Palmer et al. (1987). t. From regression of equilibrium constant data (see text). u. Calculated from $\Delta\bar{G}_f^{\circ}$ and $\bar{S}^{\circ}$ in the table, together with S° of the elements from Cox et al. (1989), ref. g, and/or ref. w. v. Calculated from ΔG_f° of WO_4^{-2} given in table together with log K at 25°C and 1 bar for reaction (11) reported by Wesolowski et al. (1984). w. Wagman et al. (1982). x. Dellien (1977). y. Gedansky and Hepler (1969). z. From regression of data reported by van Gaans et al. (1990) and corresponding property of Cl^- from Table 1. aa. From regression data reported by Swaddle and Mak (1983), together with data from ClO_4^- from the table. ab. Calculated from ΔG_f° for gibbsite solubility at high pH from Wesolowski (1992) together with ΔG_f° for gibbsite from Hemingway and Robie (1977). ac. Calculated from ΔG_f° for $Al^{+3} + 2H_2O = AlO_2^- + 4H^+$ from Couturier et al. (1984) together with data from AlO_2^- from the table, H^+ from Table 1 and ΔG_f° H_2O from ref. w. ad. Sassani and Shock (1997a). ae. Estimated with Eqn. (12) (see text). af. Calculated from data reported by Morss and McCue (1976). ag. Recalculated from data compiled by Millero (1971). ah. Values obtained by a re-evaluation of experimental data used by Shock and Helgeson (1988). ai. Estimated from both $\bar{S}^{\circ}$ and $\bar{V}^{\circ}$ as described in text.

It is important to emphasize that the purpose in constructing the following correlations is to facilitate estimates of thermodynamic data that have not been determined by experiment. It is not our purpose to replace experimental studies, but rather to build on the foundation they supply. There are uncertainties inherent in any experimental measurement, and in many cases the uncertainties in data derived from experiments can be assessed by accounting for actual procedural uncertainties in the methods. In addition, statistical fluctuations can lead to scatter of experimental measurements around a particular value. In contrast, the sources of scatter in the type of empirical correlations developed in this study are largely unknown. Uncertainty from procedural methods are impossible to assess during the creative effort of developing theoretical tools to fill the gaps in thermodynamic data. In fact, it is highly likely that the scatter around these empirical correlations reflects contributions from other factors than those selected in the construction of the correlations. In the end, a predictive scheme built on correlations of this type cannot generate values with less uncertainty than the experimental measurements on which it is based. However, it does not follow that the scatter exhibited by the correlations necessarily reflect the uncertainty in the resulting estimates. Further details about the contribution of estimated equation of state parameters to the uncertainty of predicted standard state data are given by Shock and Helgeson (1988).

3.1. Cation Correlations

Correlations among $\bar{V}^{\circ}$, $\bar{C}^{\circ}_P$, and $\bar{S}^{\circ}$ for cations and anions were constructed in the present study from experimental data in Tables 1, 3, and 4, and supersede those proposed by Shock and Helgeson (1988). For example, Fig. 9 contains a plot of $\bar{V}^{\circ}$ against $\bar{S}^{\circ}$ for aqueous cations which constitutes a revision of Fig. 17 in Shock and Helgeson (1988). The correlation lines in Fig. 9 are consistent with

$$\bar{V}^{\circ} = \mathbf{y}\bar{S}^{\circ} + \mathbf{z} \qquad (12)$$

where **z** and **y** correspond to the following parameters

Species	z	y
Monovalent monatomic cations except Li^+	−20.5	1.29
Divalent transition cations	0.0	0.92
Alkaline earth cations and Pb^{+2}	−14.8	0.19
Trivalent cations excluding rare earths	−4.0	0.50

The correlation for the trivalent cations represents a substantial change from the correlations described by Shock and

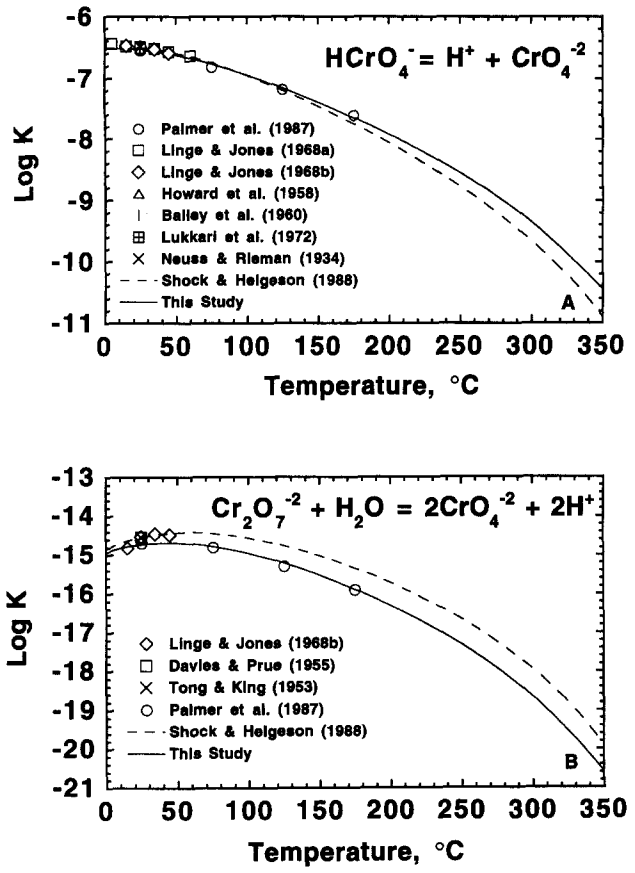

Fig. 6. The same plots as shown in Fig. 1 except that curves consistent with regression results from this study are included.

Helgeson (1988), who correlated data for Al^{+3} with the rare earth cations.

In the present study, the rare earth cations were excluded from correlations among other trivalent cations for several reasons. It was found that the rare-earth dependent correla-

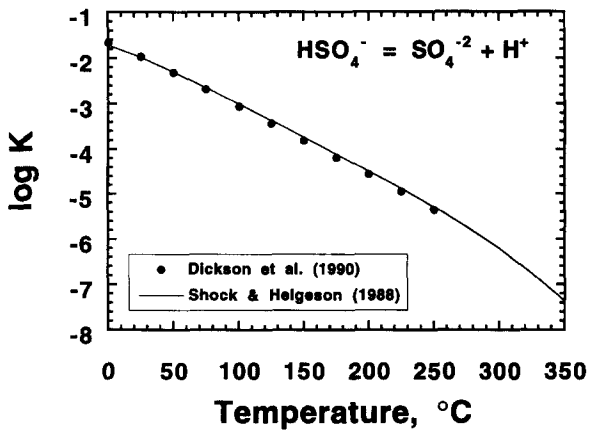

Fig. 7. The curve indicates equilibrium constants for the bisulfate dissociation reaction calculated with data and parameters from Shock and Helgeson (1988), and the symbols represent subsequent experimental data confirming the accuracy of the predicted values.

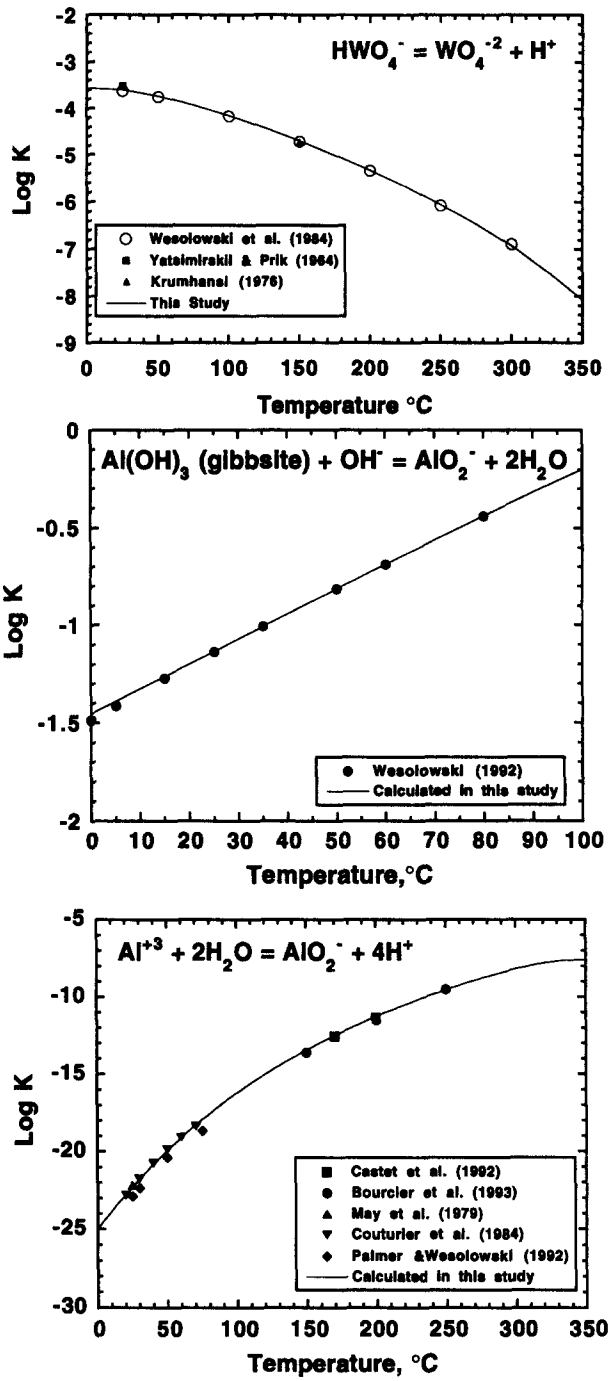

Fig. 8. Three plots comparing results obtained in this study (curves) for reactions 8, 10, and 11 with experimental data. Details of the regression procedure are given in the text. Data and parameters used to generate the curves are listed in Table 4.

tions proposed by Shock and Helgeson (1988)[‖] failed to yield estimates of $\bar{V}^{\circ}$ and $\bar{C}_P^{\circ}$ consistent with data for electrolyte solutions containing Ga^{+3}, Rh^{+3}, Fe^{+3}, and Cr^{+3}. In

[‖] It should be noted that the slope and intercept of the heat capacity vs. entropy correlation for light rare earth cations given by Shock and Helgeson (1988) are incorrect and should be replaced by −3.9 and −243.8, respectively.

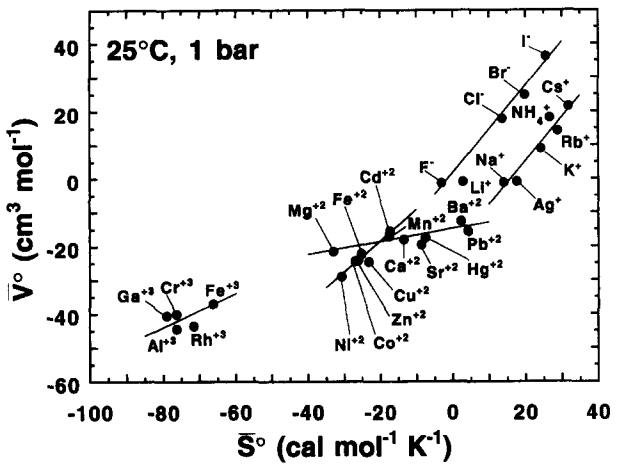

Fig. 9. Correlation of standard partial molal volumes with entropies for monatomic ions (and NH_4^+) at 25°C and 1 bar taken from Tables 1 and 4. Note that ions are grouped by charge and type. Slopes and intercepts for the lines are given in the text and are consistent with Eqn. 12.

addition, Sassani and Shock (1992) concluded that several lines of evidence indicate that the rare earth cations are in eightfold or ninefold coordination in aqueous solution in contrast to the other trivalent cations which are likely to be in sixfold coordination. Finally, there is the strictly pragmatic observation that Spedding and coworkers (Spedding et al., 1966, 1975a,b,c,d, 1979; Gildseth et al., 1975) have measured $\bar{V}°$ and $\bar{C}_P°$ for numerous rare earth electrolyte solutions over wide ranges of concentration, and estimates of standard state data at 25°C and 1 bar are generally not required. In the cases of Ce^{+3} and Pm^{+3} values obtained with correlations presented by Shock et al. (1997a) were used.

Values of the slopes of the correlation curves shown in Fig. 9 are plotted against charge in Fig. 10, where it can be seen that the slopes for the monovalent monatomic cations, divalent transition metal cations, and trivalent cations are consistent with

$$\mathbf{y} = -0.4Z_j + 1.7 \qquad (13)$$

which allows us to estimate a slope of 0.10 for a correlation of tetravalent cations consistent with those shown in Fig. 9. The only tetravalent ion for which experimental values of both $\bar{S}°$ and $\bar{V}°$ are available is Th^{+4}. Therefore, the correlation for tetravalent ions is constrained by the predicted slope and the Th^{+4} values to be

$$\bar{V}°_{+4} = 0.10\bar{S}°_{+4} - 43.3 \qquad (14)$$

Equations 12 and 14 were used in the present study to estimate values of $\bar{V}°$ for several aqueous cations listed in Table 5.

Correlations of $\bar{C}_P°$ and $\bar{V}°$ are shown in Fig. 11 which group the same sets of ions that are correlated in Fig. 9. The correlations in Fig. 11 are consistent with

$$\bar{C}_P° = \mathbf{w}\bar{V}° + \mathbf{x} \qquad (15)$$

where **x** and **w** correspond to the following intercepts and slopes

Species	z	w
Monovalent monatomic cations except Li^+	8.3	−0.68
Divalent transition cations	5.5	0.58
Alkaline earth cations and Pb^{+2}	−26.7	−1.0
Trivalent cations excluding rare earths	49.0	1.82

The slopes of the correlation curves in Fig. 11 for the monovalent monatomic cations, divalent transition cations, and trivalent cations were found to correlate with charge as shown by the line in Fig. 12, which is given by

$$\mathbf{w} = 1.25Z_j - 1.9 \qquad (16)$$

Equation 16 allows us to predict the slope for a tetravalent cation correlation which, together with the $\bar{V}°$ and $\bar{C}_P°$ data in Table 4 for Th^{+4}, yields

$$\bar{C}°_{P+4} = 3.1\bar{V}°_{+4} + 165.3 \qquad (17)$$

The correlations described above between $\bar{V}°$ and $\bar{S}°$, and between $\bar{C}_P°$ and $\bar{V}°$ require analogous correlations between $\bar{C}_P°$ and $\bar{S}°$. Combination of Eqns. 12 and 15 yields

$$\bar{C}_P° = \mathbf{u}\bar{S}° + \mathbf{v} \qquad (18)$$

where

$$\mathbf{v} = \mathbf{x} + \mathbf{wz} \qquad (19)$$

and

$$\mathbf{u} = \mathbf{wy} \qquad (20)$$

Values of **w**, **x**, **y**, and **z** listed above allow calculation of the following slope and intercept values

Species	v	u
Monovalent monatomic cations except Li^+	22.2	−0.88

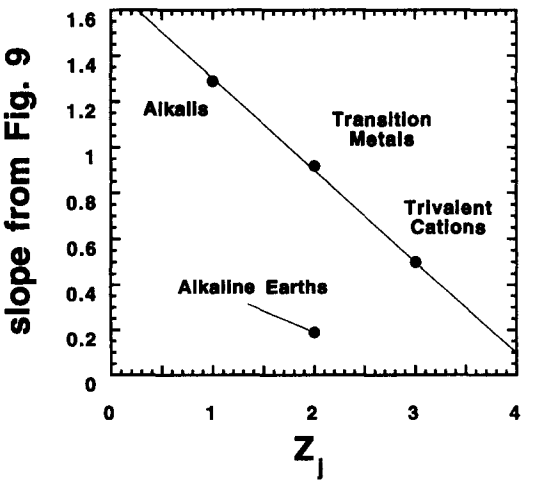

Fig. 10. The charge dependence of slopes of correlations between $\bar{V}°$ and $\bar{S}°$ shown in Fig. 9. The line is given by Eqn. 13 and was used in this study to estimate a slope of a correlation for tetravalent cations.

Table 5. Summary of standard partial molal properties of aqueous ions at 25°C and 1 bar, together with equation of state parameters needed to calculate the same properties at high temperature and pressures, which were revised or added in the present study based on estimates from new correlations.

Ion	$\Delta G^{\circ}_{f,Pr,T}$	$\Delta H^{\circ}_{f,Pr,Tr}$	S°	$\overline{Cp}^{\circ}$	V°	a_1 x10	a_2 x 10^{-2}	a^3	a_4 x 10^{-4}	c_1	c_2 x 10^{-4}	ω x 10^{-5}
Fr^{+}	-70500.[i]	-62500.[g]	35.1[h]	-6.5[k]	21.5[j]	4.7139	3.7284	4.2849	-2.9330	2.5442	-4.3586	0.0203
Be^{+2}	-90550.[x]	-91500.[w]	-32.1[l]	-5.8[k]	-20.9[j]	-0.5718	-9.1742	9.3462	-2.3996	17.0245	-4.2160	1.5475
Ra^{+2}	-134200.[w]	-126100.[w]	12.9[w]	-14.3[k]	-12.3[j]	0.3740	-6.8598	8.4279	-2.4953	5.7496	-5.9474	0.8644
In^{+3}	-23400.[m]	-25000.[m]	-63.0[m]	-15.6[k]	-35.5[j]	-2.2361	-13.2378	10.9433	-2.2316	20.3744	-6.2122	2.5346
Tl^{+}	-7740.[m]	1280.[m]	30.0[m]	-4.2[k]	18.2[j]	4.2884	2.6903	4.6910	-2.8901	4.6024	-3.8900	0.0974
Tl^{+3}	51300.[m]	47000.[m]	-46.0[m]	-0.2[k]	-27.0[j]	-1.1607	-10.6078	9.9017	-2.3404	27.0098	-3.0752	2.2752
CN^{-}	41200.[w]	36000.[w]	22.5[w]	-17.7[z]	23.9[q]	5.4714	5.5813	3.5497	-3.0096	7.6773	-6.6400	1.2900
OCN^{-}	-23280.[w]	-34900.[w]	25.5[w]	-15.8[z]	26.12[r]	5.7591	6.2815	3.2790	-3.0386	8.3509	-6.2530	1.2422
SCN^{-}	22160.[w]	18270.[w]	34.5[w]	-9.6[w]	35.7[r]	7.0244	9.3687	2.0708	-3.1662	10.7414	-4.9900	1.1073
$SeCN^{-}$	19500.[i]	18530.[g]	46.6[y]	-2.7[z]	49.68[r]	8.8752	13.8922	0.2829	-3.3532	13.0877	-3.5845	0.9230
Sn^{+2}	-6570.[i]	-2100.[t]	-4.0[t]	-15.5[k]	-15.6[j]	0.0094	-7.7516	8.7810	-2.4584	7.4160	-6.1919	1.1216
HNO_2	-12100.[u,w]	-28500.[w]	32.4[w]	6.7[s]	30.7[v]	5.9151	6.6590	3.1378	-3.0542	8.7050	-1.6697	-0.1507
HNO_3	-24730.[ab]	-45410.[ab]	42.7[ab]	18.0[ab]	40.2[v]	7.1623	9.7063	1.9367	-3.1802	13.8907	0.6320	-0.3066
$N_2O_2^{2-}$	33200.[aa]	-2590.[aa]	6.6[aa]	-59.3[s]	3.6[v]	3.3102	0.2986	5.6380	-2.7912	0.1067	-15.1139	3.1145
$HN_2O_2^{-}$	18200.[aa]	-9400.[aa]	34.0[aa]	9.3[s]	32.4[v]	6.5748	8.2753	2.4914	-3.1210	21.8724	-1.1401	1.1132
$H_2N_2O_2$	8600.[aa]	-13700.[aa]	52.0[aa]	39.0[s]	51.3[v]	8.6337	13.3019	0.5163	-3.3288	24.9004	4.9097	-0.4475
$N_2H_5^{+}$	19700.[w]	-1800.[w]	36.1[w]	16.8[w]	27.8[be]	5.5711	5.8193	3.4672	-3.0195	16.0644	0.3876	0.0057
$N_2H_6^{+2}$	21100.[ac]	-4000.[aa]	24.0[l]	15.7[k]	18.1[be]	4.4762	3.1468	4.5160	-2.9090	21.7574	0.1635	0.6936
$P_2O_7^{-4}$	-458700.[w]	-542800.[w]	-28.0[w]	-139.1[s]	21.7[v]	7.0687	9.4773	2.0273	-3.1707	-11.7223	-31.3692	6.9069
$HP_2O_7^{-3}$	-471400.[w]	-543700.[w]	11.0[w]	-28.7[s]	36.5[v]	8.3302	12.5558	0.8208	-3.2980	32.1587	-8.8807	4.6470
$H_2P_2O_7^{-2}$	-480400.[w]	-544600.[w]	39.0[w]	17.6[s]	47.1[v]	9.0963	14.4299	0.0760	-3.3754	40.6359	0.5505	2.6218
$H_3P_2O_7^{-}$	-483600.[w]	-544100.[w]	51.0[w]	37.4[s]	51.7[v]	9.1292	14.5122	0.0398	-3.3788	35.9785	4.5838	0.8568
$H_4P_2O_7$	-485700.[w]	-542200.[w]	64.0[w]	58.8[s]	56.6[v]	9.2975	14.9199	-0.1130	-3.3957	34.8301	8.9430	-0.6292
HPO_3^{-2}	-194000.[aa]	-231600.[w]	4.0[l]	-40.2[s]	4.5[v]	3.4463	0.6347	5.4974	-2.8051	11.6523	-11.2232	3.1527
$H_2PO_3^{-}$	-202350.[aa]	-231700.[w]	31.7[l]	5.5[s]	14.7[v]	4.1649	2.3899	4.8065	-2.8777	19.9762	-1.9142	1.1491
H_3PO_3	-204800.[aa]	-230600.[w]	43.6[l]	25.1[s]	19.1[v]	4.2704	2.6439	4.7145	-2.8882	17.9261	2.0783	-0.3203
$H_2PO_2^{-}$	-122400.[aa]	-146700.[w]	24.1[l]	-7.0[s]	22.0[v]	5.2026	4.9190	3.8223	-2.9823	13.7063	-4.4604	1.2637
H_3PO_2	-125100.[aa]	-145600.[aa]	36.9[l]	14.1[s]	35.4[v]	6.5352	8.1731	2.5430	-3.1168	12.4140	-0.1623	-0.2188
AsO_4^{-3}	-154970.[w]	-212270.[w]	-38.9[w]	-116.1[s]	-18.7[v]	1.0308	-5.2609	7.8091	-2.5614	-12.1352	-26.6841	5.3990
$HAsO_4^{-2}$	-170790.[w]	-216620.[w]	-0.4[w]	-47.5[s]	11.3[v]	4.3994	2.9611	4.5853	-2.9013	7.9908	-12.7102	3.2197
$H_2AsO_4^{-}$	-180010.[w]	-217390.[w]	28.0[w]	-0.6[s]	33.4[v]	6.7429	8.6835	2.3351	-3.1379	16.9206	-3.1567	1.2055
H_3AsO_4	-183100.[w]	-215700.[w]	44.0[w]	25.8[s]	45.9[v]	7.9357	11.5925	1.1990	-3.2581	18.2805	2.2209	-0.3263
AsO_2^{-}	-83650.[w]	-102540.[w]	9.7[w]	-28.0[s]	6.9[v]	3.2101	0.0554	5.7305	-2.7812	3.4104	-8.7381	1.4820
$HAsO_2$	-96240.[w]	-109110.[w]	30.1[w]	2.9[s]	28.3[v]	5.5984	5.8913	3.4280	-3.0224	6.7990	-2.4438	-0.1158
SbO_2^{-}	-82400.[ac]	-110000.[ad]	-17.1[l]	-44.1[s]	-21.3[v]	-0.5113	-9.0269	9.2893	-2.4057	-2.2802	-12.0177	1.8885
$HSbO_2$	-97400.[w]	-116600.[w]	11.1[w]	-28.5[s]	8.4[v]	2.9726	-0.5203	5.9475	-2.7574	-8.9525	-8.8400	0.1719
Bi^{+3}	22880.[i]	19360.[g]	-45.[h]	0.8[k]	-26.5[j]	-1.0957	-10.4536	9.8506	-2.3467	27.5027	-2.8715	2.2651
HO_2^{-}	-16090.[w]	-38320.[w]	5.7[w]	-37.4[s]	2.7[v]	2.6566	-1.2961	6.2619	-2.7253	-1.5190	-10.6529	1.5449
H_2O_2	-32030.[w]	-45690.[w]	34.4[w]	10.0[s]	32.8[v]	6.1922	7.3370	2.8686	-3.0822	10.3600	-0.9975	-0.1809
SO_3^{-2}	-116300.[m]	-151900.[m]	-7.[m]	-67.5[s]	-3.1[v]	2.4632	-1.7691	6.4494	-2.7058	-2.7967	-16.7843	3.3210
HSO_3^{-}	-152370.[m]	-185380.[m]	50.7[m]	36.9[s]	50.3[v]	8.9391	14.0430	0.2349	-3.3594	35.7254	4.4819	0.8611
$HS_2O_3^{-}$	-127200.[bb]	-153900.[ai]	30.5[bd]	3.5[s]	29.5[v]	6.1964	7.3510	2.8549	-3.0828	18.9745	-2.3216	1.1676
$H_2S_2O_3$	-128000.[bc]	-150400.[ai]	45.0[bd]	27.5[s]	42.2[v]	7.4242	10.3493	1.6762	-3.2067	19.1373	2.5672	-0.3415
$S_2O_4^{-2}$	-143500.[m]	-180100.[m]	22.0[m]	-50.1[s]	28.8[v]	6.6784	8.5280	2.3917	-3.1314	3.3115	-13.2399	2.8772
$HS_2O_4^{-}$	-146900.[w]	-179100.[ai]	36.5[bd]	13.4[s]	40.1[v]	7.6159	10.8142	1.5005	-3.2260	23.9326	-0.3049	1.0760
$H_2S_2O_4$	-147400.[w]	-175300.[ai]	51.0[bd]	37.4[s]	51.4[v]	8.6525	13.3462	0.5023	-3.3306	24.1023	4.5838	-0.4323
$S_2O_5^{-2}$	-189000.[m]	-232000.[m]	25.[m]	-48.3[s]	33.9[v]	7.3618	10.1945	1.7414	-3.2003	3.9715	-12.8732	2.8343
$S_2O_6^{-2}$	-231000.[m]	-280400.[m]	30.[m]	-45.3[s]	40.4[v]	8.2257	12.3054	0.9087	-3.2876	5.0331	-12.2621	2.7587
$S_3O_6^{-2}$	-229000.[m]	-279000.[m]	33.[m]	-43.5[s]	41.9[v]	8.4155	12.7691	0.7268	-3.3068	5.6683	-11.8954	2.7131
$S_4O_6^{-2}$	-248700.[m]	-292600.[m]	61.5[m]	-26.4[s]	56.5[v]	10.2672	17.2902	-1.0502	-3.4937	11.7042	-8.4122	2.2805
$S_5O_6^{-2}$	-229000.[m]	-281000.[m]	40.[m]	-39.3[s]	45.5[v]	8.8725	13.8806	0.2986	-3.3527	7.1576	-11.0399	2.6076
HSe^{-}	10500.[w]	3800.[w]	19.[w]	-19.8[z]	20.2[y]	4.9823	4.3855	4.0227	-2.9602	6.9147	-7.0678	1.340
SeO_3^{-2}	-88400.[w]	-121700.[w]	3.1[w]	-61.4[s]	5.7[v]	3.6149	1.0478	5.3323	-2.8222	-0.6517	-15.5417	3.1658
$HSeO_3^{-}$	-98340.[w]	-122980.[w]	32.3[w]	6.5[s]	31.1[v]	6.4061	7.8624	2.6551	-3.1039	20.4808	-1.7105	1.1402
H_2SeO_3	-101850.[w]	-121290.[w]	49.7[w]	35.2[s]	46.2[v]	7.9475	11.6240	1.1819	-3.2594	22.9944	4.1356	-0.4127
SeO_4^{-2}	-105500.[w]	-143200.[w]	12.9[w]	-55.6[s]	21.7[v]	5.7548	6.2678	3.2916	-3.0380	1.3971	-14.3602	3.0192
$HSeO_4^{-}$	-108100.[w]	-139000.[w]	35.7[w]	12.1[s]	39.4[v]	7.5244	10.5922	1.5837	-3.2168	23.2855	-0.5697	1.0885
ClO^{-}	-8800.[w]	-25600.[w]	10.[w]	-27.8[s]	0.7[v]	2.3599	-2.0164	6.5356	-2.6955	3.4786	-8.6974	1.4767
$HClO$	-19100.[w]	-28900.[w]	33.9[w]	9.1[s]	28.4[v]	5.5927	5.8751	3.4387	-3.0218	9.9023	-1.1808	-0.1734
ClO_2^{-}	4100.[w]	-15900.[w]	24.2[w]	-19.3[s]	22.1[v]	5.2163	4.9580	3.7949	-2.9839	6.4977	-6.9659	1.2637
$HClO_2$	1400.[w]	-12400.[w]	45.0[w]	27.5[s]	44.0[v]	7.6706	10.9455	1.4527	-3.2314	19.1373	2.5672	-0.3415
BrO^{-}	-8000.[m]	-22500.[m]	9.7[l]	-28.0[s]	0.4[v]	2.3206	-2.1131	6.5758	-2.6915	3.4104	-8.7381	1.4820
$HBrO$	-19700.[w]	-27000.[w]	33.8[l]	9.0[s]	28.3[v]	5.5795	5.8410	3.4565	-3.0204	9.8576	-1.2012	-0.1719
BrO_4^{-}	28200.[m]	3100.[m]	47.6[l]	-5.2[s]	48.7[v]	8.7361	13.5515	0.4200	-3.3391	11.4884	-4.0937	0.9085
IO^{-}	-9200.[m]	-25700.[m]	-1.4[l]	-34.6[s]	-12.5[v]	0.6131	-6.2757	8.1983	-2.5195	1.1172	-10.0825	1.6530
HIO	-23700.[w]	-33000.[w]	22.8[l]	-9.2[s]	15.6[v]	3.8979	1.7354	5.0694	-2.8506	0.7260	-4.9085	-0.0053
HIO_3	-31700.[w]	-50500.[w]	39.9[l]	19.0[s]	37.7[v]	6.8346	8.9050	2.2530	-3.1470	14.8674	0.8357	-0.2642
IO_4^{-}	-14000.[m]	-36200.[m]	53.0[l]	-2.0[s]	52.9[v]	9.2831	14.8827	-0.0933	-3.3942	12.6081	-3.4419	0.8264
Sc^{+3}	-140200.[w]	-146800.[w]	-61.[w]	-13.8[k]	-34.5[j]	-2.1109	-12.9294	10.8170	-2.2444	21.1134	-5.8456	2.5003
V^{+2}	-52000.[af]	-54000.[af]	-31.[af]	-10.9[k]	-28.5[j]	-1.6188	-11.7289	10.3473	-2.2940	13.8458	-5.2548	1.5269
V^{+3}	-57900.[af]	-62000.[af]	-55.[af]	-8.4[k]	-31.5[j]	-1.7304	-11.9981	10.4465	-2.2829	23.4604	-4.7456	2.4115
VO^{+2}	-106700.[w]	-116300.[w]	-32.[w]	31.4[p]	-26.2[ag]	-1.2971	-10.9431	10.0377	-2.3265	38.8261	3.3616	1.5475
VO_2^{+}	-140300.[w]	-155300.[w]	-10.1[w]	-13.7[p]	9.2[ag]	3.2606	0.1790	5.6817	-2.7863	4.5892	-5.8252	0.7003

Table 5. (Continued)

VO_4^{-3}	-214900.[w]	-270600.[ai]	-35.2[ah]	38.0[p]	-16.9[ag]	1.2579	-4.7015	7.5797	-2.5845	77.6555	4.7060	5.3424
HVO_4^{-2}	-233000.[w]	-277000.[w]	4.[w]	87.3[aj]	12.5[ag]	4.5410	3.3077	4.4469	-2.9156	86.3755	14.7484	3.1527
$H_2VO_4^-$	-243990.[w]	-280620.[w]	29.0[w]	35.8[aj]	31.3[ag]	6.4502	7.9653	2.6252	-3.1082	38.1088	4.2579	1.1898
H_3VO_4	-249200.[ak]	-284600.[ai]	37.1[bf]	19.1[aj]	38.3[ag]	6.9310	9.1392	2.1640	-3.1567	15.3166	0.8561	-0.2218
Cr^{+2}	-39400.[al]	-39000.[ai]	-24.2[h]	-7.3[k]	-22.3[j]	-0.8036	-9.7400	9.5688	-2.3762	15.0502	-4.5215	1.4287
Mn^{+3}	-20300.[am]	-30700.[ai]	-74.[h]	-25.6[k]	-41.0[j]	-2.9320	-14.9340	11.6041	-2.1615	16.0611	-8.2492	2.7025
MnO_4^{-2}	-120400.[ba]	-156600.[ba]	15.5[l]	-66.4[p]	21.1[ag]	5.6596	6.0368	3.3786	-3.0285	-5.2910	-16.5602	2.9803
Fe^{+2}	-21870.[n]	-22050.[n]	-25.3[n]	-7.9[n]	-22.2[m]	-0.7867	-9.6969	9.5479	-2.3780	14.7860	-4.6437	1.4382
Fe^{+3}	-4120.[n]	-11850.[n]	-66.3[n]	-18.6[k]	-37.0[q]	-2.4256	-13.6961	11.1141	-2.2127	19.0459	-6.8233	2.5812
Co^{+3}	32000.[m]	22000.[m]	-73.[m]	-24.7[k]	-40.5[j]	-2.8678	-14.7777	11.5439	-2.1680	16.4739	-8.0659	2.6901
Cu^+	11950.[m]	17132.[m]	9.7[m]	13.7[k]	-8.0[j]	0.8070	-5.8040	8.0165	-2.5390	17.9233	-0.2438	0.4046
Y^{+3}	-163800.[m]	-170900.[m]	-60.[m]	-12.9[k]	-34.0[j]	-2.0463	-12.7741	10.7611	-2.2508	21.5366	-5.6622	2.4890
Zr^{+4}	-133270.[an]	-150330.[ai]	-110.3[h]	-3.1[ap]	-54.3[ag]	-4.3670	-18.4377	12.9811	-2.0167	39.7423	-3.6660	3.8417
NbO_3^-	-227100.[g]	-255300.[ai]	3.2[g]	-41.1[p]	20.4[ar]	5.0915	4.6485	3.9273	-2.9711	-3.3376	-11.4066	1.5829
$HNbO_3$	-236800.[g]	-257950.[ai]	31.1[az]	31.4[aj]	30.0[ar]	5.7110	6.1642	3.3252	-3.0337	20.2299	3.3616	-0.4710
$HMoO_4^-$	-206400.[ay]	-238500.[ai]	32.5[ax]	28.6[aj]	40.8[ar]	7.7320	11.0966	1.3908	-3.2376	33.3930	2.7912	1.1359
RuO_4^{-2}	-71600.[g]	-110200.[g]	6.6[l]	-48.1[aj]	30.2[p]	6.9502	9.1887	2.1387	-3.1588	6.6707	-12.8325	3.1145
Ce^{+3}	-161600.[m]	-167400.[m]	-49.[m]	-47.7[as]	-44.1[as]	-3.4833	-16.2789	12.1302	-2.1059	-0.3550	-12.7510	2.3265
Pm^{+3}	-158000.[i]	-164000.[at]	-50.[at]	-44.6[as]	-42.4[as]	-3.2471	-15.7059	11.9125	-2.1296	1.5577	-12.1195	2.3369
Hf^{+4}	-132600.[g]	-150250.[ai]	-111.2[h]	-3.4[ap]	-54.4[aq]	-4.3761	-18.4638	12.9996	-2.0156	39.6914	-3.7271	3.8552
Au^+	39000.[m]	47900.[ai]	25.6[h]	-0.3[k]	12.5[j]	3.5312	0.8428	5.4139	-2.8137	7.5089	-3.0956	0.1648
Au^{+3}	103600.[m]	97800.[ai]	-54.8[h]	-8.2[k]	-31.4[j]	-1.7167	-11.9654	10.4352	-2.2843	23.5775	-4.7048	2.4115
Hg_2^{+2}	36710.[i]	39880.[t]	15.71[t]	13.8[k]	14.5[j]	4.0263	2.0479	4.9491	-2.8636	21.8090	-0.2234	0.8201
U^{+3}	-113550.[au]	-116900.[au]	-46.1[au]	-36.4[as]	-39.3[as]	-2.8438	-14.7220	11.5280	-2.1703	5.7945	-10.4492	2.2752
U^{+4}	-126650.[au]	-141300.[au]	-99.6[au]	0.2[ap]	-53.3[aq]	-4.2836	-18.2319	12.8955	-2.0252	40.2193	-2.9938	3.6835
UO_2^+	-229690.[au]	-245000.[au]	-6.0[au]	-22.1[p]	10.2[ar]	3.3767	0.4614	5.5725	-2.7980	-0.9002	-7.5363	0.6388
La^{+2}	-77700.[j]	-72200.[at]	0.7[at]	-12.0[av]	-14.7[aw]	0.1064	-7.5128	8.6835	-2.4683	8.7551	-5.4789	1.0444
Ce^{+2}	-74900.[i]	-70300.[at]	1.4[at]	-12.2[av]	-14.5[aw]	0.1315	-7.4538	8.6653	-2.4708	8.5755	-5.5196	1.0376
Pr^{+2}	-92700.[i]	-88400.[at]	0.7[at]	-12.0[av]	-14.7[aw]	0.1064	-7.5128	8.6835	-2.4683	8.7551	-5.4789	1.0444
Nd^{+2}	-100200.[i]	-96100.[at]	-0.5[at]	-11.8[av]	-14.9[aw]	0.0860	-7.5654	8.7097	-2.4661	9.0616	-5.4382	1.0649
Pm^{+2}	-92700.[i]	-88400.[at]	-1.9[at]	-11.5[av]	-15.2[aw]	0.0520	-7.6511	8.7496	-2.4626	9.4303	-5.3771	1.0858
Sm^{+2}	-123000.[i]	-120500.[at]	-6.2[at]	-10.7[av]	-16.0[aw]	-0.0353	-7.8592	8.8194	-2.4540	10.5009	-5.2141	1.1512
Eu^{+2}	-129200.[i]	-126150.[at]	-2.4[at]	-11.4[av]	-15.3[aw]	0.0407	-7.6776	8.7578	-2.4615	9.5539	-5.3567	1.0929
Gd^{+2}	-70600.[i]	-67400.[at]	-4.3[at]	-11.1[av]	-15.6[aw]	0.0094	-7.7516	8.7810	-2.4584	9.9946	-5.2956	1.1216
Tb^{+2}	-79400.[i]	-76200.[at]	-2.9[at]	-11.3[av]	-15.4[aw]	0.0294	-7.7042	8.7663	-2.4604	9.6780	-5.3363	1.1000
Dy^{+2}	-102800.[i]	-99900.[at]	-3.6[at]	-11.2[av]	-15.5[aw]	0.0206	-7.7248	8.7724	-2.4596	9.8690	-5.3159	1.1144
Ho^{+2}	-96900.[i]	-94200.[at]	-4.3[at]	-11.1[av]	-15.6[aw]	0.0094	-7.7516	8.7810	-2.4584	9.9946	-5.2956	1.1216
Er^{+2}	-91600.[i]	-89150.[at]	-5.5[at]	-10.9[av]	-15.8[aw]	-0.0104	-7.7996	8.7981	-2.4565	10.3150	-5.2548	1.1437
Tm^{+2}	-107600.[i]	-105600.[at]	-6.7[at]	-10.6[av]	-16.1[aw]	-0.0464	-7.8863	8.8296	-2.4529	10.6286	-5.1937	1.1587
Yb^{+2}	-128500.[i]	-126800.[at]	-11.2[at]	-9.8[av]	-16.9[aw]	-0.1323	-8.0980	8.9173	-2.4441	11.7413	-5.0308	1.2285
Ce^{+4}	-121300.[i]	-137700.[at]	-100.1[at]	0.1[ap]	-53.3[aq]	-4.2792	-18.2247	12.8996	-2.0255	40.2790	-3.0141	3.6964
Pr^{+4}	-72700.[i]	-88700.[at]	-98.5[at]	0.6[ap]	-53.2[aq]	-4.2742	-18.2128	12.8958	-2.0260	40.3357	-2.9123	3.6707
Nd^{+4}	-47000.[i]	-62900.[at]	-98.7[at]	0.5[ap]	-53.2[aq]	-4.2742	-18.2128	12.8958	-2.0260	40.2772	-2.9327	3.6707
Pm^{+4}	-34200.[i]	-50400.[at]	-99.7[at]	0.2[ap]	-53.3[aq]	-4.2836	-18.2319	12.8955	-2.0252	40.2193	-2.9938	3.6835
Sm^{+4}	-39900.[i]	-56400.[at]	-101.1[at]	-0.2[ap]	-53.4[aq]	-4.2886	-18.2500	12.9154	-2.0244	40.2222	-3.0752	3.7093
Eu^{+4}	5000.[i]	-12700.[at]	-103.3[at]	-0.9[ap]	-53.6[aq]	-4.3071	-18.2951	12.9322	-2.0226	40.0515	-3.2178	3.7353
Gd^{+4}	12600.[i]	-5700.[at]	-107.6[at]	-2.3[ap]	-54.1[aq]	-4.3532	-18.4052	12.9700	-2.0180	39.8394	-3.5030	3.8013
Tb^{+4}	-88200.[i]	-105900.[at]	-104.2[at]	-1.2[ap]	-53.7[aq]	-4.3164	-18.3144	12.9330	-2.0218	39.9963	-3.2789	3.7484
Dy^{+4}	-55700.[i]	-73400.[at]	-104.0[at]	-1.1[ap]	-53.7[aq]	-4.3164	-18.3144	12.9330	-2.0218	40.0550	-3.2586	3.7484
Ho^{+4}	-30500.[i]	-48300.[at]	-104.2[at]	-1.2[ap]	-53.7[aq]	-4.3164	-18.3144	12.9330	-2.0218	39.9963	-3.2789	3.7484
Er^{+4}	-28100.[i]	-45900.[at]	-104.7[at]	-1.4[ap]	-53.8[aq]	-4.3256	-18.3402	12.9496	-2.0207	40.0003	-3.3197	3.7615
Tm^{+4}	-30100.[i]	-48300.[at]	-105.6[at]	-1.6[ap]	-53.9[aq]	-4.3349	-18.3596	12.9511	-2.0199	40.0047	-3.3604	3.7747
Yb^{+4}	3800.[i]	-13600.[at]	-106.6[at]	-1.9[ap]	-54.0[aq]	-4.3441	-18.3854	12.9683	-2.0188	39.9511	-3.4215	3.7880
Lu^{+4}	27000.[i]	9800.[at]	-108.0[at]	-2.4[ap]	-54.1[aq]	-4.3487	-18.3921	12.9608	-2.0186	39.9042	-3.5234	3.8147

a. cal mol^{-1}. b. cal mol^{-1} K^{-1}. c. cm^3 mol^{-1}. d. cal mol^{-1} bar^{-1}. e. cal K mol^{-1} bar^{-1}. f. cal K mol^{-1}. g. Glushko (1965, 1966, 1968, 1970, 1971, 1972, 1973, 1974, 1978, 1979, 1981, 1982). h. Sassani and Shock (1992, 1994). i. Calculated from ΔH_f° and S° in the table using values of S° of the elements from Cox et al. (1989), ref. g, and/or ref. w. j. Estimated with Eqn. (12). k. Estimated with Eqn. (18). l. Calculated from ΔG_f° and ΔH_f° given in table, together with $S^\circ$of the elements from Cox et al (1989) and/or ref. w. m. Shock and Helgeson (1988). n. Shock and Helgeson (1989). p. Estimated with Eqn. (31) using the lower correlation in Fig. 25. q. Calculated in this study from data given in Table 2. r. Millero (1971). s. Estimated with Eqn. (18) using parameters for nonmetal oxygen-bearing species given in text. t. Cox et al. (1989). u. Calculated from pK_a reported by Li and Ritter (1953). v. Estimated with Eqn. (12) using parameters for nonmetal oxygen-bearing species given in text or estimated with Eqns. (25) and (26). w. Wagman et al. (1982). x. Calculated from log K for α-$Be(OH)_2 + 2H^+ = Be^{+2} + 2H_2O$ given by Baes and Mesmer (1976), together with ΔG_f°, α-$Be(OH)_2$ from Wagman et al. (1982) and ΔG_f°, H_2O = -56687 cal mol^{-1}. y. Estimated with Eqn. (23). z. Estimated with Eqn. (24). aa. Latimer (1952). ab. Shock et al. (1989). ac. Calculated from ΔG_f° of $N_2H_5^+$ in table and K for the reaction $N_2H_5^+ + H^+ = N_2H_6^{+2}$ given by Latimer (1952). ad. Estimated by assuming that ΔH_r° for the dissociation reaction of $HSbO_2$ is equal to that for $HAsO_2$. ae. Calculated from ΔG_f° for $HSbO_2$ in the table and Latimer's (1952) estimate of log K for the dissociation reaction. af. Hill et al. (1971). ag. Estimated with Eqn. (12) using parameters for first-row transition metal oxygen-bearing species given in text. ah. Estimated from S° of HVO_4^{-2} using data plotted in the correlation shown in Fig. 25C. ai. Calculated from ΔG_f° and S° given in the table together with values of S° of the elements from Cox et al. (1989), ref. g., and /or ref. w. aj. Estimated with Eqn. (31) using the upper curve in Fig. 25. ak. Langmuir (1978). al. Calculated from the standard redox potential for Cr^{+3}/Cr^{+2} couple reported by Beiderman and Romano (1975) and value of ΔG_f° for Cr^{+3} from Table 4. am. Calculated from data given by Latimer (1952) and the value of ΔG_f° for Mn^{+2} from Table 1. an. Calculated from solubility product for ZrO_2 given by Baes and Mesmer (1976) together with ΔG_f° of ZrO_2 from ref. w. ap. Estimated with Eqn. (22). aq. Estimated with Eqn. (14). ar. Estimated with Eqn. (12) using parameters for higher-order transition-metal oxygen-bearing species given in text or estimated with Eqns. (28) and (29). as. Estimated from value of S° in table, together with revised rare earth correlations from Shock et al. (1997a) which are also applicable to trivalent actinides. at. Morss (1976). au. Grenthe et al. (1992). av. Estimated with Eqn. (18) using parameters for the alkaline earth cations. aw. Estimated with Eqn. (12) using parameters for the alkaline earth cations. ax. Estimated from S° of MoO_4^{-2} from Table 4 and Eqn. (32). ay. Re-calculated from data given in ref. g using ΔG_f° of MoO_4^{-2} from table 4. az. Estimated from S° of NbO_3^- using Eqn. (32). ba. Re-calculated from value given by Wagman et al. (1982) to be consistent with Mn^{+2} value in Table 4. bb. Calculated from the log K given by Page (1953) for the reaction $HS_2O_3^- = H^+ + S_2O_3^{-2}$ using ΔG_f° of $S_2O_3^{-2}$ from Table 1. bc. Calculated from the log K estimated by Page (1953) for the reaction $H_2S_2O_3 = H^+ + HS_2O_3^-$ using ΔG_f° of $HS_2O_3^-$ from the Table. bd. Estimated by assuming $\Delta S^\circ_{n,H^+}$ = 14.5 cal mol^{-1} K^{-1} consistent with the lower correlation in Fig. 26A. be. Estimated by assuming that the correlation shown as a dashed line in Fig. 13 has an analog on Fig. 9 which can be constrained by the data for Li^+ and NH_4^+. The resulting expression is $\nabla^* = 0.80\ S^* - 1.1$. bf. Estimated from S° of $H_2VO_4^-$ using Eqn. (32).

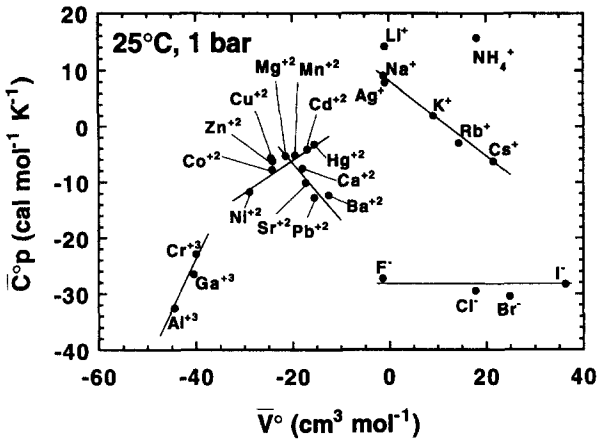

Fig. 11. Correlation of standard partial molal heat capacities with volumes for monatomic ions (and NH_4^+) at 25°C and 1 bar taken from Tables 1 and 4. Note that ions are grouped by charge and type. Slopes and intercepts for the lines are given in the text and are consistent with Eqn. 15.

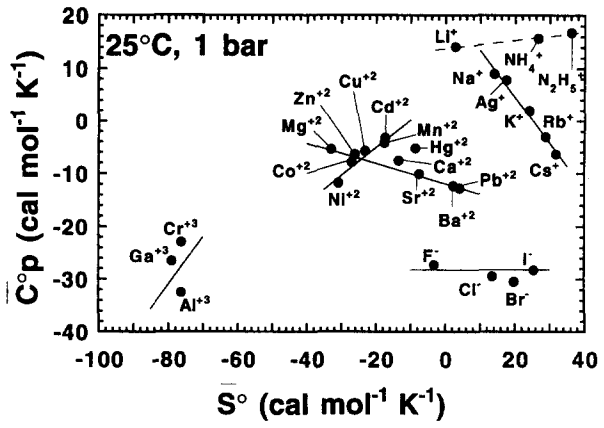

Fig. 13. Correlation of standard partial molal heat capacities with entropies for monatomic ions (and NH_4^+ and $N_2H_5^+$) at 25°C and 1 bar taken from Tables 1 and 4. Note that ions are grouped by charge and type. All of the solid lines in this figure are calculated, and are consistent with the lines given in Figs. 9 and 11. Slopes and intercepts for the lines are given in the text and are consistent with Eqn. 18.

Other monovalent cations (dashed line)	14.2	0.064
Divalent transition cations	5.5	0.53
Alkaline earth cations and Pb^{+2}	−11.9	−0.19
Trivalent cations other than rare earths	41.7	0.91

which were used to construct the lines shown in Fig. 13. Both of the correlations for alkali and alkaline earth cations in Fig. 13 are identical to those proposed by Shock and Helgeson (1988). In addition, the divalent transition cation slope and intercept differ only slightly from values obtained by Shock and Helgeson (1988) (0.61 and 7.5, respectively). However, exclusion of the rare earth elements yields a trivalent cation correlation which differs considerably from those adopted by Shock and Helgeson (1988). This new correlation should allow more accurate estimates for trivalent cations other than the rare earths, and was used in the present study to estimate values of $\bar{C}°_P$ for those trivalent species for which no reliable values of $\bar{V}°$ are available from experiments (see Table 5). The dashed correlation between NH_4^+ and $N_2H_5^+$ shown in Fig. 13 passes close to the position of Li^+ and may shed some light on why Li^+ does not correlate with the other alkali cations.

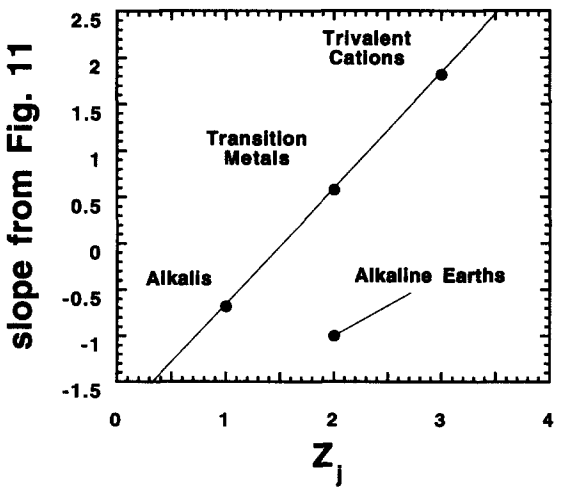

Fig. 12. The charge dependence of slopes of correlations between $\bar{C}°_P$ and $\bar{V}°$ shown in Fig. 11. The line is given by Eqn. 16 and was used in this study to estimate a slope of a correlation for tetravalent cations.

In order to obtain a predicted correlation for $\bar{C}°_P$ and $\bar{S}°$ of tetravalent cations, which is consistent with the predicted $\bar{V}°$ vs. $\bar{S}°$ and $\bar{C}°_P$ vs. $\bar{V}°$ correlations described above, the relations among slopes and charge depicted in Figs. 10 and 12 must be taken into account. Because the slopes of correlations between $\bar{C}°_P$ and $\bar{S}°$ shown in Fig. 13 are products of the slopes of the $\bar{V}°$ vs. $\bar{S}°$ and $\bar{C}°_P$ vs. $\bar{V}°$ correlations (see Eqn. 20), the slope vs. charge dependence for the $\bar{C}°_P$ vs. $\bar{S}°$ correlation will be the product of Eqns. 13 and 16. As a result, the relation between **u** and charge is second order and given by

$$\mathbf{u} = -0.5Z_j^2 + 2.885Z_j - 3.23 \qquad (21)$$

The resulting slope for the predicted $\bar{C}°_P$ vs. $\bar{S}°$ correlation for tetravalent cations is 0.31 which, together with the data for Th^{+4} in Table 4, yields

$$\bar{C}°_{P+4} = 0.31\ \bar{S}°_{+4} + 31.1 \qquad (22)$$

This correlation was used in the present study to estimate values of $\bar{C}°_P$ from $\bar{S}°$ for several tetravalent cations listed in Table 5. The correlations expressed by Eqns. 12, 14, 18, and 22 are also used by Sassani and Shock (1996a) to estimate values of $\bar{V}°$ and $\bar{C}°_P$ for Pd^{+2}, Pt^{+2}, Ru^{+2}, Rh^{+2}, Ru^{+3}, and Rh^{+3}, and by Willis and Shock (1997) to estimate values for Ti^{+3} and Ti^{+4}. Additional correlations involving rare earth and actinide cations are described by Shock et al. (1997a).

3.2. Anion Correlations

Correlations among $\bar{S}°$, $\bar{V}°$, and $\bar{C}°_P$ at 25°C and 1 bar for various groups of anions were constructed during the course

of the present study. Those involving halides, cyanides, OH^-, and HS^- are described in this section, and correlations for oxyanions are discussed in the following section.

Standard partial molal properties of aqueous halides adopted by Shock and Helgeson (1988) were not revised in the present study. Therefore, the values of **z** (1.8) and **y** (1.29) in Eqn. 12, and **v** (−28.2) and **u** (0.0) in Eqn. 18 determined by Shock and Helgeson (1988) were not changed during this study. The corresponding values of **x** and **w** in Eqn. 15 are −28.2 and 0.0, respectively.

Standard partial molal properties of other monovalent anions (other than oxyanions, see below) do not fall on the halide correlations described by Shock and Helgeson (1988). These authors placed OH^- and HS^- on correlations for oxyanions, but it was found in the present study that there are stronger correlations between these anions and CN^-, OCN^-, and SCN^-. These correlations of $\bar{V}°$ and $\bar{S}°$, and $\bar{C}_P°$ and $\bar{S}°$ are shown in Fig. 14, and the correlations lines are given by

$$\bar{V}° = 1.06\ \bar{S}° + 0.07 \qquad (23)$$

and

$$\bar{C}_P° = 0.62\ \bar{S}° - 31.6 \qquad (24)$$

Equation 24 was used in this study to estimate values of $\bar{C}_P°$ for CN^-, OCN^-, and $SeCN^-$, and Eqn. 23 was rearranged to estimate a value of $\bar{S}°$ for $SeCN^-$ from an experimental value of $\bar{V}°$ (see Table 5).

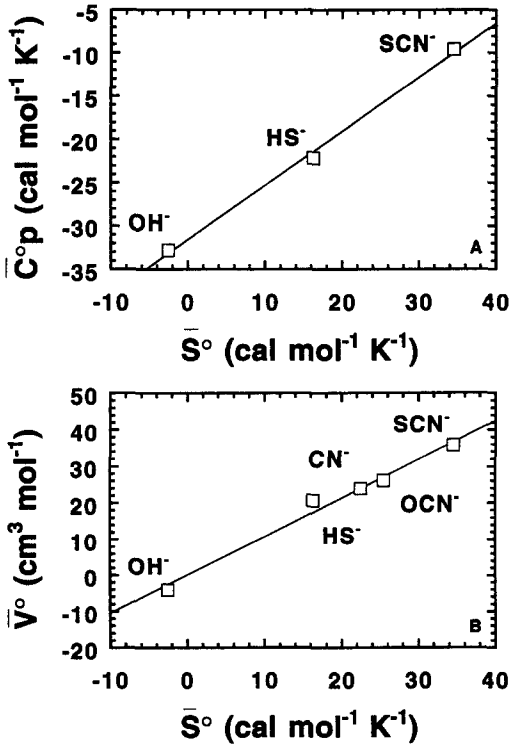

Fig. 14. Correlations of standard partial molal heat capacities and volumes with entropies for several monovalent anions at 25°C and 1 bar, taken from Tables 1 and 5. Lines are given by Eqns. 23 and 24 in text.

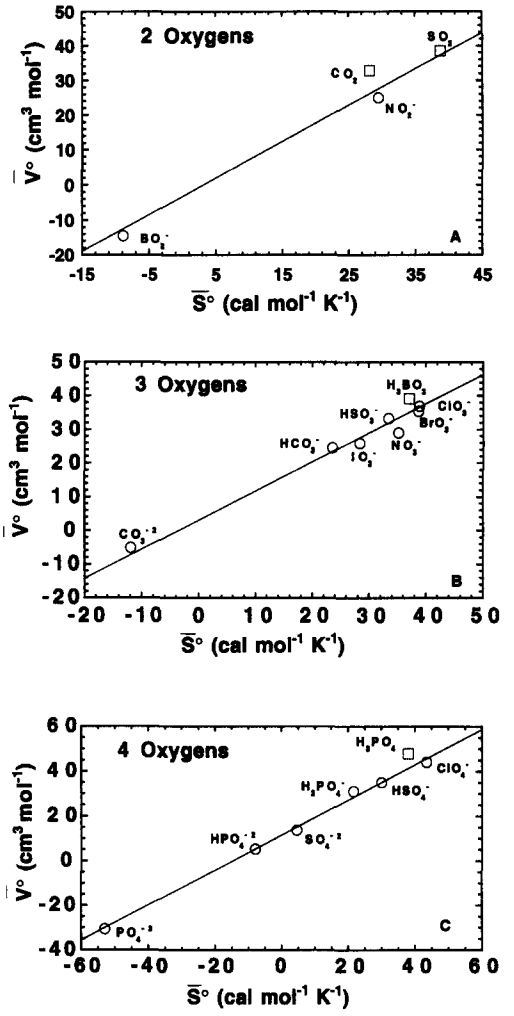

Fig. 15. Correlations of standard partial molal volumes with entropies at 25°C and 1 bar for nonmetal oxygen-bearing species, which depend on the number of oxygen atoms in the species. Experimental data are from Table 1, 4, and 5; lines are consistent with Eqn. 12 and the slopes and intercepts given in the text.

3.3. Correlations for Oxygen-Bearing Anions and Neutral Species

The disparity between experimental and calculated values of log K for reactions involving CrO_4^{-2}, $HCrO_4^-$, and $Cr_2O_7^{-2}$ shown in Fig. 1 arises in part from uncertainties in predictive methods for standard partial molal properties of oxyanions at 25°C and 1 bar adopted by Shock and Helgeson (1988). In the present study, several new correlations were developed in order to decrease the uncertainty attending such predictions. Central to these new correlations is the separation of metal oxygen-bearing aqueous species from nonmetal oxygen-bearing species.[#] In both cases, correlations were found with the number of oxygen atoms in the aqueous species, the charge of the species, and, in some cases,

[#] The term "oxygen-bearing species" is adopted in the present communication to include oxyanions, acid oxyanions, dissolved oxide gases, neutral oxyacid species, and hydroxide complexes (see below).

whether or not the aqueous species contains hydrogen. In constructing the following correlations, B, C, N, P, S, Cl, Br, and I are considered nonmetals, and Mn, Tc, Cr, W, Mo, U, Al, Si, and Re are grouped as metals.

3.3.1. *Nonmetal oxygen-bearing aqueous species*

Correlations between $\bar{V}^\circ$ and $\bar{S}^\circ$ for nonmetallic oxygen-bearing species based on their number of oxygens are shown in Fig. 15a–c. It can be seen in this figure that the correlations include hydrogen-bearing species. The correlation curves given in Fig. 15a–c correspond to Eqn. 12 with the following values of **z** and **y**

Number of oxygens	y	z
2	1.05	−3.3
3	0.87	3.0
4	0.78	11.6

Values of the slopes (**y**) and intercepts (**z**) shown in Fig. 15a–c are correlated with the number of oxygen atoms (#O) in the species as shown in Fig. 16. The correlation lines for the nonmetal oxygen-bearing species shown in Fig. 16 are given by

$$\mathbf{y} = -0.13(\#O) + 1.29 \qquad (25)$$

and

$$\mathbf{z} = 7.2(\#O) - 18.1 \qquad (26)$$

for the slopes and intercepts, respectively. Equations 25 and 26 allow estimates of **y** and **z** for many values of #O. As examples, values for #O = 1 were used to estimate $\bar{V}^\circ$ for ClO^-, BrO^-, and other one-oxygen-bearing species, and those for #O = 7 were used to estimate $\bar{V}^\circ$ for $P_2O_7^{-4}$ and its protonated analogs.

It was found in the present study that correlations involving $\bar{C}_P^\circ$ of nonmetal oxygen-bearing species and either $\bar{V}^\circ$ or $\bar{S}^\circ$ that are based on the number of oxygens lead to greater uncertainty than correlations based on charge. Therefore, the correlations based on charge are presented here and incorporated in the revised correlation algorithm described below. There are remarkably few experimental determinations of $\bar{C}_P^\circ$ for oxygen-bearing aqueous species and it is exceedingly rare to find duplicate studies for the same electrolyte or acid. It is therefore likely that additional experimental work will permit revision of the correlations obtained in the present study.

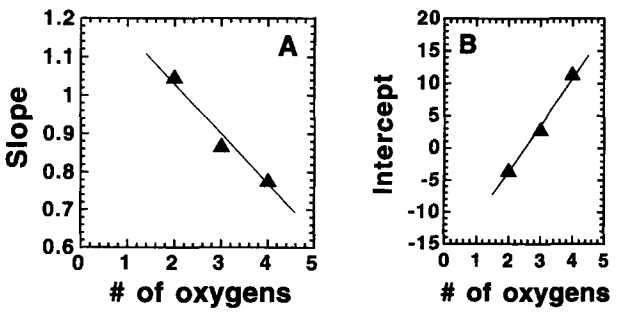

Fig. 16. Slopes and intercepts from correlations of $\bar{V}^\circ$ with $\bar{S}^\circ$ from Fig. 15.

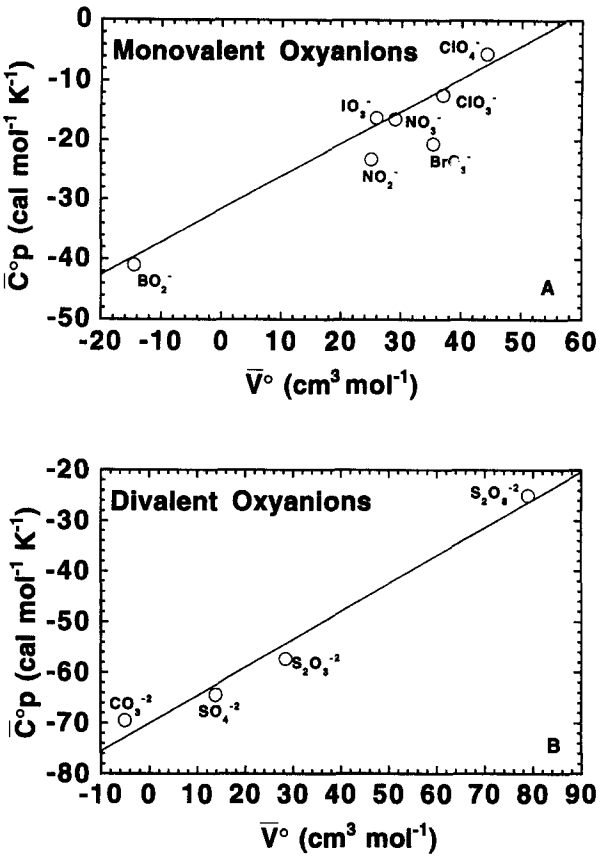

Fig. 17. Correlations between experimental values of $\bar{C}_P^\circ$ and $\bar{V}^\circ$ at 25°C and 1 bar for nonmetal oxygen-bearing monovalent and divalent anions which do not contain hydrogen. Data are taken from Tables 1 and 4. Lines are consistent with Eqn. 15, and values of the slope and intercept are given in the text.

Correlations between $\bar{C}_P^\circ$ and $\bar{V}^\circ$ for nonmetal oxygen-bearing species are shown in Fig. 17 for charges of −1 and −2. The correlation lines shown in these plots are consistent with Eqn. 15 where **x** and **w** correspond to −32. and 0.55 for a charge of −1, and −70. and 0.55 for a charge of −2. Assuming that these two correlations indicate charge independence of the slopes of $\bar{C}_P^\circ$ vs. $\bar{V}^\circ$ correlations for species of this type, and that the difference in intercepts between the $Z_j = -1$ and $Z_j = -2$ correlations can be used to estimate the difference between the $Z_j = -2$ and $Z_j = -3$ correlations, the corresponding values of **x** and **w** for $Z_j = -3$ are −108. and 0.55, respectively. These parameters, together with the value of $\bar{V}^\circ$ for PO_4^{-3} selected by Shock and Helgeson (1988) (−30.6 cm^3 mol^{-1}) yields an estimated value of $\bar{C}_P^\circ$ for PO_4^{-3} of −124.8 cal mol^{-1} K^{-1}. Although this value is about 6 cal mol^{-1} K^{-1} more negative than that obtained by Larson et al. (1982), it is closely consistent with the value predicted from the $\bar{C}_P^\circ$ vs. $\bar{S}^\circ$ correlation described below. Possible reasons for the discrepancy between the value of $\bar{C}_P^\circ$ for PO_4^{-3} adopted in the present study and that advocated by Larson et al. (1982) are discussed below.

Figure 18 contains a plot of $\bar{C}_P^\circ$ vs. $\bar{V}^\circ$ for nonmetal oxy-

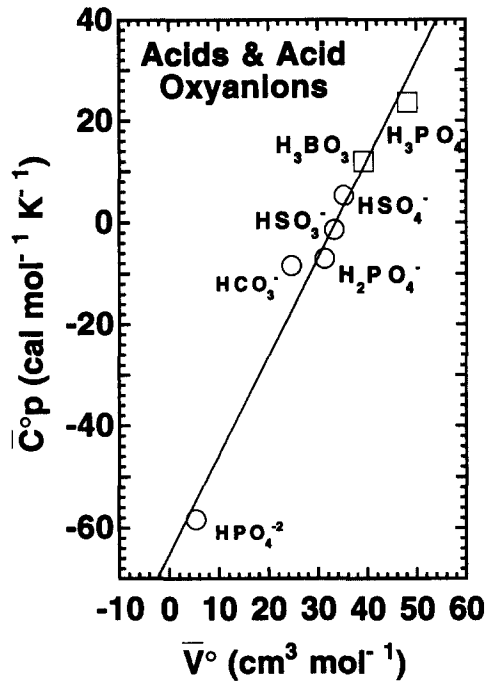

Fig. 18. Correlation between experimental values of $\bar{C}^\circ_P$ and $\bar{V}^\circ$ at 25°C and 1 bar for nonmetal oxygen-bearing species which contain hydrogen (inorganic acids and acid oxyanions). Data are taken from Table 1 (circles) and Shock et al. (1989) (squares). See text for slope and intercept of the line which is consistent with Eqn. 15.

gen-bearing species containing hydrogen. It can be seen that a single correlation line represents the data for acid oxyanions and oxyacid species regardless of charge. It should be emphasized that the correlation in Fig. 18 may be a fortuitous consequence of the relative paucity of experimental data for these types of species. At any rate, the line in Fig. 18 is

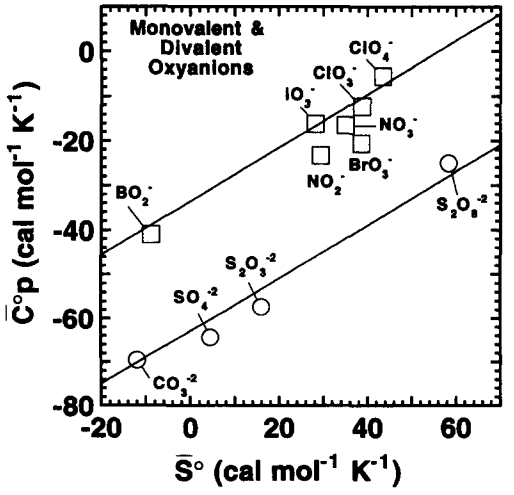

Fig. 19. Correlations of $\bar{C}^\circ_P$ with $\bar{S}^\circ$ at 25°C and 1 bar for nonmetal oxygen-bearing monovalent (squares) and divalent anions (circles) which do not contain hydrogen from data given in Tables 1 and 4. Lines are consistent with Eqn. 18, with slopes and intercepts given in the text.

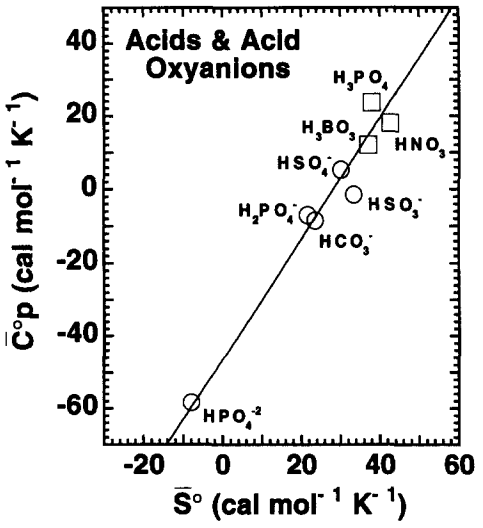

Fig. 20. Correlation of $\bar{C}^\circ_P$ with $\bar{S}^\circ$ at 25°C and 1 bar for nonmetal acid and acid oxyanion species from Table 1 (circles) and Shock et al. (1989) (squares). Line is consistent with Eqn. 18 with slope and intercept given in the text.

consistent with Eqn. 15, where **x** and **w** equal −65.8 and 1.94, respectively.

Correlations of $\bar{C}^\circ_P$ and $\bar{S}^\circ$, analogous to those between $\bar{C}^\circ_P$ and $\bar{V}^\circ$ shown in Figs. 17 and 18, are depicted in Figs. 19 and 20. The correlation lines in these figures are consistent with Eqn. 18 where the parameters **u** and **v** correspond to 0.60 and −33.8 for oxygen-bearing species with $Z_j = -1$, 0.60 and −63.3 for those with $Z_j = -2$, and 1.65 and −46.8 for all acid oxyanions and neutral oxyacid species. As in the case of the charge dependence of the correlations among $\bar{C}^\circ_P$ and $\bar{V}^\circ$, if we assume that **u** is independent of charge, and that the increment in **v** between $Z_j = -3$ and $Z_j = -2$ is the same as that between $Z_j = -2$ and $Z_j = -1$, we obtain values of **u** and **v** for $Z_j = -3$ of 0.60 and −92.8, respectively. Using this correlation for $Z_j = -3$ and the value of $\bar{S}^\circ$ adopted for PO_4^{-3} by Shock and Helgeson (1988) (−3.5 cal mol^{-1} K^{-1}) yields an estimate of −124.6 cal mol^{-1} K^{-1} for $\bar{C}^\circ_P$ of PO_4^{-3}. This value is in close agreement with that estimated from $\bar{V}^\circ$ as described above.

Larson et al. (1982) measured heat capacities of Na_3PO_4 solutions at 25°C and 1 bar and obtained a value of −87.7 cal mol^{-1} K^{-1} for $\bar{C}^\circ_P$ of Na_3PO_4 from which they calculated $\bar{C}^\circ_P$ for PO_4^{-3} equal to −118.6 cal mol^{-1} K^{-1}. These data were re-evaluated by Shock and Helgeson (1988) who obtained $\bar{C}^\circ_P$ for PO_4^{-3} = −114.9 cal mol^{-1} K^{-1}. This difference is directly attributable to different choices of $\bar{C}^\circ_P$ for Na^+. Additional uncertainties arise from the fact that the experimental solutions used by Larson et al. (1982) and coworkers had to be kept at high pH by the addition of NaOH. Problems in resolving the experimental measurements into apparent molal heat capacities of the electrolyte Na_3PO_4 were addressed by explicitly accounting for the degree of dissociation of NaOH and extent of formation of the HPO_4^{-2} ion. Nevertheless, Larson et al. (1982) estimate an uncertainty of ±5 cal mol^{-1} K^{-1} in their $\bar{C}^\circ_P$ for PO_4^{-3}. The value of $\bar{C}^\circ_P$ adopted in the present study for PO_4^{-3} (−124.6 cal mol^{-1}

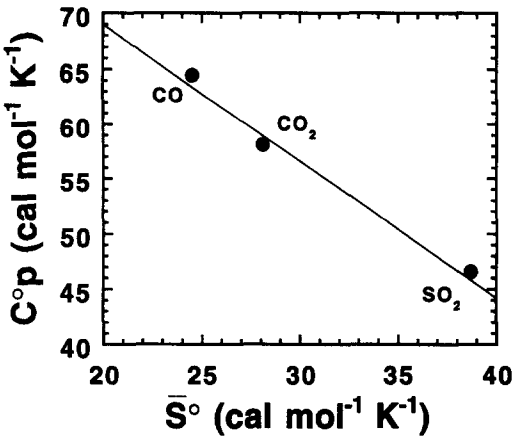

Fig. 21. Correlation of $\bar{C}_P^\circ$ with $\bar{S}^\circ$ at 25°C and 1 bar for dissolved oxygen-bearing gases from data given by Shock et al. (1989) (CO_2 and SO_2) and Shock and McKinnon (1993) (CO).

K^{-1}) is only slightly outside the range of uncertainty claimed by Larson et al. (1982), and is consistent with the correlations among all other experimental data shown in Figs. 18 and 20.

Following the arguments above for estimating **u** and **v** for $Z_j = -3$, and the reasonable degree of success in estimating $\bar{C}_P^\circ$ for PO_4^{-3}, values of **u** and **v** adopted in this study for $Z_j = -4$ are 0.60 and −122.3, respectively, which were used to estimate $\bar{C}_P^\circ$ for $P_2O_7^{-4}$. In contrast, extrapolation to $Z_j = 0$ does not yield a correlation expression consistent with the data for dissolved oxygen-bearing gases shown in Fig. 21, where the correlation line is given by

$$\bar{C}_P^\circ = -1.24\,\bar{S}^\circ + 93.8 \qquad (27)$$

This is to be expected given the vast differences in the interactions between H_2O molecules and ions and that between H_2O molecules and uncharged dissolved gases (see Shock et al., 1989).

3.3.2. *Metal oxygen-bearing aqueous species*

Correlations between $\bar{V}^\circ$ and $\bar{S}^\circ$ for metal oxygen-bearing species are shown in Fig. 22a–d. As in the case of the nonmetal species (see Fig. 15), these correlations are distinguished by the number of oxygen atoms in the aqueous species. However, there is the added complexity in this set of correlations that there are two possibilities for species

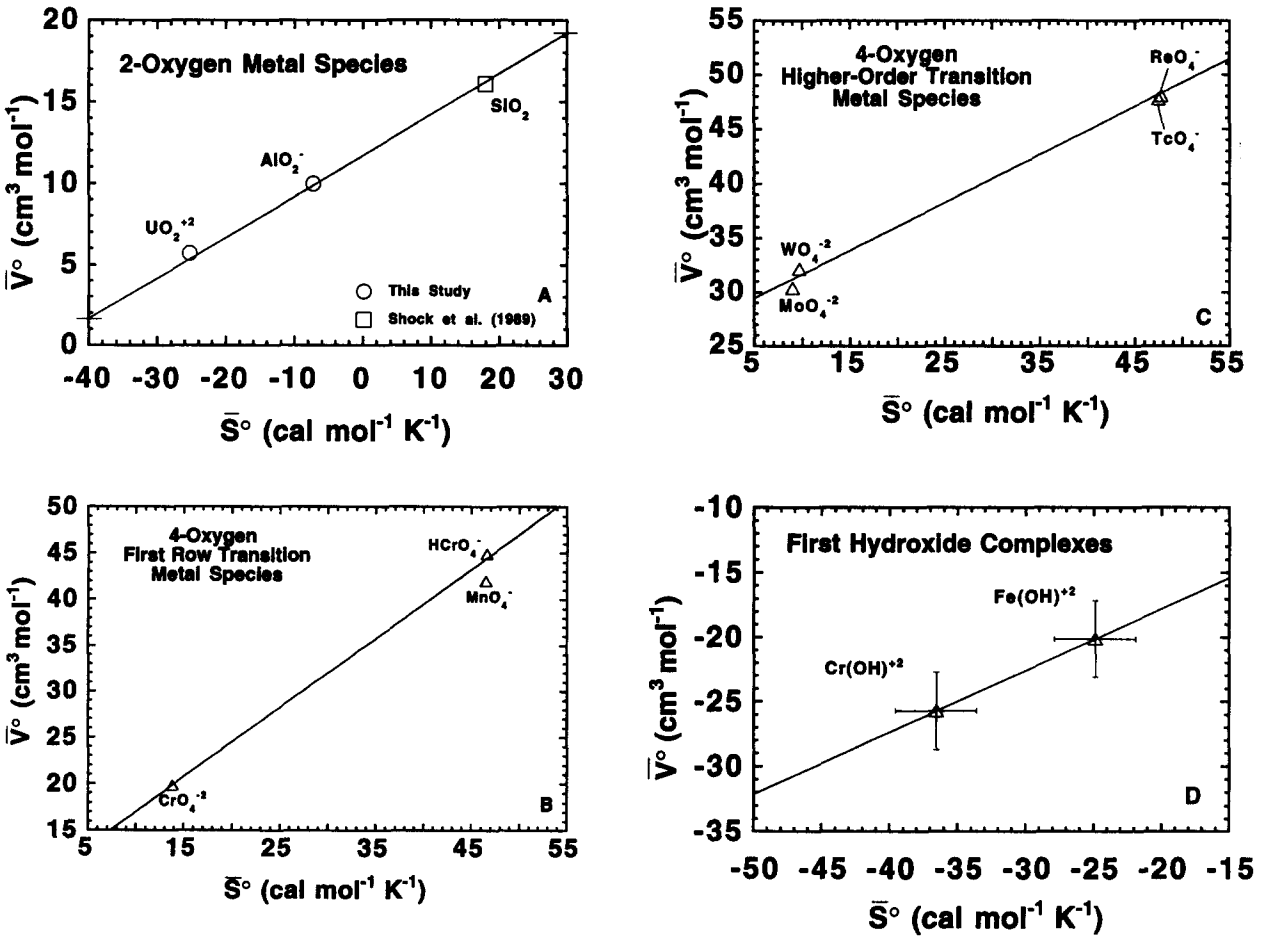

Fig. 22. Correlation plots of $\bar{V}^\circ$ against $\bar{S}^\circ$ at 25°C and 1 bar for metal oxygen-bearing aqueous species constructed with data from Table 4, Shock et al. (1989), and values given in the text. Lines are consistent with Eqn. 12 with slopes and intercepts given in the text. Slope and intercept values are plotted in Fig. 23.

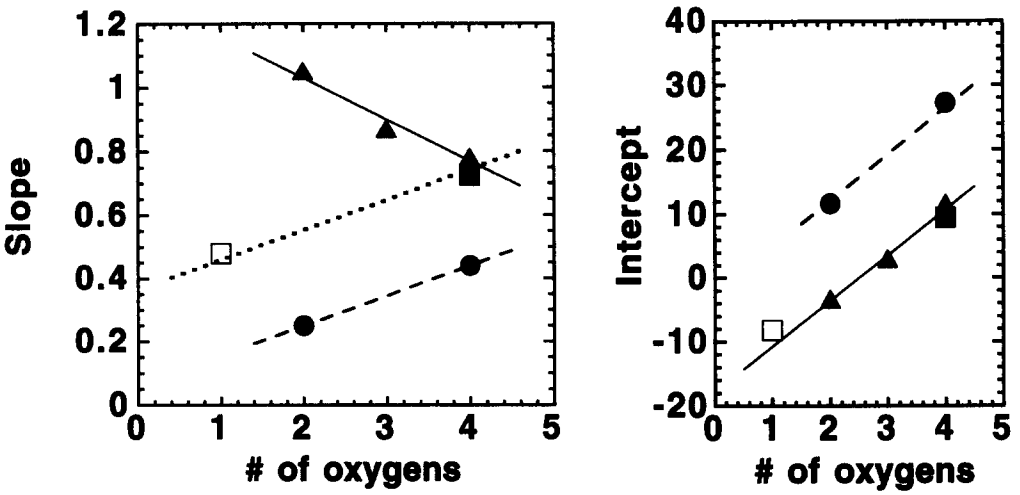

Fig. 23. Slopes and intercepts from correlations of $\bar{V}^\circ$ and $\bar{S}^\circ$ from Fig. 15 (triangles) and Fig. 22 (circles and squares) against the number of oxygen atoms in the species. Solid lines are consistent with Eqns. 25 and 26 which can be used for nonmetal oxygen-bearing aqueous species. Dashed lines are given by Eqns. 28 and 29 and can be used for higher-order transition-metal oxygen-bearing species. The dotted line is given by Eqn. 30 and can be used for first-row-transition-metal oxygen-bearing species.

containing four oxygen atoms. Our interpretation is that the first-row, transition-metal, oxygen-bearing anions and the higher-order transition metal oxyanions fall on different trends. All of the correlation curves in Fig. 22a–c are consistent with Eqn. 12 where **y** and **z** are given by 0.25 and 11.7 for two-oxygen species, 0.44 and 27.3 for four-oxygen species of the higher-order transition elements, and 0.75 and 9.5 for four-oxygen species of the first-row transition elements, respectively. Asano and Le Noble (1978) review two experimental studies which provide values of $\Delta\bar{V}^\circ_r$ for reactions in which metal hydroxide complexes are formed. From these we can calculate values of $\bar{V}^\circ$ for $FeOH^{+2}$ and $CrOH^{+2}$ (-24.9 cm^3 mol^{-1} and -36.6 cm^3 mol^{-1}, respectively). These values are plotted in Fig. 22d against values of $\bar{S}^\circ$ calculated from the values of $\Delta\bar{S}^\circ_r$ for the association reactions given by Smith and Martell (1989) (43 and 44 cal mol^{-1} K^{-1} for the association reactions to form $CrOH^{+2}$ and $FeOH^{+2}$, respectively). Values of **y** and **z** for the correlation curve in Fig. 22 are 0.48 and -8.2, respectively. This observation allows estimates of $\bar{V}^\circ$ for hydroxide complexes as described below.

Slopes and intercepts from Fig. 22 are plotted against number of oxygen atoms (#O) in Fig. 23, together with the slopes and intercepts of the correlations for nonmetal oxygen-bearing species taken from Fig. 16 (triangles). Squares in Fig. 23 indicate values for first-row transition-metal oxygen-bearing species and circles represent higher-order, transition-metal, oxygen-bearing species. The slope and intercept for the one-oxygen first-row transition metal species are shown as open symbols in Fig. 23 as they are constrained by only two data points. In the case of the intercept values plotted in Fig. 23b, it would appear that the one-oxygen and four-oxygen first-row transition-metal species correlate with the nonmetal species. This suggests that Eqn. 26 can be used to estimate intercept values for these species. The intercepts for the higher order transition-metal species appear to be consistent with a parallel correlation indicated by the dashed line. In contrast, the slope for the one-oxygen, first-row, transition-metal species, shown as an open square in Fig. 23a, does not correlate with the nonmetal slopes. There does

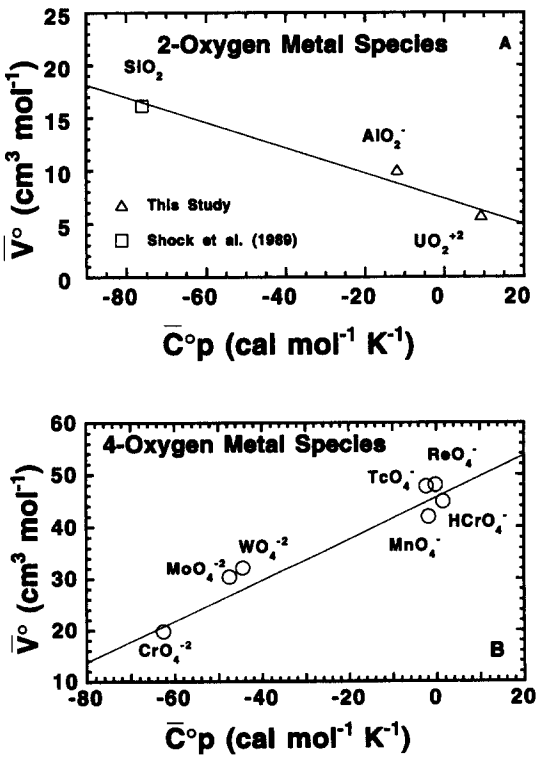

Fig. 24. Correlations between experimental values of $\bar{V}^\circ$ and $\bar{C}^\circ_p$ at 25°C and 1 bar taken from Table 4, and Shock et al. (1989) for metal oxygen-bearing aqueous species. Correlation lines are consistent with Eqn. 15 using slopes and intercepts given in the text.

appear to be a first-row transition-metal correlation among slopes which parallels the corresponding correlation for the higher order transition metal species. The dashed lines in Fig. 23a and b are consistent with

$$y = 0.095(\#O) + 0.06 \quad (28)$$

and

$$z = 7.2(\#O) - 2.3 \quad (29)$$

The dotted line in Fig. 23a, corresponding to a correlation for first row transition cation slopes is drawn parallel to the dashed line and is given by

$$y = 0.095(\#O) + 0.365 \quad (30)$$

Correlations among $\bar{C}^\circ_P$ and $\bar{V}^\circ$ for metal oxygen-bearing species are shown in Fig. 24. The lines in Fig. 24 are consistent with Eqn. 15 and **w** and **x** are given by −0.12 and 7.3 for two-oxygen species and 0.40 and 45.8 for four-oxygen species, respectively. It would be possible to place two parallel correlations through the four-oxygen species in order to separate first-row and higher order transition metals. However, it was decided in the present study that, unlike the relations between $\bar{V}^\circ$ and $\bar{S}^\circ$ shown in Fig. 22, the available experimental values of $\bar{C}^\circ_P$ do not compel the use of two correlations. Additional experimental work may help to clarify this issue.

The plot in Fig. 25 contains correlations of $\bar{C}^\circ_P$ and $\bar{S}^\circ$ for metal oxygen-bearing species. The curves are given by

$$\bar{C}^\circ_P = -2.06\bar{S}^\circ + \mathbf{h} \quad (31)$$

where **h** is given by −34.5 for the lower curve and 95.5 for the upper curve. The reasons for the distribution of data in Fig. 25 are not completely clear. One possible interpretation is that the location of the upper curve reflects the standard molal entropy and heat capacity changes of protonating a metal oxyanion, based on the $CrO_4^{-2}/HCrO_4^-$ and WO_4^{-2}/HWO_4^- pairs shown in Fig. 25. However, it is not evident why MnO_4^-, ReO_4^-, and TcO_4^- fall on or near a correlation which includes acid oxyanions. Nevertheless, similar parallel correlations between $\bar{C}^\circ_P$ and $\bar{S}^\circ$ can be constructed for analogous protonation reactions among hydroxide complexes as discussed below.

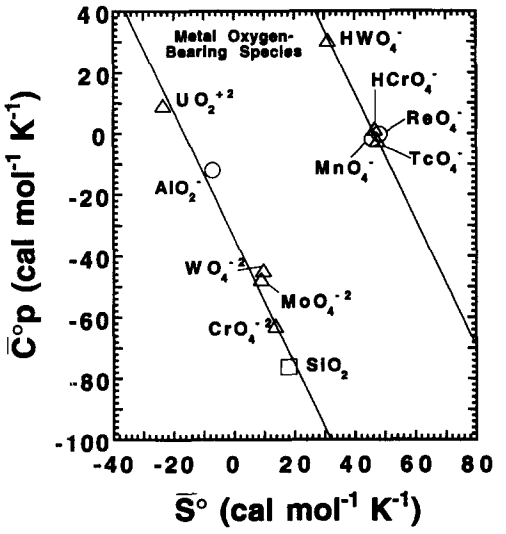

Fig. 25. Correlations of $\bar{C}^\circ_P$ with $\bar{S}^\circ$ at 25°C and 1 bar showing data from Table 4 and Shock et al. (1989) for metal oxygen-bearing species. Lines are consistent with Eqn. 31 using intercept values given in the text.

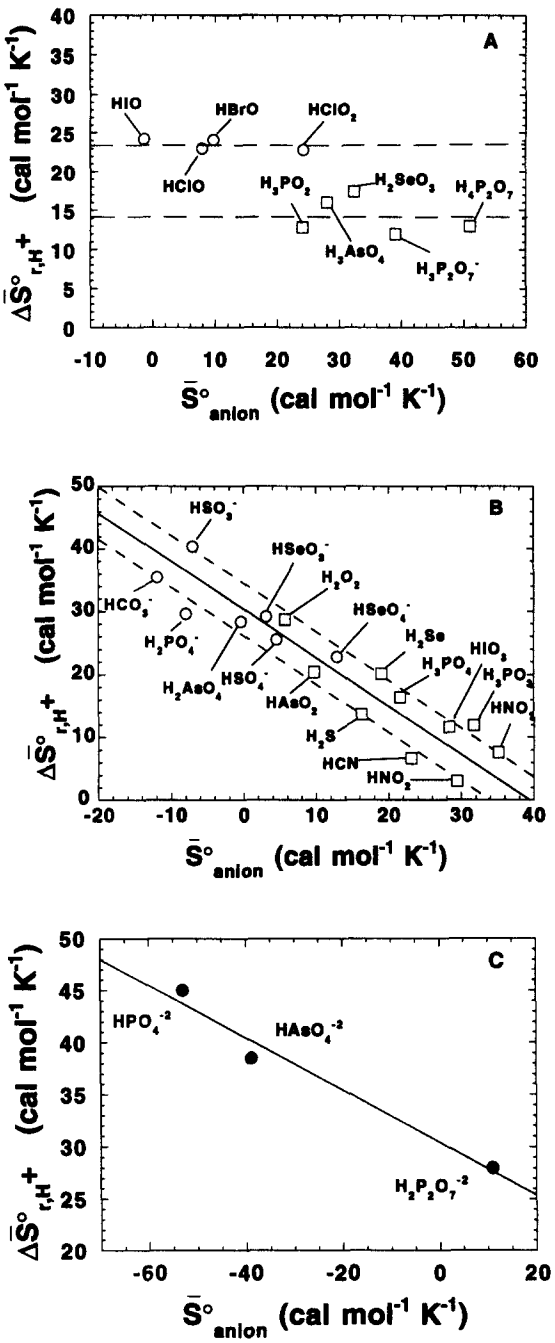

Fig. 26. Correlations of the standard partial molal entropy of association for protonation reactions at 25°C and 1 bar against $\bar{S}^\circ$ values of the anions to which the proton is added. Equations corresponding to the lines are given in the text.

Table 6. Correlation algorithm for estimating standard partial molal volumes and heat capacities of aqueous oxygen-bearing ions at 25°C and 1 bar.[a]

Case 1 — Nonmetal oxygen-bearing species

A. If $\bar{S}^\circ$ and $\bar{V}^\circ$ are known but $\bar{C}p^\circ$ is not, use charge-dependent correlations for hydrogen-free anions (Eqn. 15)

$\bar{C}p^\circ = 0.55\ \bar{V}^\circ - 32.$	for $z_j = -1$	(Fig. 17)
$\bar{C}p^\circ = 0.55\ \bar{V}^\circ - 70.$	for $z_j = -2$	(Fig. 17)
$\bar{C}p^\circ = 0.55\ \bar{V}^\circ - 108.$	for $z_j = -3$	(estimate, see text)

For hydrogen-bearing anions use $\bar{C}p^\circ = 1.94\ \bar{V}^\circ - 65.8$ (Fig. 18)

B. If $\bar{S}^\circ$ is known but $\bar{V}^\circ$ is not, use number-of-oxygen (#O) dependent correlations for $\bar{V}^\circ$(Eqn. 12)

$\bar{V}^\circ = 1.05\ \bar{S}^\circ - 3.3.$	for #O = 2	(Fig. 15A)
$\bar{V}^\circ = 0.87\ \bar{S}^\circ + 3.0.$	for #O = 3	(Fig. 15B)
$\bar{V}^\circ = 0.78\ \bar{S}^\circ + 11.6.$	for #O = 4	(Fig. 14C)

For all other values of #O use combined form of Eqns. (12), (25) and (26)
$\bar{V}^\circ = [-0.13\ (\#O) + 1.29]\ \bar{S}^\circ + 7.2(\#O) - 18.1$ (Fig. 16)

C. If $\bar{S}^\circ$ is known but $\bar{C}p^\circ$ is not, use charge-dependent correlations for hydrogen-free anions

$\bar{C}p^\circ = 0.60\ \bar{S}^\circ - 33.8.$	for $z_j = -1$	(Fig. 19A)
$\bar{C}p^\circ = 0.60\ \bar{S}^\circ - 63.3.$	for $z_j = -2$	(Fig. 19B)
$\bar{C}p^\circ = 0.60\ \bar{S}^\circ - 92.8.$	for $z_j = -3$	(estimated, see text)

For hydrogen-bearing anions use
$\bar{C}p^\circ = 1.65\ \bar{S}^\circ - 46.8.$ (Fig. 20)

Case 2 — Metal oxygen-bearing species

A. If $\bar{S}^\circ$ is known but $\bar{V}^\circ$ is not, use oxygen-number dependent correlations.

All 2-oxygen species:

$\bar{V}^\circ = 0.25\ \bar{S}^\circ + 11.7.$	all 2-oxygen species	(Fig. 22A)

4-oxygen species

$\bar{V}^\circ = 0.75\ \bar{S}^\circ + 9.5.$	for first-row transition metals	(Fig. 22C)
$\bar{V}^\circ = 0.44\ \bar{S}^\circ + 27.3.$	for higher-order transition metals	(Fig. 22B)

4-oxygen species

$\bar{V}^\circ = 0.48\ \bar{S}^\circ - 8.2$	for first-row transition metals	(Fig. 22D)

For other first-row transition metal species

$\bar{V}^\circ = [0.095\ (\#O) + 0.365\ \bar{S}^\circ + 7.2(\#O) - 18.1$ (Fig. 23)

For other higher-order transition metal species
$\bar{V}^\circ = [0.095\ (\#O) + 0.06]\ \bar{S}^\circ + 7.2(\#O) - 2.3$ (Fig. 23)

B. If $\bar{S}^\circ$ is known but $\bar{C}p^\circ$ is not, use correlations in Fig. 24 (Eqn. 31).

For most species
$\bar{C}p^\circ = -2.06\ \bar{S}^\circ - 34.5$ (lower correlation)

For their protonated analogues
$\bar{C}p^\circ = -2.06\ \bar{S}^\circ + 95.5$ (upper correlation)

a. These expressions are based on the empirical correlations shown in various figures in this paper. Therefore, the units are those typically used for these properties ($cm^3\ mol^{-1}$ for $\bar{V}^\circ$, and $cal\ mol^{-1}\ K^{-1}$ for $\bar{S}^\circ$ and $\bar{C}p^\circ$)

3.4. Correlations Among $\bar{S}^\circ$ Values of Aqueous Species

Despite the plethora of standard state thermodynamic data for aqueous species at 25°C and 1 bar, it is occasionally necessary to estimate a value of $\bar{S}^\circ$ for aqueous species in chemical systems which have not been studied extensively by experiments. The wealth of data at 25°C and 1 bar, which allows construction of the correlations among $\bar{V}^\circ$, $\bar{C}^\circ_P$, and $\bar{S}^\circ$ described above, also permit the development of correlation methods for estimating $\bar{S}^\circ$. These correlations are depicted in the diagrams in Fig. 26 where values of the standard partial molal entropies of proton association reactions, $\Delta\bar{S}^\circ_{r,H^+}$, are plotted against values of $\bar{S}^\circ$ of the anion to which the proton is added. It can be seen in Fig. 26a that for some groups of aqueous species $\Delta\bar{S}^\circ_{r,H^+}$ is independent of $\bar{S}^\circ$. In this figure it appears that $\Delta\bar{S}^\circ_{r,H^+}$ is approximately 23 cal mol^{-1} K^{-1} for many oxygenated-halogen acid association reactions, and approximately 14.5 cal mol^{-1} K^{-1} for associa-

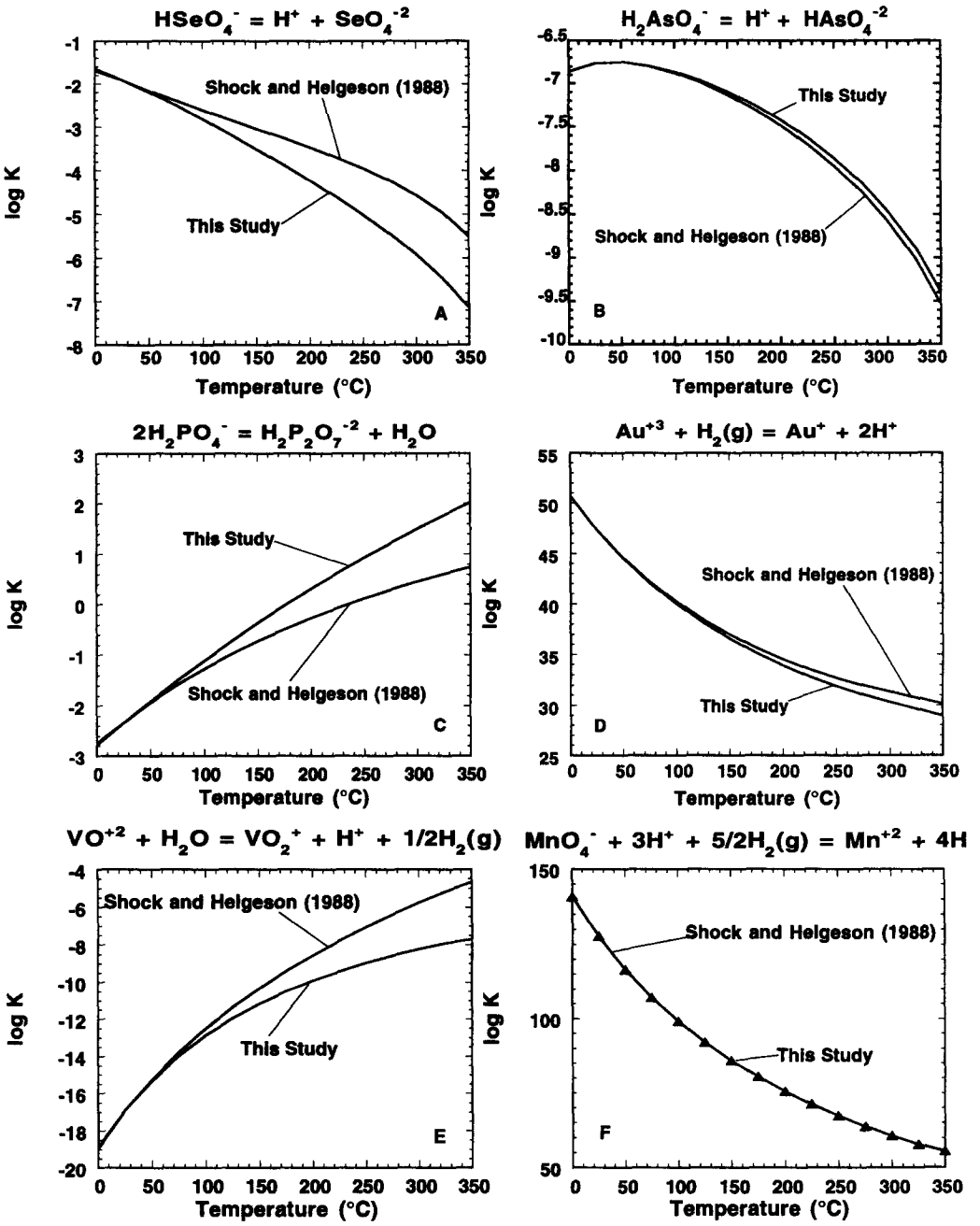

Fig. 27. Comparison of predicted log K values at P_{SAT} for several dissociation, redox and polymerization reactions calculated with data and parameters obtained in this study and those presented by Shock and Helgeson (1988). Differences at 350°C can be as much as three log units, although in general the differences are less. In the case of the reaction shown in plot F, the differences are too small to differentiate at this scale so values from the present study are shown as symbols.

tion reactions which form species bearing unusually oxidized forms of P, As, and Se. This lower correlation was used in this study to estimate values of $\bar{S}^\circ$ for $HS_2O_3^-$, $H_2S_2O_3$, $HS_2O_4^-$, and $H_2S_2O_4$. In contrast, the data plotted in Fig. 26b indicate that there are many species for which values of $\Delta\bar{S}^\circ_{r,H^+}$ differ from those shown in Fig. 26a. Nevertheless, trends are discernable within these arrays. One interpretation of these data yields the correlation shown in Fig. 26b corresponding to

$$\Delta\bar{S}^\circ_{r,H^+} = -0.77\bar{S}^\circ_{anion} + 30.4 \quad (32)$$

The dashed lines indicate an uncertainty envelope of ±4.2 calories around the values estimated with Eqn. 32. This correlation was adopted in the present study to estimate values of $\bar{S}^\circ$ for $HMoO_4^-$, $HNbO_3$, and H_3VO_4.

In contrast to data plotted in Fig. 26a and b which refer to protonation reactions of monovalent and divalent anions, the data plotted in Fig. 26c refer to protonation of trivalent anions represented by the subscript −3. Although these data are severely limited, the dashed correlation is given by

$$\Delta\bar{S}^\circ_{r,H^+} = -0.25(\bar{S}^\circ_{-3}) + 30.4 \quad (33)$$

The same data, recast into a correlation of $\bar{S}^\circ_{-2}$ vs $\bar{S}^\circ_{-3}$, were used in this study to estimate $\bar{S}^\circ$ for VO_4^{-3} from experimental data for HVO_4^{-2}.

The correlations among $\bar{V}^\circ$, $\bar{C}^\circ_P$, and $\bar{S}^\circ$ for oxygen-bearing species shown in Figs. 22–26 were used in the present study to estimate data for several species listed in Table 5. Further application of these correlations for estimating standard state properties should be facilitated with the algorithm outlined in Table 6. If estimates are to be made for hydroxide complexes, the procedure outlined in the next section should be followed.

Examples of predicted equilibrium constants obtained with the revised-HKF equations and new parameters from Tables 4 and 5 are plotted in Fig. 27, together with the corresponding predicted values calculated with parameters from Shock and Helgeson (1988). It can be seen that there are substantial differences for certain dissociation, polymerization, and redox reactions. We believe that the new values will yield new insights into geochemical processes once these data are incorporated into theoretical models. This belief is based on the improvements shown in Figs. 6–8, improved estimates of $\bar{S}^\circ$ for aqueous cations, and the numerous new correlations discussed above and incorporated in the algorithm in Table 6. In many cases these correlations exhibit less scatter than those proposed by Shock and Helgeson

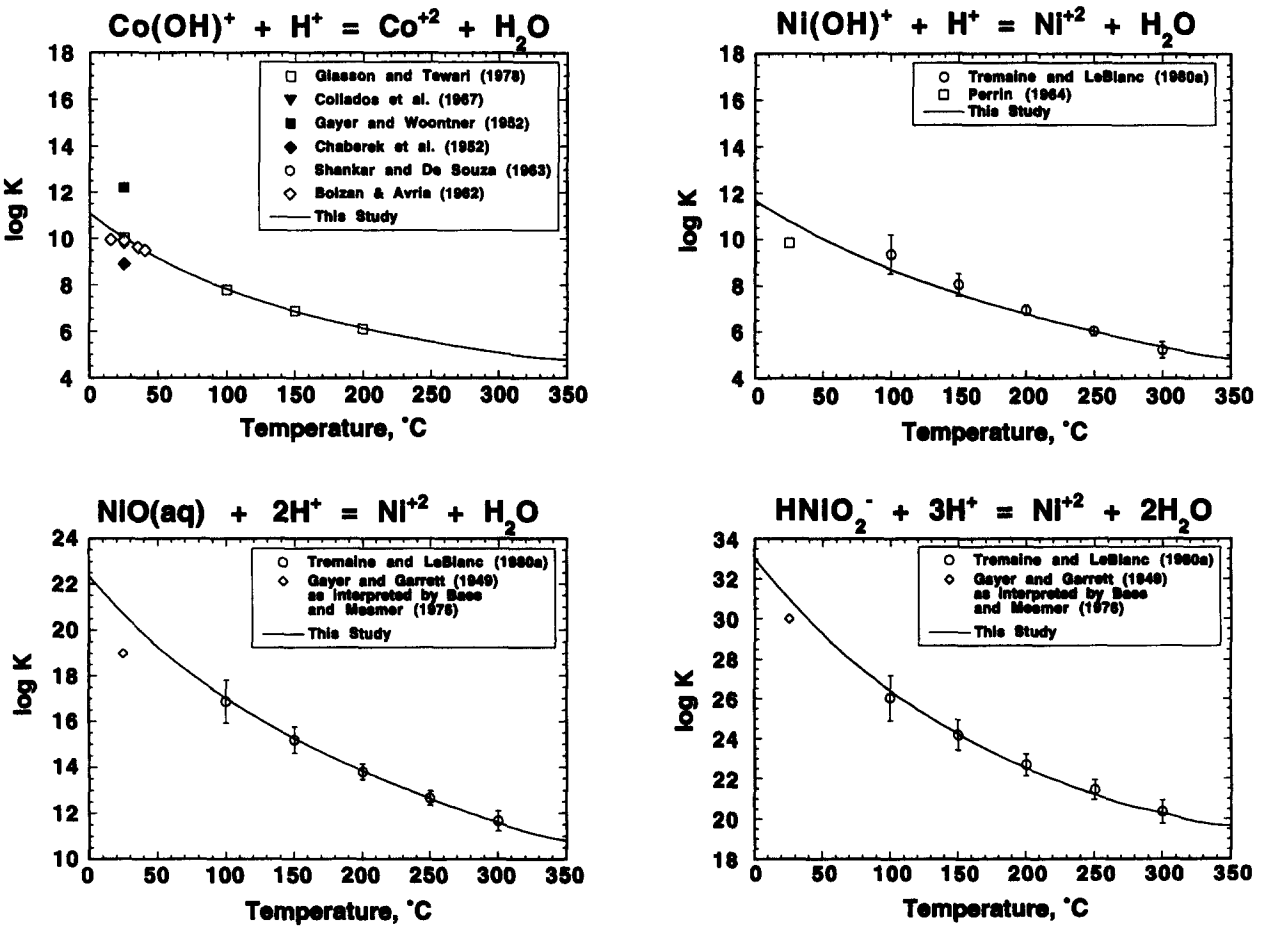

Fig. 28. Experimental (symbols) and calculated (curves) values of log K for Co^{+2} and Ni^{+2} hydrolysis reactions 34 through 37. Data and equation of state parameters consistent with the curves are given in Tables 7 and 10.

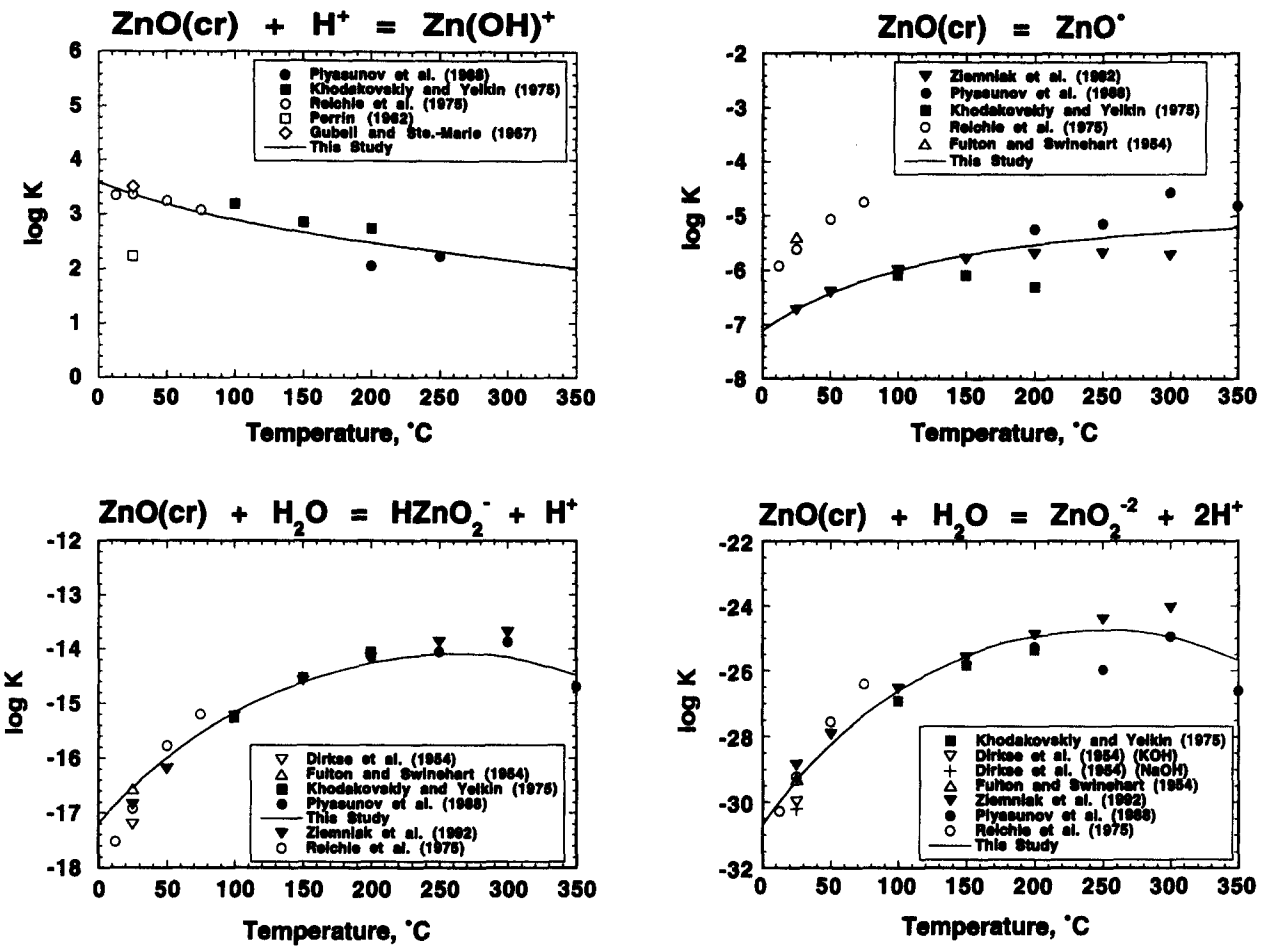

Fig. 29. Experimental (symbols) and calculated (curves) values of log K for Zn^{+2} hydrolysis reactions 38 through 41. The high temperature studies (solid symbols) contain log K values determined from zincite solubility experiments. Many of the lower temperature studies (open symbols) employed solid $Zn(OH)_2$ and the values of log K were evaluated in the present study by combining equilibrium constants for mineral hydrolysis reactions and the dissociation of H_2O with those reported by the investigators. Data and equation of state parameters consistent with the curves are given in Tables 7 and 10.

(1988), and it is likely that the uncertainty attending the use of these new correlations is less than the uncertainty in estimates made with the earlier sets of data and parameters. Further details concerning uncertainties in correlation methods can be found in the discussion by Shock and Helgeson (1988), and those arguments apply, in full, to the present study. Each of the examples in Fig. 27 provides an excellent opportunity for experimental tests of the predictions possible as a result of the present study. Dozens of other equilibria can be calculated with parameters in Tables 1, 4, and 5 that can help with modelling of geochemical processes and design of experimental studies.

4. STANDARD PARTIAL MOLAL PROPERTIES OF HYDROXIDE COMPLEXES

There are hundreds of reports in the literature of experiments which yields values of equilibrium constants for reactions involving metal-hydroxide complexes. The literature through the mid-1970s is summarized by Baes and Mesmer (1976, 1981), who tackled the formidable task of systematically addressing the entire periodic table. As demonstrated by these comprehensive reviews, there are very few determinations of standard partial molal properties or equilibrium constants for hydroxide complexes at temperatures >100°C. This situation persists, despite considerable interest in the myriad geochemical processes involving aqueous fluids that occur at high temperatures and pressures. Despite this lack of directly applicable data, it is possible to detect systematic behavior in the available high-temperature data for hydroxide complexes of Al^{+3} and several divalent metal cations as described here. This systematic behavior can then be used to predict properties for hydroxide complexes of other types of cations. In the present study, high-temperature equilibrium constants for reactions involving hydroxide complexes were regressed for standard partial molal entropies and heat capacities of the complexes at 25°C and 1 bar as described above for the HWO_4^- dissociation reaction. Correlations involving $\bar{S}^\circ$ and $\bar{C}_P^\circ$ of hydroxide complexes were developed to help estimate these properties for the many other metals of geologic interest for which no high-temperature data exist. It should be kept in mind that the regression procedure has

two goals: (1) an adequate representation of the experimental data and (2) construction of correlations for predictive algorithms. Because of this dual purpose, it is likely in some cases that we have accepted fairly large differences between experimental data and calculations, especially at low temperature.

4.1. Regression of Equilibrium Constant Data for Hydroxide Complexes of Divalent Metals

Experimental log K values which extend to temperatures >100°C for reactions involving hydroxide complexes of divalent metal cations are shown by the symbols in Figs. 28–31. The reactions are indicated in the figures and correspond to

$$CoOH^+ + H^+ = Co^{+2} + H_2O \quad (34)$$

$$NiOH^+ + H^+ = Ni^{+2} + H_2O \quad (35)$$

$$NiO + 2H^+ = Ni^{+2} + H_2O \quad (36)$$

$$HNiO_2^- + 3H^+ = Ni^{+2} + 2H_2O \quad (37)$$

$$ZnO_{(cr)} + H^+ = ZnOH^+ \quad (38)$$

$$ZnO_{(cr)} = ZnO \quad (39)$$

$$ZnO_{(cr)} + H_2O = HZnO_2^- + H^+ \quad (40)$$

$$ZnO_{(cr)} + H_2O = ZnO_2^{-2} + 2H^+ \quad (41)$$

$$PbO_{(cr)} + H^+ = PbOH^+ \quad (42)$$

$$PbO_{(cr)} = PbO \quad (43)$$

$$PbO_{(cr)} + H_2O = HPbO_2^- + H^+ \quad (44)$$

$$FeOH^+ + H^+ = Fe^{+2} + H_2O \quad (45)$$

$$FeO + 2H^+ = Fe^{+2} + H_2O \quad (46)$$

$$HFeO_2^- + 3H^+ = Fe^{+2} + 2H_2O \quad (47)$$

where the subscript (cr) refers to the crystalline solid oxide. Note that these reactions do not involve the conventional stepwise hydroxide complex species adopted by Baes and Mesmer (1976, 1981) and many other authors. In the present study a decision was made to treat the conventional hydroxide complexes like other conventional aqueous species such as NH_4OH, H_2CO_3, and H_4SiO_4 whose properties are evaluated from reactions such as

$$NH_3(aq) + H_2O = NH_4OH \quad (48)$$

$$CO_2(aq) + H_2O = H_2CO_3 \quad (49)$$

$$SiO_2(aq) + 2H_2O = H_4SiO_4 \quad (50)$$

and the convention that thermodynamic properties of such reactions are equal to zero (Wagman et al., 1982). Following Wagman et al. (1982) and Shock et al. (1989), H_2O was subtracted from the stoichiometry of the hydroxide complexes whenever possible yielding the species in the reactions above, and the properties of H_2O were subtracted from those of the conventional stepwise hydroxide complex species to yield the properties of the nonconventional species used in the present study. This is largely a pragmatic decision that helps in the construction of correlations and does not, in every case, necessarily reflect the molecular structure of the hydroxide complex.

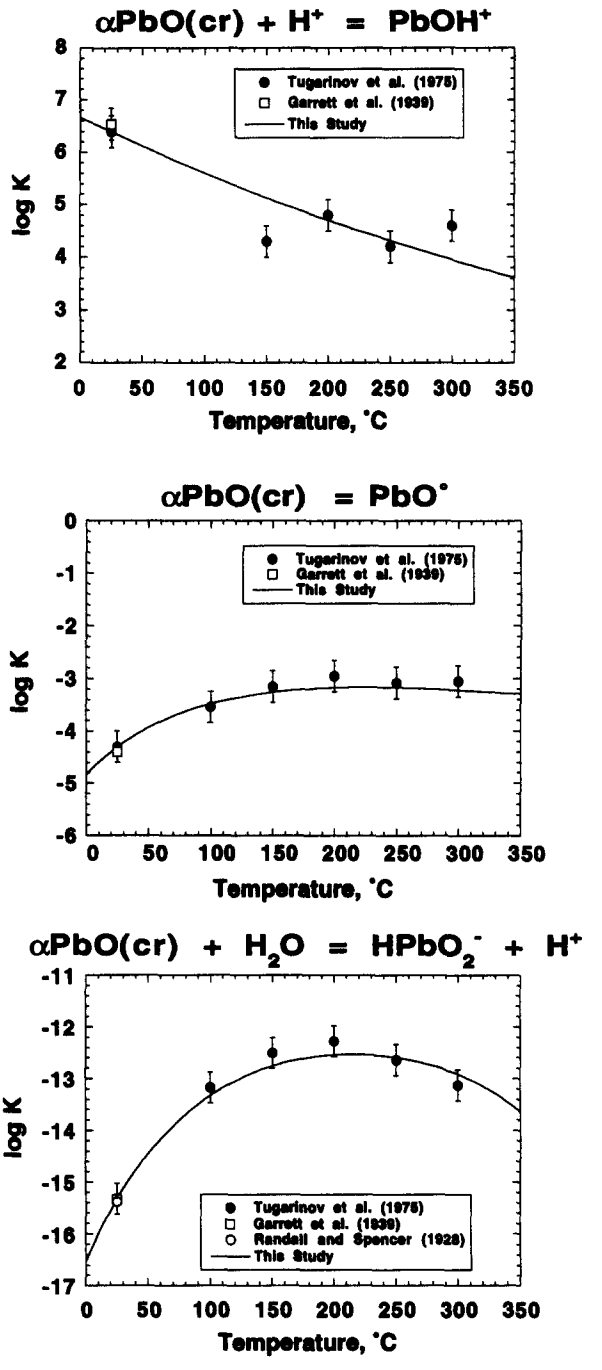

Fig. 30. Experimental (symbols) and calculated (curves) values of log K for Pb^{+2} hydrolysis reactions 42 through 44. Data and equation of state parameters consistent with the curves are given in Tables 7 and 10.

The curves in Figs. 28 through 31 correspond to regression results, and the resulting values of $\Delta\bar{G}^\circ_f$, $\bar{S}^\circ$, and $\bar{C}^\circ_P$ at 25°C and 1 bar are listed in Table 7. Some discussion of these regression results is necessary before moving on to correla-

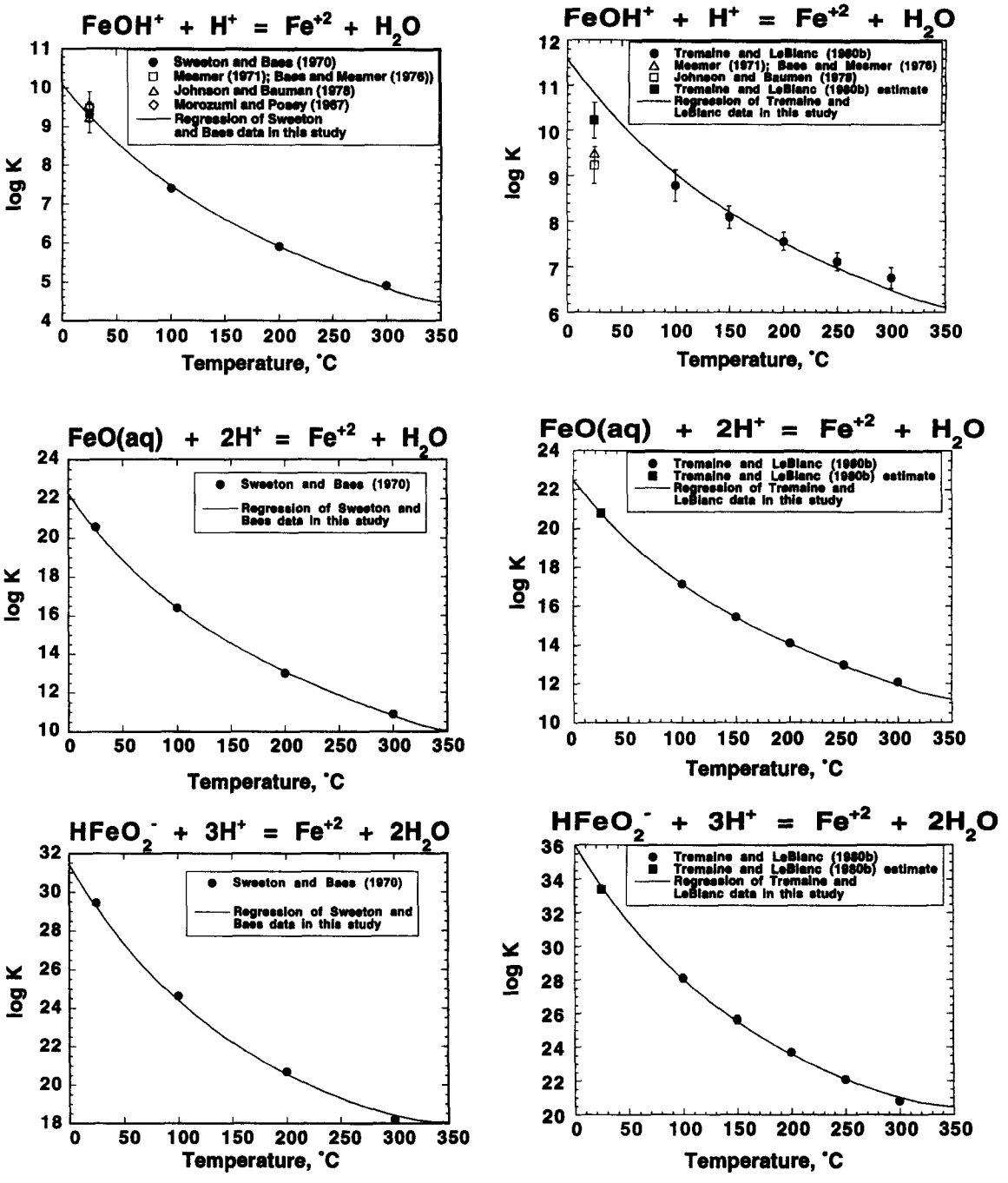

Fig. 31. Experimental (symbols) and calculated (curves) values of log K for Fe^{+2} hydrolysis reactions 45 through 47 from two studies of magnetite solubility (see text). Data consistent with each set of curves are given in Table 7. Data and equation of state parameters consistent with the regression of data from Sweeton and Baes (1970) are given in Table 10.

tions involving the data in Table 7. In several cases ($CoOH^+$, $NiOH^+$, NiO, $HNiO_2^-$, $PbOH^+$, PbO, $HPbO_2^-$) there is a single study at high temperature for the reactions considered, and the regression was constrained to represent those data as closely as possible while allowing the construction of correlations. At the same time, it is amply evident in Figs. 28–31 that there is a considerable range of log K values for some of these reactions at 25°C and 1 bar, and it follows that it is not at all evident that the lone sets of high-temperature data are intrinsically accurate. In fact, in cases where there are several sets of high-temperature data ($ZnOH^+$, ZnO, $HZnO_2^-$, ZnO_2^{-2}, $FeOH^+$, FeO, $HFeO_2^-$, see below) there is considerable disagreement between the various studies. Nevertheless, every attempt has been made to incorporate the available data in the regression process.

The ambiguity in equilibrium constants for reactions in-

Table 7. Summary of standard partial molal properties of nonconventional aqueous hydroxide complexes at 25°C obtained in the present study by regression of experimental data shown in Figures 28-32.

Aqueous Species	ΔG_f°[a]	$\bar{S}^{\circ}$[b]	$\bar{C}p^{\circ}$[b]
$CoOH^+$	-56025.	-10.	24.
$ZnOH^+$	-81190.	15.	10.
$NiOH^+$	-52850.	-18.	31.
$PbOH^+$	-53950.	30.	-20
$FeOH^+$	-65850.[c]	-10.[c]	15.[c]
$FeOH^+$	-63820.[d]	-18.[d]	15.[d]
$AlOH^{+2}$	-165475.	-44.2	13.2
$ZnO(aq)$	-67420.	-2.	-10.
$NiO(aq)$	-39340.	-25.	10.
$PbO(aq)$	-39350.	22.	-42.
$FeO(aq)$	-50720.[c]	-10.[c]	0.[c]
$FeO(aq)$	-50175.[d]	-20.[d]	5.[d]
AlO^+	-158188.	-27.	-30.
$HZnO_2^-$	-110720.	-16.	20.
$HNiO_2^-$	-81980.	-36.	48.
$HPbO_2^-$	-81000.	18.	-70.
$HFeO_2^-$	-95400.[c]	-15.[c]	22.[c]
$HFeO_2^-$	-89540.[d]	-19.[d]	25.[d]
$HAlO_2(aq)$	-207700.	5.	-50.
ZnO_2^{-2}	-93290.	-40.	-15.

a. cal mol^{-1}. b. cal mol^{-1} K^{-1}, the uncertainty in $\bar{S}^{\circ}$ is generally ± 3 cal mol^{-1} K^{-1}, and that in $\bar{C}p^{\circ}$ is generally ± 5 cal mol^{-1} K^{-1}. c. Based on regression of log K data from Sweeton and Baes (1970). d. Based on regression of log K data from Tremaine and LeBlanc (1980b).

volving metal hydroxide complexes is emphasized by a comparison of the two sets of high-temperature data for Fe^{+2}-hydroxide complexes shown in Fig. 30. Both sets of data were obtained from measurements of magnetite solubility in solutions of varying pH, but there is as much as two log units of difference in the derived equilibrium constants for the hydroxide complexes. Possible sources of this uncertainty include characterization of the purity and crystallinity of the magnetite, the degree to which chloride complexing may be involved in the low pH solutions (initial pH set by addition of HCl), the degree of dissociation of NaOH and/or KOH complexes at high temperatures, precipitation of hydroxide solids on magnetite surfaces, and control of the oxidation state. We were unable to quantify the contributions from each of these possible sources based on the available information. Therefore, each set of data was regressed separately and values of $\Delta\bar{G}_f^{\circ}$, $\bar{S}^{\circ}$, and $\bar{C}_P^{\circ}$ obtained from both experimental studies are given in Table 7. A possible resolution of this state of confusion is attempted with the aid of the correlations described below.

4.2. Regression of Equilibrium Constant Data for Hydroxide Complexes of Al^{+3}

Experimental log K values for the reaction,

$$Al^{+3} + H_2O = AlOH^{+2} + H^+ \quad (51)$$

are shown in Fig. 32a, together with a curve which represents the results of regression of these data with the revised-HKF equations and correlation algorithms to obtain the values of $\bar{S}^{\circ}$ and $\bar{C}_P^{\circ}$ at 25°C and 1 bar listed in Table 7. Note that these regression results are dependent on the regression for Al^{+3} and AlO_2^- described above and depicted in Fig. 8. Unlike values of log K_{11}, measurements from Bourcier et al. (1993) for log K_{51} diverge increasingly with increasing temperature from those reported by Castet et al. (1992, 1993). Other disagreement between these two datasets can be observed in other plots in Fig. 32. In the present study it was found that regression of data from Castet et al. (1992, 1993) leads to predictions in the supercritical region which are more closely consistent with mineral solubility data than those obtained from regressing the Bourcier et al. (1993) data. For this reason, regression results in the present study were constrained by the Castet et al. (1992, 1993) data.

Three sets of equilibrium constants corresponding to the reactions

$$Al^{+3} + H_2O = AlO^+ + 2H^+ \quad (52)$$

$$AlOH^{+2} = AlO^+ + H^+ \quad (53)$$

$$AlO^+ + H_2O = AlO_2^- + 2H^+ \quad (54)$$

were regressed simultaneously to obtain values of $\bar{S}^{\circ}$ and $\bar{C}_P^{\circ}$ listed in Table 7 for AlO^+ using the data and parameters for Al^{+3}, AlO_2^-, and $AlOH^+$ outlined above. In the regression, a value for log K_{52} at 25°C and 1 bar was estimated with the method proposed by Sassani and Shock (1997b). It can be seen in Fig. 32b that this independent value is

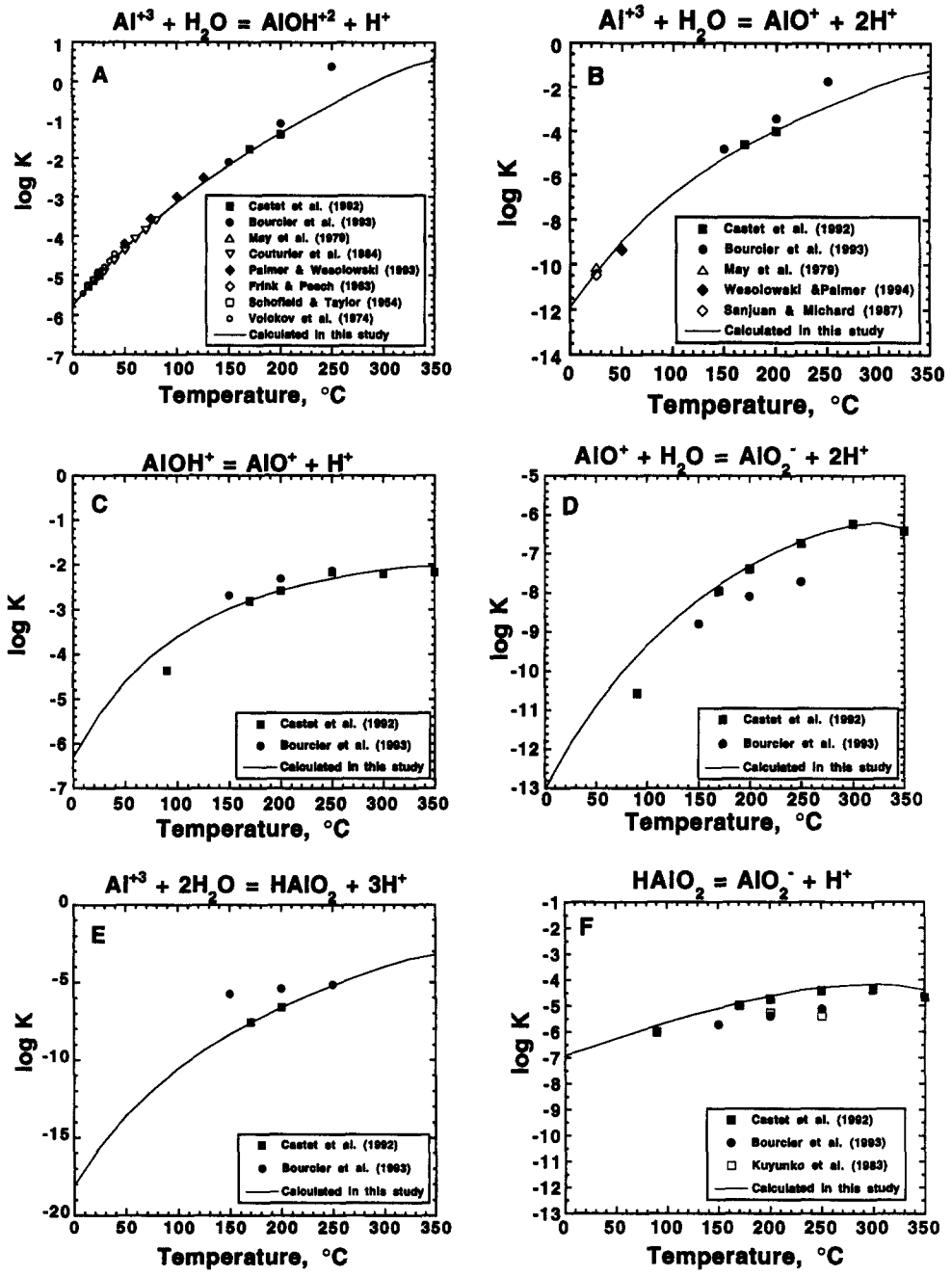

Fig. 32. Experimental (symbols) and calculated (curves) values of log K for Al^{+3} hydrolysis reactions 50 through 55. Data and equation of state parameters consistent with the curves are given in Tables 7 and 10.

nearly an average of the experimental values reported by May et al. (1979) and Sanjuan and Michard (1987). Comparison of regression results with experimental data for reaction 53 and 54 is made in Fig. 32c and d, where it can be seen that there is considerable close agreement with the data from the study of Castet et al. (1992, 1993) which extend to higher temperatures that those for reaction 52.

Regression results for $HAlO_2$ listed in Table 7 depend on a value of the equilibrium constant at 25°C and 1 bar for

$$Al^{+3} + 2H_2O = HAlO_2 + 3H^+ \quad (55)$$

estimated with methods described by Sassani and Shock (1997b). These results are also constrained by the data for reaction 55 at higher temperatures shown in Fig. 32e and for

$$HAlO_2 = AlO_2^- + H^+ \quad (56)$$

shown in Fig. 32f. As in the case of equilibrium constants for reactions 51–54, the regression procedure for reactions involving $HAlO_2$ was guided by the study of Castet et al. (1992, 1993).

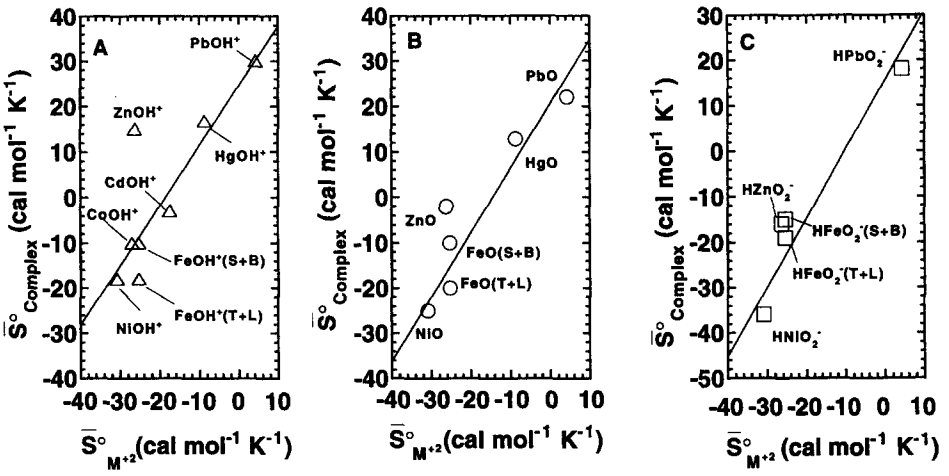

Fig. 33. Correlations of standard partial molal entropies of nonconventional hydroxide complexes (see text) with $\bar{S}^\circ$ values of the corresponding divalent metal cations at 25°C and 1 bar. Data refer to regression results from Table 7, and lines are consistent with Eqn. 57 using parameters given in the text.

The fairly complete set of experimental data for reactions 51–56 at elevated temperatures is a remarkably unique situation for hydrolysis reactions of aqueous trivalent metal cations. The theoretical interpretation allowed by these data, together with the interpretation of data for divalent metal cation hydrolysis described above, permits the construction of an estimation algorithm based on correlations among values of $\bar{S}^\circ$ and $\bar{C}_P^\circ$ of the hydrolyzed metal complexes and $\bar{S}^\circ$ of the metal cations as described in the next section. These methods provide estimates for geochemical calculations which can be used to fill the enormous gaps in experimental data. Many experimental tests of these estimates are called for, and we hope that future developments will enlighten the realm of high-temperature metal hydrolysis and eventually supersede these predicted data.

4.3. Correlations Among Standard Partial Molal Properties of Hydroxide Complex Species at 25°C and 1 Bar

A set of correlations involving $\bar{S}^\circ$ and $\bar{C}_P^\circ$ for hydroxide complex species of divalent metals from Table 7 are shown in Figs. 33 through 36. Some of these correlations are expanded to include hydroxide complexes of metal cations with charges other than +2 in the subsequent discussion. Figure 33 contains a plot of $\bar{S}^\circ$ for divalent metal-hydroxide complex species against $\bar{S}^\circ$ for the divalent metal cations. These correlations are arranged by conventional hydroxide order such that $MOH^+ = 1$, $MO = 2$, and $HMO_2^- = 3$. The values of $\bar{S}^\circ$ for $CdOH^+$, $HgOH^+$, and HgO shown in Fig. 33 were taken from Baes and Mesmer (1981) who indicate that these values of $\bar{S}^\circ$ for divalent metal hydroxide complex species are the only values which come from calorimetric measurements in the literature they reviewed. All other literature values of $\bar{S}^\circ$ for divalent metal hydroxide complex species were obtained from regression of log K values over a range of low temperatures in a manner similar to that used in the present study.

It can be seen in Fig. 33 that the $\bar{S}^\circ$ value for $ZnOH^+$ falls well off of the correlation line constrained by the other first-hydroxide species. The source of this discrepancy is not fully known, although similar peculiarities in $\bar{S}^\circ$ values of chloride

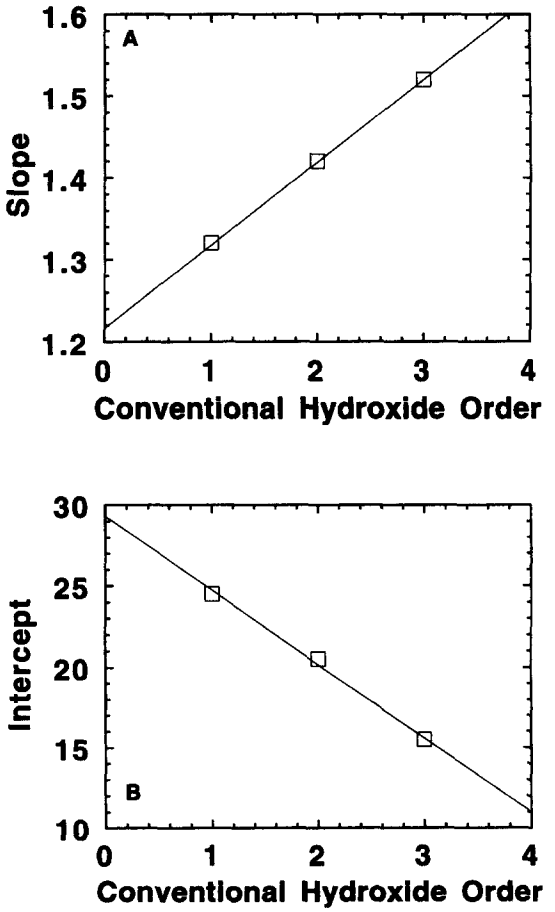

Fig. 34. Correlations of slopes and intercepts of the lines shown in Fig. 33 against conventional hydroxide order. Lines are consistent with Eqns. 58 and 59.

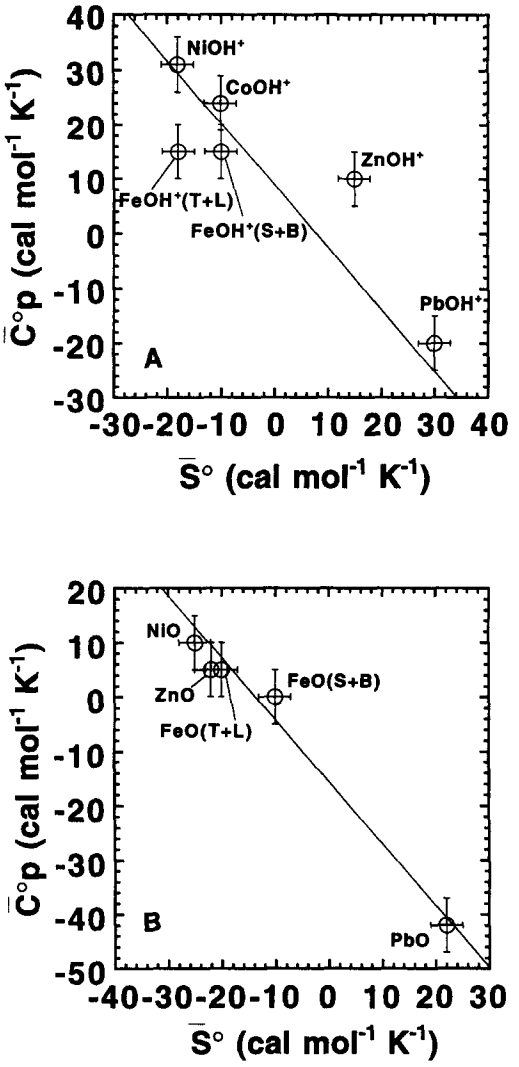

Fig. 35. Correlation of $\bar{C}_P^\circ$ with $\bar{S}^\circ$ at 25°C and 1 bar for nonconventional hydroxide complexes of divalent metal cations using data from Table 7. Lines are consistent with Eqn. 60 using intercept values given in the text.

and acetate complexes of Zn^{+2} are noted by Sverjensky et al. (1996) who suggest that a change in coordination of Zn^{+2} upon complex formation would explain this behavior. Note also that the $\bar{S}^\circ$ value for $FeOH^+$ regressed from the data of Sweeton and Baes (1970) appears more consistent with the correlation shown in Fig. 33 than that obtained from the data reported by Tremaine and LeBlanc (1980b). On the other hand, the value of $\bar{S}^\circ$ for $HFeO_2^-$ from the data of Tremaine and LeBlanc (1980b) falls slightly closer to the corresponding correlation than that obtained from the results of Sweeton and Baes (1970). Finally, the correlation among the MO species splits the difference between the values of $\bar{S}^\circ$ for FeO obtained from these two studies. These observations influenced our recommendations of which data to use in speciation and mass transfer calculations (see below).

The curves in Fig. 33 are given by

$$\bar{S}^\circ_{\text{complex}} = \mathbf{e}\bar{S}^\circ_{M^{+2}} + \mathbf{f} \qquad (57)$$

where **e** and **f** correspond to the following parameters

Conventional Hydroxide Order	e	f
1	1.32	24.5
2	1.42	20.5
3	1.52	15.5

These slopes and intercepts can be correlated with conventional hydroxide order (CHO) as shown in Fig. 34, where the correlation curves are consistent with

$$\mathbf{e} = 0.1(\text{CHO}) + 1.22 \qquad (58)$$

$$\mathbf{f} = -4.6(\text{CHO}) + 29.4 \qquad (59)$$

Equations 58 and 59 allow estimates of **e** and **f** for CHO = 4 of 1.62 and 11.0, respectively. We return to this prediction below. Values of $\bar{S}^\circ$ obtained in this study for the nonconventional hydroxide complexes of Al^{+3} are used below with data from several literature sources to generate correlations which account for the charge dependence of the intercepts of lines such as those shown in Fig. 33.

Values of $\bar{C}_P^\circ$ for the first and second nonconventional hydroxide complexes of divalent metals (MOH^+ and MO) from Table 7 are plotted against corresponding $\bar{S}^\circ$ values in Fig. 35. The parallel correlation curves in Fig. 35 are given by

$$\bar{C}_P^\circ = -1.14\bar{S}^\circ + \mathbf{d} \qquad (60)$$

where **d** corresponds to 9.0 for MOH^+ species and −15.5 for MO species. These parallel curves are offset in much the same manner as the two curves in Fig. 25, and, as in the WO_4^{-2}/HWO_4^- and $CrO_4^{-2}/HCrO_4^-$ pairs in Fig. 25, the species on the upper curve are protonated versions of those on

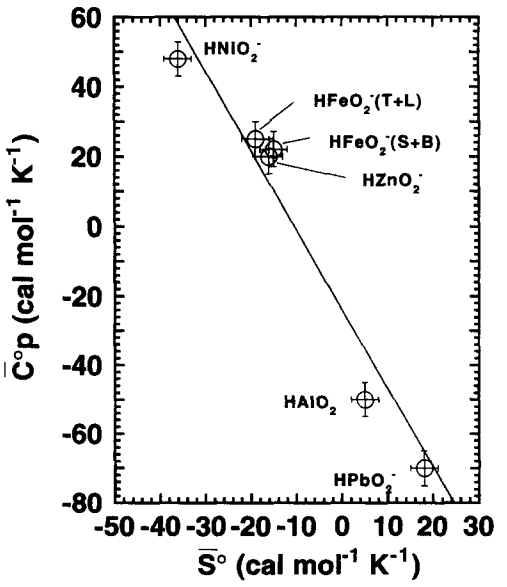

Fig. 36. Correlation of $\bar{C}_P^\circ$ with $\bar{S}^\circ$ at 25°C and 1 bar for nonconventional third hydroxide complexes of divalent metals using regression results from this study given in Table 7. Correlation line is given by Eqn. 61.

Table 8. Summary of $\bar{S}^*$ values at 25°C and 1 bar for nonconventinal aqueous hydroxide complexes based on reaction data reported in the literature.

Complex	$\bar{S}^*$	Complex	$\bar{S}^*$
LiOH(aq)	2.1[b], 1.9[c]	PbO(aq)	3.3[c]
NaOH(aq)	10.4[b], 10.8[c], -22.4[g]	InO^+	-2.6[g]
TlOH(aq)	32.4[b], 32.5[d,e,f]	CrO^+	-4.1[b], -3.1[k]
$BeOH^+$	-9.5[g]	FeO^+	-21.4[g]
$MgOH^+$	-16.6[j], -15.9[g]	TiO^{+2}	-45.7[g]
$CaOH^+$	-3.3[c], -3.5[g], -3.8[d,h], -4.8[f], -5.7[d,e,f]	ZrO^{+2}	-53.4[g]
$SrOH^+$	-2.1[b], -2.5[d,e,f,h]	HfO^{+2}	-46.2[g]
$BaOH^+$	8.7[b], 8.5[d,e,f], 13.3[g], 13.7[h], 18.3[h]	$UO_3(aq)$	-4.6[g]
$MnOH^+$	1.2[b], 0.3[c], 1.0[g]		
$FeOH^+$	-7.8[c], -9.5[c], -5.0[g], -10.9[j]	$HFeO_2^-$	-23.7[k], -16.6[c]
$CoOH^+$	-5.5[c]	$HNiO_2^-$	-56.8[c]
$NiOH^+$	-19.5[c], -11.1[h]	$HZnO_2^-$	-21.9[c]
$ZnOH^+$	-5.7[c], -5.6[g], -3.8[i]	$HPbO_2^-$	0.5[c]
$CdOH^+$	-2.9[c,g], -4.9[c]	$HCuO_2^-$	0.3[g]
$HgOH^+$	16.7[c]		
VOH^+	11.3[g]	ZnO_2^{-2}	-42.9[c]
$SnOH^+$	11.3[g]	CdO_2^{-2}	-20.3[g]
$PbOH^+$	21.3[c]	CuO_2^{-2}	-23.1[g]
$BiOH^{+2}$	-19.5[c]		
$AlOH^{+2}$	-43.8[c], -31.3[j]		
$InOH^{+2}$	-44.7[g]		
$ScOH^{+2}$	-15.7[c], -36.8[g]		
$FeOH^{+2}$	-25.4[c], -18.9[d,e,f], -24.6[e,f], -30.2[g]		
$CoOH^{+2}$	-28.5[c], -36.9[g]		
VOH^{+2}	-10.7[g], -12.1[d]		
$CrOH^{+2}$	-46.1[c], -36.6[b], -36.3[e], -35.6[f]		
UO_2OH^+	4.1[l], 12.8[g]		
UOH^{+3}	-48.3[c], -52.3[c], -52.2[b], -46.9[e,f], -50.2[e,f], -49.9[f], -47.8[l]		
$ThOH^{+3}$	-61.4[c]		
$PuOH^{+3}$	-65.6[c]		
FeO(aq)	-4.3[c], -6.6[k]		
CoO(aq)	-9.8[c]		
NiO(aq)	-37.9[c]		
ZnO(aq)	-14.6[c]		
HgO(aq)	12.8[c], 16.4[f], 22.4[g]		

a. cal mol^{-1} K^{-1}. b. Calculated from $\Delta\bar{S}^*_r$ for the association reaction given by Smith and Martell (1976). c. Calculated from $\Delta\bar{S}^*_r$ for the hydrolysis reaction given by Baes and Mesmer (1981). d. Calculated from $\Delta\bar{S}^*_r$ for the association reaction given by Christensen and Izatt (1983). e. Calculated from $\Delta\bar{S}^*_r$ for the association reaction given by Bjerrum et al. (1958). f. Calculated from $\Delta\bar{S}^*_r$ for the association or hydrolysis reaction given by Sillen and Martell (1964). g. Glushko (1965, 1966, 1968, 1970, 1971, 1972, 1973, 1974, 1978, 1979, 1981, 1982). h. Calculated from $\Delta\bar{S}^*_r$ for the association or hydrolysis reaction given by Sillen and Martell (1971). i. Calculated from $\Delta\bar{S}^*_r$ for the association reaction given by Martell and Smith (1982). j. Calculated from $\Delta\bar{S}^*_r$ for the dissociation reaction given by Helgeson (1969). k. Calculated for $\Delta\bar{S}^*_r$ for the association reaction given by Smith and Martell (1989). l. Grenthe et al. (1992)

the lower curve. An analogous correlation for the HMO_2^- species is shown in Fig. 36 and is given by

$$\bar{C}^\circ_P = -2.28\bar{S}^\circ - 24.0 \qquad (61)$$

The doubling of the slope between the correlations in Fig. 35 and that in Fig. 36 may correspond to the factor of two increase in the number of oxygen atoms in the species. The only MO_2^{-2} species for which values of $\bar{S}^\circ$ and $\bar{C}^\circ_P$ were obtained by regression of log K data in this study is ZnO_2^{-2}. Using these values from Table 7 and assuming a correlation parallel to that shown in Fig. 36 yields

$$\bar{C}^\circ_P = -2.28\bar{S}^\circ - 106.2 \qquad (62)$$

for MO_2^{-2} species.

In the case of the nonconventional hydroxide complexes of Al^{+3}, it was shown above that AlO_2^- plots on the $\bar{C}^\circ_P$ vs. $\bar{S}^\circ$ correlation for metal oxygen-bearing species depicted in Fig. 25. Regression results for $HAlO_2$ are shown in Fig. 35 where it can be seen that $HAlO_2$ plots close to the correlation for other nonconventional versions of the third conventional hydroxide complexes. In the absence of other values of $\bar{C}^\circ_P$ and $\bar{S}^\circ$ for third and fourth hydroxide complexes of trivalent cations, we propose using Eqn. 61 to estimate $\bar{C}^\circ_P$ for nonconventional third hydroxide complexes and Eqn. 31, with $\mathbf{h} = -34.5$, for estimating $\bar{C}^\circ_P$ of nonconventional fourth hydroxide complexes. We have also adopted these correlations for estimating $\bar{C}^\circ_P$ of the nonconventional third and fourth hydroxide complexes of tetravalent cations. In the case of the first and second hydroxide complexes, a decision was made in the present study to use the $\bar{C}^\circ_P$ and $\bar{S}^\circ$ data for $AlOH^{+2}$ and AlO^+ to constrain the intercepts of hypothetical correlations which are parallel to those shown in Fig. 35. As a result, the following expressions

$$\bar{C}^\circ_P = -1.14\bar{S}^\circ - 37.2 \qquad (63)$$

$$\bar{C}^\circ_P = -1.14\bar{S}^\circ - 60.8 \qquad (64)$$

were used in this study to estimate values of $\bar{C}^\circ_P$ for first and nonconventional second hydroxide complexes of trivalent cations, respectively. Note that the intercept of the proposed correlation represented by Eqn. 63 is 46.2 cal mol^{-1} K^{-1} more negative than that given by Eqn. 60 for MOH^+ species

which compares very well with the 45.8 cal mol^{-1} K^{-1} offset in intercepts between Eqn. 64 and that given by Eqn. 60 for *MO* species. In addition to estimates of $\bar{C}_P^\circ$ for hydroxide complexes of trivalent metal cations made in the present study, Eqns. 63 and 64 were used by Haas et al. (1995) to estimate $\bar{C}_P^\circ$ for trivalent rare earth cation complexes, by Sassani and Shock (1997b) to estimate $\bar{C}_P^\circ$ for Rh^{+3} and Ru^{+3} complexes, and by Willis and Shock (1997) to estimate $\bar{C}_P^\circ$ for Ti^{+3} complexes. Until definitive experimental data are generated, we recommend using Eqns. 61–64 to estimate values of $\bar{C}_P^\circ$ for nonconventional counterparts of conventional hydroxide complexes of tetravalent cations as well.

4.4. Charge Dependence of $\bar{S}^\circ$ Correlations

The correlations described above rely on the values of $\bar{S}^\circ$ and $\bar{C}_P^\circ$ for hydroxide complexes of divalent transition metal cations obtained through regression of experimental data. The general lack of experimental data for hydroxide complexes precludes a regression treatment for all metals of geochemical interest. There are, however, numerous values of $\bar{S}^\circ$ reported in the literature for hydroxide complexes of metal cations as summarized in Table 8. Many of these experimentally based values for $\bar{S}^\circ$ were obtained from values of $\Delta\bar{S}_r^\circ$ which were in turn obtained from fitting the distribution of log *K* values for association or hydrolysis reactions over narrow ranges of temperature. In addition, many investigators regress their experimental data without benefit of an equation of state for aqueous species. As a result, there is considerable uncertainty associated with many of the values in Table 8. Nevertheless, it can be seen in Fig. 37 that many of these data are consistent with a postulate that correlations can be constructed which are parallel to that for the first hydroxide complexes of divalent metal cations shown in Fig. 33, which is reproduced in Fig. 37. It can be seen that groups of cations can be distinguished by charge and type of species and that the resulting parallel correlations correspond to

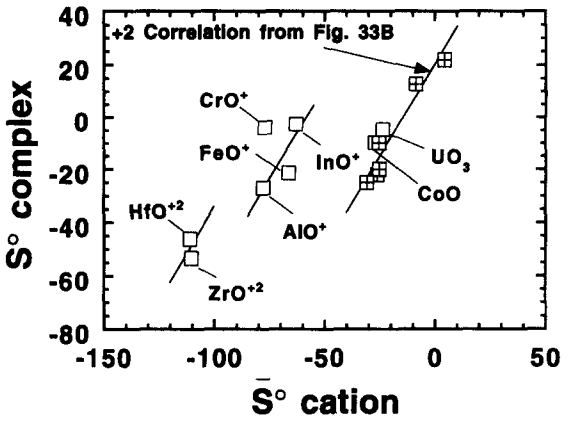

Fig. 38. Plot showing the charge dependence of the type of correlation shown in Fig. 33 for nonconventional second hydroxide complexes of various cations using data from Tables 7 and 8. Lines are consistent with Eqn. 66 using intercepts given in text.

$$\bar{S}^\circ_{MOH^{(Z-1)}} = 1.32\bar{S}^\circ_{M^{+Z}} + \mathbf{b} \qquad (65)$$

where *M* represents any metal cation, *Z* stands for the charge of the metal cation, *M*OH designates the first hydroxide complex, $\bar{S}^\circ_{M^{+Z}}$ refers to the standard molal entropy of the metal cation (taken from Tables 1, 4, or 5), and **b** is given by the following parameters

Cation type	**b**
monovalent cations	−6.0
divalent cations	24.5
trivalent transition metal cations (and Al^{+3})	62.0
other trivalent cations	37.0
tetravalent cations	74.0

Data from Tables 1, 4, 5, 7, and 8 also permit the construction of a set of parallel correlations for the $MO^{(Z-2)}$ species as shown in Fig. 38. In this case there are many fewer data with which to work. The correlations in Fig. 38 are given by

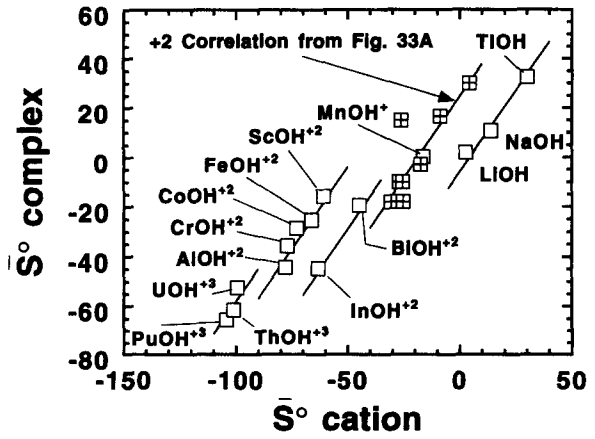

Fig. 37. Plot showing the charge dependence of the type of correlation shown in Fig. 33 for first hydroxide complexes of various cations using data from Tables 7 and 8. Lines are consistent with Eqn. 65 using intercepts given in text.

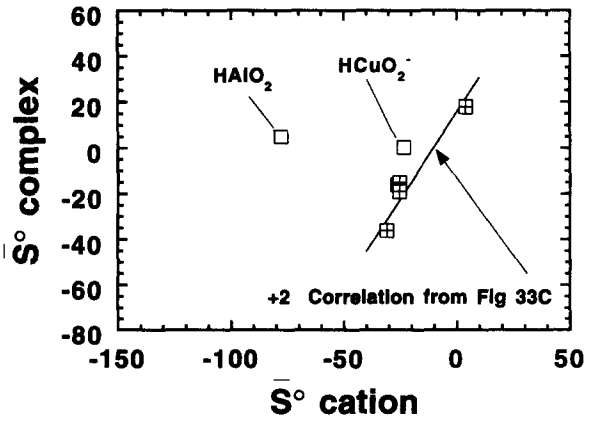

Fig. 39. Plot showing the charge dependence of the type of correlation shown in Fig. 33 for nonconventional third hydroxide complexes of various cations using data from Tables 7 and 8. Line is consistent with Eqn. 57 using intercepts given in text.

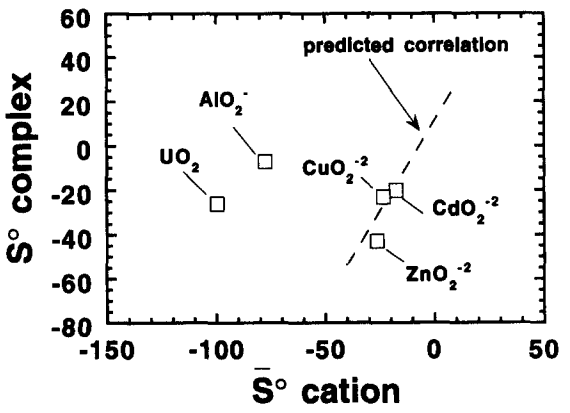

Fig. 40. Plot showing the charge dependence of the type of correlation shown in Fig. 33 for nonconventional fourth hydroxide complexes of various cations using data from Tables 7 and 8. Predicted dashed line is consistent with Eqns. 57, 58, and 59, using CHO = 4.

$$\bar{S}^\circ_{MO^{(Z-2)}} = 1.42\bar{S}^\circ_{M^{+Z}} + \mathbf{a} \qquad (66)$$

where $MO^{(Z-2)}$ designates the nonconventional second hydroxide complex, and values of **a** correspond to

Species	a
divalent cations	20.5
all trivalent cations	78.0
tetravalent cations	108.0 .

Until there are more experimental data, the strongest case for the correlations shown in Fig. 38 is made by analogy to those shown in Fig. 37.

In the case of the $HMO_2^{(Z-3)}$ species, a correlation can only be constructed for the divalent transition metals shown in Fig. 33c, and reproduced in Fig. 39, together with the values for $HAlO_2$ and $HCuO_2^-$ found in Tables 7 and 8. If we assume that slopes parallel to that for divalent metals are appropriate for other cation types, as appears to be the case for $MOH^{(Z-1)}$ and $MO^{(Z-2)}$ species, we can use the value of $\bar{S}^\circ$ for $HAlO_2$ obtained above to constrain an intercept of 123 for trivalent cations. It can be seen in Fig. 40 that there is fairly close agreement between experimental values and the predicted correlation for nonconventional fourth hydroxide complexes of divalent metals obtained from Eqns. 57–59 as described above. Again, by assuming parallel slopes, we can use the value of $\bar{S}^\circ$ for AlO_2^- to constrain an intercept of 118 for trivalent cations and that for UO_2 from Shock et al. (1997b) to obtain an intercept of 135 for tetravalent cations. First approximations for $\bar{S}^\circ$ values of nonconventional third and fifth hydroxide complexes of tetravalent metal ions of interest to geochemistry were made with the correlation shown in Fig. 41 which allows estimates for intercept values of $\bar{S}^\circ$ correlations. Until experimental data are collected to examine directly the process of metal hydroxide complex formation at elevated temperatures, we recommend making estimates with the expressions listed in Table 9 which are consistent with all of the regression results described above, as well as the plots shown in Figs. 37 through 41. The algorithm in Table 9 can be combined with algorithms proposed by Shock and Koretsky (1993, 1995) and Sverjensky et al. (1997) to estimate the data necessary to evaluate speciation of metals in fluids containing a wide variety of organic and inorganic ligands.

4.5. The Hydroxide Correlation Algorithm

The correlations described above for metal hydroxide complex species are summarized in the algorithm listed in Table 9. The available data for standard molal volumes of hydroxide complexes are reviewed above, and there were no such data found in the present study for hydroxide complexes of divalent metal cations. As a first approximation, therefore, we have adopted the correlations between $\bar{V}^\circ$ and $\bar{S}^\circ$ shown in Fig. 22 together with predicted correlations for other numbers of oxygen atoms obtained with Fig. 23 and Eqns. 26 and 28 through 31. In the present study, the algorithm in Table 9 was followed in order to predict many of the values of standard partial molal properties for nonconventional metal-hydroxide species listed in Table 10. A few of the values in Table 10 are referenced to regression results listed in Table 7. Note that the data and parameters for Fe^{+2}-hydroxide complexes listed in Table 10 are those obtained from regression of the Sweeton and Baes (1970) experiments. This decision was influenced, in part, by the correlations shown in Figs. 33, 35, and 36.

4.6. Comparison of Predicted and Experimental Log *K* Values at High Temperatures

It is intended that using the algorithm in Table 9 will minimize uncertainty at high temperatures and pressures in predicted thermodynamic data for aqueous hydroxide complexes of many cations of geochemical interest. Confirma-

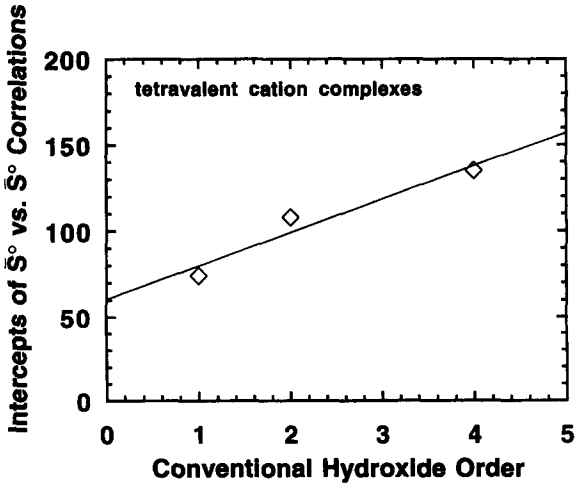

Fig. 41. Plot of intercepts of possible correlation lines for tetravalent cation correlations estimated as described in the text, against conventional hydroxide order. Intercepts estimated with this plot are given in the text and used to estimate values of $\bar{S}^\circ$ for some nonconventional third and fifth hydroxide complexes given in Table 10.

Table 9. Summary of correlations for estimating standard partial molal entropies, heat capacities and volumes of aqueous hydroxide complexes at 25°C and 1 bar.[a]

Complexes of Monovalent Cations (M^{+})

First (MOH)
$\bar{S}^{\circ}_{complex} = 1.32\,\bar{S}^{\circ}_{cation} - 6.$
$\bar{C}^{\circ}_{p,complex} = -1.14\,\bar{S}^{\circ}_{complex} + 9.$
$\bar{V}^{\circ}_{complex}$ calculated with methods proposed by Sverjensky et al. (1997) for first complexes of metal cations

Second (MO^{-}) [b]
$\bar{S}^{\circ}_{complex} = 1.42\,\bar{S}^{\circ}_{cation} - 11.$
$\bar{C}^{\circ}_{p,complex} = -1.14\,\bar{S}^{\circ}_{complex} - 15.5$
$\bar{V}^{\circ}_{complex} = 0.45\,\bar{S}^{\circ}_{complex} - 12.$

Complexes of Divalent Cations (M^{+2})

First (MOH^{+})
$\bar{S}^{\circ}_{complex} = 1.32\,\bar{S}^{\circ}_{cation} + 24.5$
$\bar{C}^{\circ}_{p,complex} = -1.14\,\bar{S}^{\circ}_{complex} + 9.$
$\bar{V}^{\circ}_{complex} = 0.45\,\bar{S}^{\circ}_{complex} - 12.$ (transition metals)
$\bar{V}^{\circ}_{complex} = 0.16\,\bar{S}^{\circ}_{complex} + 4.9$ (alkaline earths)

Second (MO)
$\bar{S}^{\circ}_{complex} = 1.42\,\bar{S}^{\circ}_{cation} + 20.5$
$\bar{C}^{\circ}_{p,complex} = -1.14\,\bar{S}^{\circ}_{complex} - 15.5$
$\bar{V}^{\circ}_{complex} = 0.45\,\bar{S}^{\circ}_{complex} - 12.$ (transition metals)
$\bar{V}^{\circ}_{complex} = 0.16\,\bar{S}^{\circ}_{complex} + 4.9$ (alkaline earths)

Third (HMO_2^{-})
$\bar{S}^{\circ}_{complex} = 1.52\,\bar{S}^{\circ}_{cation} + 15.5$
$\bar{C}^{\circ}_{p,complex} = -2.28\,\bar{S}^{\circ}_{complex} - 24.0$
$\bar{V}^{\circ}_{complex} = 0.54\,\bar{S}^{\circ}_{complex} - 4.8$ (transition metals)
$\bar{V}^{\circ}_{complex} = 0.25\,\bar{S}^{\circ}_{complex} + 11.7$ (alkaline earths)

Fourth (MO_2^{-2})
$\bar{S}^{\circ}_{complex} = 1.62\,\bar{S}^{\circ}_{cation} + 11.$
$\bar{C}^{\circ}_{p,complex} = -2.28\,\bar{S}^{\circ}_{complex} - 106.2$
$\bar{V}^{\circ}_{complex} = 0.54\,\bar{S}^{\circ}_{complex} - 4.8$ (transition metals)
$\bar{V}^{\circ}_{complex} = 0.25\,\bar{S}^{\circ}_{complex} + 11.7$ (alkaline earths)

Complexes of Trivalent Cations (M^{+3})

First (MOH^{+2})
$\bar{S}^{\circ}_{complex} = 1.32\,\bar{S}^{\circ}_{cation} + 37.$ (Ga, In, Tl, Bi)
$\bar{S}^{\circ}_{complex} = 1.32\,\bar{S}^{\circ}_{cation} + 62.$ (all others)
$\bar{C}^{\circ}_{p,complex} = -1.14\,\bar{S}^{\circ}_{complex} - 37.2$
$\bar{V}^{\circ}_{complex} = 0.45\,\bar{S}^{\circ}_{complex} - 12.$ (1st row transition metals)
$\bar{V}^{\circ}_{complex} = 0.16\,\bar{S}^{\circ}_{complex} + 4.9$ (all others)

Second (MO^{+})
$\bar{S}^{\circ}_{complex} = 1.42\,\bar{S}^{\circ}_{cation} + 83.$
$\bar{C}^{\circ}_{p,complex} = -1.14\,\bar{S}^{\circ}_{complex} - 60.8$
$\bar{V}^{\circ}_{complex} = 0.45\,\bar{S}^{\circ}_{complex} - 12.$ (1st row transition metals)
$\bar{V}^{\circ}_{complex} = 0.16\,\bar{S}^{\circ}_{complex} + 4.9$ (all others)

Third (HMO_2)
$\bar{S}^{\circ}_{complex} = 1.52\,\bar{S}^{\circ}_{cation} + 123.$
$\bar{C}^{\circ}_{p,complex} = -2.28\,\bar{S}^{\circ}_{complex} - 24.0$
$\bar{V}^{\circ}_{complex} = 0.54\,\bar{S}^{\circ}_{complex} - 4.8$ (1st row transition metals)
$\bar{V}^{\circ}_{complex} = 0.25\,\bar{S}^{\circ}_{complex} + 11.7$ (all others)

Fourth (MO_2^{-})
$\bar{S}^{\circ}_{complex} = 1.62\,\bar{S}^{\circ}_{cation} + 118.$
$\bar{C}^{\circ}_{p,complex} = -2.06\,\bar{S}^{\circ}_{complex} - 34.5$
$\bar{V}^{\circ}_{complex} = 0.54\,\bar{S}^{\circ}_{complex} - 4.8$ (1st row transition metals)
$\bar{V}^{\circ}_{complex} = 0.25\,\bar{S}^{\circ}_{complex} + 11.7$ (all others)

Table 9. (Continued)

Complexes of Tetravalent Cations (M^{+4})

First (MOH^{+3})
$\bar{S}^{\circ}_{complex} = 1.32\,\bar{S}^{\circ}_{cation} + 74.$
$\bar{C}^{\circ}_{p,complex} = -1.14\,\bar{S}^{\circ}_{complex} - 37.2$
$\bar{V}^{\circ}_{complex} = 0.16\,\bar{S}^{\circ}_{complex} + 4.9$

Second (MO^{+2})
$\bar{S}^{\circ}_{complex} = 1.42\,\bar{S}^{\circ}_{cation} + 108.$
$\bar{C}^{\circ}_{p,complex} = -1.14\,\bar{S}^{\circ}_{complex} - 60.8$
$\bar{V}^{\circ}_{complex} = 0.16\,\bar{S}^{\circ}_{complex} + 4.9$

Third (HMO_2^{+})
$\bar{S}^{\circ}_{complex} = 1.52\,\bar{S}^{\circ}_{cation} + 140.$
$\bar{C}^{\circ}_{p,complex} = -2.28\,\bar{S}^{\circ}_{complex} - 24.0$
$\bar{V}^{\circ}_{complex} = 0.25\,\bar{S}^{\circ}_{complex} + 11.7$

Fourth (MO_2)
$\bar{S}^{\circ}_{complex} = 1.62\,\bar{S}^{\circ}_{cation} + 135.$
$\bar{C}^{\circ}_{p,complex} = -2.06\,\bar{S}^{\circ}_{complex} - 34.5$
$\bar{V}^{\circ}_{complex} = 0.25\,\bar{S}^{\circ}_{complex} + 11.7$

Fifth (HMO_3^{-})
$\bar{S}^{\circ}_{complex} = 1.72\,\bar{S}^{\circ}_{cation} + 130.$
$\bar{C}^{\circ}_{p,complex} = -2.28\,\bar{S}^{\circ}_{complex} - 24.0$
$\bar{V}^{\circ}_{complex} = 0.35\,\bar{S}^{\circ}_{complex} + 19.3$

a. These expressions are based on the empirical correlations shown in various figures in the paper. Therefore, the units are those typically associated with these properties (cal mol^{-1} K^{-1} for $\bar{S}^{\circ}$ and $\bar{C}p^{\circ}$, and cm^3 mol^{-1} for $\bar{V}^{\circ}$). b. The intercept value for this entropy was obtained from the intercept of the MOH correlation by analogy to the difference in intercepts for divalent cation correlations.

tion comes through comparison of predicted data with experimental studies, which is possible in a few cases described in this section. We suspect that additional experimental studies will lead to substantial improvements in the predictive methods described above.

Recently, equilibrium constants for the reaction

$$Mg^{+2} + H_2O = MgOH^{+} + H^{+} \qquad (67)$$

were reported by Wesolowski et al. (1996) at elevated temperatures, and these data are shown as symbols in Fig. 42. The curve in Fig. 42 corresponds to values predicted in the present study using the estimated data and parameters for $MgOH^{+}$ listed in Table 10. Similar close agreement between predicted and experimental data for the reaction

$$Ca^{+2} + H_2O = CaOH^{+} + H^{+} \qquad (68)$$

is shown in Fig. 43. Note that the comparison in Fig. 43 involves log K values at 500 bars and 1 kb as well as Psat. As in the case of Fig. 42, the curves in Fig. 43 are *independent* of the experimental data except at 25°C. It was found in this study that use of the predicted value of $\bar{S}^{\circ}$ listed in Table 10 for $CaOH^{+}$ leads to high-temperature/pressure estimates of log K_{68} which are more consistent with experimental data than those obtained from any of the literature values listed in Table 8.

Table 10. Summary of standard partial molal properties of nonconventional aqueous hydroxide complexes of metal cations at 25°C and 1 bar, together with parameters for calculating the corresponding properties at elevated temperatures and pressures with the revised-HKF equation of state.

Species	ΔG_f° [a]	ΔH_f° [a]	S° [b]	$\bar{C}_p^{\circ}$ [b]	V° [c]	a_1 [d] x 10	a_2 [a] x 10^{-2}	a_3 [e]	a_4 [f] x 10^{-4}	c_1 [b]	c_2 [f] x 10^{-4}	ω [a] x 10^{-5}
LiOH	-108000.[h]	-121500.[j]	1.9[i]	6.8[v]	3.8[y]	2.2749	-2.2242	6.6181	-2.6870	9.8752	-1.6493	-0.0300
NaOH	-99900.[h]	-112300.[n]	10.7[p]	-3.2[v]	3.5[y]	2.2338	-2.3287	6.6683	-2.6826	4.0146	-3.6863	-0.0300
KOH	-104500.[h]	-120200.[j]	25.9[l]	-20.5[v]	14.9[y]	3.7938	1.4839	5.1619	-2.8402	-6.1240	-7.2104	-0.0300
RbOH	-105100.[u]	-113000.[j]	32.0[l]	-27.5[v]	20.7[y]	4.5875	3.4168	4.4132	-2.9202	-10.2264	-8.6363	-0.0300
CsOH	-105000.[u]	-112300.[j]	35.9[l]	-31.9[v]	28.6[y]	5.6685	6.0571	3.3740	-3.0293	-12.8052	-9.5325	-0.0300
$BeOH^+$	-139900.[h]	-153200.[j]	-17.9[l]	29.4[v]	2.1[x]	2.3302	-2.0945	6.5792	-2.6923	30.9714	2.9542	0.8222
BeO	-128600.[h]	-144100.[j]	-25.1[l]	13.1[v]	1.0[x]	1.8917	-3.1609	6.9887	-2.6482	13.5675	-0.3660	-0.0300
$HBeO_2^-$	-172200.[h]	-206700.[j]	-33.3[l]	51.9[z]	3.4[af]	2.9518	-0.5719	5.9708	-2.7553	56.2537	7.5374	2.1351
BeO_2^{-2}	-152900.[h]	-189700.[j]	-41.0[l]	-12.7[aa]	1.5[af]	3.2657	0.1906	5.6788	-2.7868	34.0366	-5.6215	3.8330
$MgOH^+$	-149255.[h]	-152955.[j]	-19.1[l]	30.8[v]	1.9[x]	2.3105	-2.1365	6.5827	-2.6906	32.0008	3.2394	0.8449
$CaOH^+$	-171300.[h]	-179600.[j]	6.7[l]	1.4[v]	5.9[x]	2.7243	-1.1303	6.1958	-2.7322	11.1286	-2.7493	0.4496
$SrOH^+$	-173300.[h]	-180000.[j]	14.6[l]	-7.6[v]	7.2[x]	2.8620	-0.7922	6.0586	-2.7462	4.7576	-4.5826	0.3306
$BaOH^+$	-172300.[h]	-175900.[j]	27.5[l]	-22.4[v]	9.2[x]	3.0700	-0.2825	5.8541	-2.7672	-5.7064	-7.5974	0.1362
$SnOH^+$	-58600.[h]	-63800.[j]	19.2[l]	-12.9[v]	7.9[x]	2.9337	-0.6181	5.9928	-2.7533	0.9969	-5.6622	0.2595
SnO	-53600.[h]	-60100.[j]	14.8[l]	-32.4[v]	7.2[x]	2.7401	-1.0905	6.1776	-2.7338	-13.0981	-9.6344	-0.0300
$HSnO_2^-$	-97300.[h]	-122100.[j]	9.4[l]	-45.4[z]	14.1[af]	4.1971	2.4678	4.7779	-2.8809	-6.7372	-12.2825	1.4874
$PbOH^+$	-53950.[q]	-68900.[j]	-10.[q]	-20.[q]	3.4[x]	2.4669	-1.7600	6.4461	-2.7061	0.8970	-7.1085	0.7003
PbO	-39350.[q]	-44700.[j]	22.[q]	-42.[q]	8.3[x]	2.8906	-0.7236	6.0351	-2.7490	-18.7244	-11.5899	-0.0300
$HPbO_2^-$	-81000.[q]	-104200.[j]	18.[q]	-70.[q]	16.2[af]	4.4403	3.0599	4.5482	-2.9054	-22.3600	-17.2935	1.3566
$BiOH^{+2}$	-32300.[h]	-44800.[j]	-19.5[i]	-15.0[k]	1.8[x]	2.4693	-1.7539	6.4433	-2.7064	9.8610	-6.0900	1.3552
BiO^+	-29300.[h]	-30300.[j]	19.1[l]	-82.6[ab]	8.0[x]	2.9487	-0.5825	5.9810	-2.7548	-39.8159	-19.8601	0.2634
$HBiO_2$	-79300.[h]	-86300.[j]	54.6[m]	-148.5[z]	25.4[x]	5.2306	4.9892	3.7912	-2.9852	-81.1398	-33.2840	-0.0300
BiO_2^-	-61700.[h]	-71600.[j]	45.1[m]	-127.4[ac]	23.0[x]	5.2319	4.9920	3.7909	-2.9853	-59.7858	-28.9859	0.9456
$AlOH^{+2}$	-165475.[q]	-183300.[j]	-44.2[q]	13.2[q]	-2.2[x]	2.0469	-2.7813	6.8376	-2.6639	29.7923	-0.3457	1.7247
AlO^+	-158188.[q]	-170900.[j]	-27.[q]	-30.[q]	0.6[x]	2.1705	-2.4811	6.7241	-2.6763	-2.5983	-9.1455	0.9570
$HAlO_2$	-207700.[q]	-227500.[j]	5.[q]	-50.[q]	13.0[x]	3.5338	0.8485	5.4132	-2.8140	-23.4129	-13.2195	-0.0300
$GaOH^{+2}$	-91100.[h]	-116700.[j]	-67.3[l]	39.5[k]	-5.9[x]	1.6572	-3.7321	7.2107	-2.6246	48.3870	5.0115	2.0700
GaO^+	-86600.[h]	-100900.[j]	-29.2[l]	-27.5[ab]	0.2[x]	2.1299	-2.5806	6.7629	-2.6722	-0.7503	-8.6363	0.9986
$HGaO_2$	-137300.[h]	-158600.[j]	2.9[m]	-30.6[z]	12.4[x]	3.4470	0.6328	5.5060	-2.8051	-12.1716	-9.2677	-0.0439
GaO_2^-	-128700.[h]	-153900.[j]	-10.0[m]	-13.9[ac]	9.2[x]	3.6247	1.0721	5.3221	-2.8232	14.3978	-5.8659	1.7777
$InOH^{+2}$	-74600.[h]	-94700.[j]	-44.7[i]	13.8[k]	-2.3[x]	2.0372	-2.8058	6.8493	-2.6629	30.2531	-0.2234	1.7366
InO^+	-69400.[h]	-76900.[j]	-2.6[l]	-57.8[ab]	4.5[x]	2.5804	-1.4833	6.3385	-2.7176	-22.2654	-14.8084	0.5907
$HInO_2$	-119800.[h]	-135100.[j]	27.2[m]	-86.0[z]	18.5[x]	4.2864	2.6831	4.6987	-2.8898	-44.5111	-20.5527	-0.0300
InO_2^-	-106700.[h]	-125300.[j]	15.9[m]	-67.3[ac]	15.7[x]	4.3832	2.9224	4.5983	-2.8997	-20.4685	-16.7435	1.3901
TlOH	-65550.[ac]	-66660.[ac]	32.5[i]	-28.1[v]	25.0[y]	5.1759	4.8579	3.8372	-2.9797	-10.5781	-8.7585	-0.0300
$TlOH^{+2}$	-4500.[h]	-18800.[j]	-23.7[l]	-10.2[k]	1.1[x]	2.3952	-1.9341	6.5118	-2.6989	13.2638	-5.1122	1.4192
TlO^+	-3200.[h]	-5150.[j]	17.7[l]	-81.0[ab]	7.7[x]	2.9144	-0.6673	6.0161	-2.7513	-38.6952	-19.5342	0.2832
$HTlO_2$	-57600.[h]	-65600.[j]	53.1[m]	-145.1[z]	25.0[x]	5.1759	4.8579	3.8372	-2.9797	-79.1473	-32.5914	-0.0300
TlO_2^-	-41600.[h]	-52500.[j]	43.5[m]	-124.1[ac]	22.6[x]	5.1854	4.8830	3.8238	-2.9808	-57.6278	-28.3137	0.9699
$ScOH^{+2}$	-19100.[h]	-200700.[n]	-15.7[p,i]	-19.3[k]	-19.1[x]	-0.4111	-8.7778	9.1827	-2.4160	6.7806	-6.9659	1.2944
ScO^+	-183600.[h]	-189800.[j]	-3.6[l]	-56.7[ab]	-13.6[x]	0.1089	-7.5069	8.6817	-2.4686	-21.4773	-14.5843	0.6063
$HScO_2$	-231600.[h]	-244300.[j]	30.3[m]	-91.9[z]	11.6[x]	3.3422	0.3770	5.6066	-2.7945	-47.9689	-21.7545	-0.0300
ScO_2^-	-218100.[h]	-234100.[j]	19.2[m]	-74.1[ac]	5.6[x]	2.9831	-0.4979	5.9465	-2.7583	-24.9439	-18.1287	1.3369
VOH^+	-99800.[r]	-114100.[j]	-16.4[l]	27.7[v]	-26.0[x]	-1.5223	-11.4950	10.2591	-2.3037	29.7729	2.6079	0.8002
VOH^{+2}	-111500.[h]	-119400.[j]	-10.6[l]	-25.1[k]	-16.8[x]	-0.1213	-8.0707	8.9058	-2.4453	2.7011	-8.1474	1.2206
VO^+	-106100.[s]	-109400.[j]	4.9[l]	-66.4[ac]	-36.8[x]	-3.1084	-15.3641	11.7711	-2.1437	-28.3270	-16.5602	0.4799
$VOOH^+$	-155700.[t]	-177600.[j]	-17.7[l]	29.2[v]	-26.4[x]	-1.5696	-11.6082	10.2984	-2.2990	30.8543	2.9134	0.8222
$CrOH^{+2}$	-100500.[h]	-118600.[n]	-46.1[p,i]	15.4[k]	-36.6[ad]	-2.6482	-14.2423	11.3347	-2.1901	31.4127	0.1024	1.7607
CrO^+	-92800.[h]	-105000.[j]	-26.3[l]	-30.8[ab]	-23.8[x]	-1.1728	-10.6385	9.9161	-2.3391	-3.1901	-9.3085	0.9437
$HCrO_2$	-138100.[h]	-157300.[j]	6.0[m]	-37.7[z]	-1.6[x]	1.5359	-4.0259	7.3211	-2.6125	-16.2043	-10.7140	-0.0300
CrO_2^-	-125300.[h]	-148300.[j]	-6.7[m]	-20.7[ac]	-8.4[x]	1.2013	-4.8403	7.6350	-2.5788	10.0021	-7.2511	1.7331
$MnOH^+$	-97300.[h]	-106800.[n]	0.3[p,i]	8.7[v]	-11.9[x]	0.3213	-6.9901	8.4821	-2.4899	16.2994	-1.2623	0.5464
MnO	-81500.[h]	-99100.[j]	-2.5[l]	-12.7[v]	-13.1[x]	-0.0376	-7.8656	8.8229	-2.4537	-1.5528	-5.6215	-0.0300
$HMnO_2^-$	-121000.[h]	-149900.[j]	-9.1[l]	-3.3[z]	-9.7[x]	1.0354	-5.2480	7.8003	-2.5619	20.5255	-3.7067	1.7685
MnO_2^{-2}	-102600.[h]	-133300.[j]	-15.2[l]	-71.5[aa]	-13.0[x]	1.1489	-4.9713	7.6937	-2.5734	-4.0375	-17.5991	3.4408
$FeOH^+$	-65850.[q]	-78080.[j]	-10.[q]	15.[q]	-16.5[x]	-0.2561	-8.4039	9.0457	-2.4315	21.4093	0.0209	0.7003
FeO	-50720.[q]	-62950.[j]	-10.[q]	0.[q]	-16.5[x]	-0.5029	-9.0053	9.2791	-2.4066	5.8901	-3.0345	-0.0300
$HFeO_2^-$	-95400.[q]	-125700.[j]	-15.[q]	22.[q]	-12.9[x]	0.6272	-6.2440	8.1905	-2.5208	36.1624	1.4468	1.8564
$FeOH^{+2}$	-57800.[h]	-70000.[n]	-25.4[p,i]	-8.2[k]	-24.9[ad]	-1.1562	-10.6009	9.9077	-2.3407	14.6102	-4.7048	1.4382
FeO^+	-53100.[h]	-61000.[j]	-11.1[l]	-48.1[ab]	-41.8[x]	-3.7118	-16.8408	12.3595	-2.0827	-15.3982	-12.8325	0.7191
$HFeO_2$	-101100.[h]	-120300.[j]	22.2[m]	-74.6[z]	7.2[x]	2.7401	-1.0905	6.1776	-2.7338	-37.8300	-18.2305	-0.0300
FeO_2^-	-88000.[h]	-110700.[j]	10.6[m]	-56.3[ac]	0.9[x]	2.3837	-1.9602	6.5182	-2.6979	-13.3207	-14.5028	1.4662
$CoOH^+$	-56025.[q]	-68450.[j]	-10.[q]	24.[q]	-16.5[x]	-0.2561	-8.4039	9.0457	-2.4315	26.6839	1.8542	0.7003
CoO	-44000.[h]	-58800.[j]	-17.8[l]	4.8[v]	-24.2[x]	-1.5566	-11.5736	10.2791	-2.3004	8.7031	-2.0567	-0.0300
$HCoO_2^-$	-83400.[h]	-117100.[j]	-25.5[l]	34.1[z]	-18.6[x]	-0.0971	-8.0155	8.8926	-2.4475	44.7712	3.9116	2.0211
CoO_2^{-2}	-63200.[h]	-99000.[j]	-32.7[l]	-31.6[aa]	-22.5[x]	-0.0590	-7.9219	8.8540	-2.4514	21.8518	-9.4714	3.7127
$CoOH^{+2}$	-23000.[h]	-36100.[n]	-27.8[p]	-5.5[k]	-24.5[x]	-1.0884	-10.4353	9.8425	-2.3475	16.5492	-4.1549	1.4769
$NiOH^+$	-52850.[q]	-67650.[j]	-18.[q]	31.[q]	-20.1[x]	-0.7075	-9.5051	9.4760	-2.3860	31.9091	3.2801	0.8222
NiO	-39340.[q]	-56230.[j]	25.[q]	10.[q]	-23.3[x]	-1.4334	-11.2786	10.1751	-2.3126	11.7507	-0.9975	-0.0300
$HNiO_2^-$	-81980.[q]	-118760.[j]	-36.[q]	48.[q]	-24.2[x]	-0.8143	-9.7619	9.5688	-2.3753	54.2564	6.7430	2.1664
NiO_2^{-2}	-64200.[h]	-101800.[j]	-38.9[l]	-17.5[aa]	-25.8[x]	-0.4814	-8.9493	9.2495	-2.4089	30.9114	-6.5993	3.7992
$CuOH^+$	-30200.[h]	-41700.[j]	-6.1[l]	16.0[v]	-14.7[x]	-0.0277	-7.8416	8.8142	-2.4547	21.5062	0.2246	0.6472
CuO	-20800.[s]	-34200.[j]	-12.4[l]	-1.4[v]	-17.6[x]	-0.3937	-8.7360	9.1675	-2.4178	12.1490	-3.3197	0.7384
$HCuO_2^-$	-60100.[s]	-86300.[j]	0.3[l]	-24.7[z]	-4.6[x]	1.3202	-4.5527	7.5282	-2.5907	-3.2749	-8.0659	0.5464
CuO_2^{-2}	-41200.[s]	-74400.[j]	-23.1[i]	-53.5[aa]	-17.3[x]	0.6024	-6.3038	8.2129	-2.5183	7.6532	-13.9325	3.5647

Table 10. (Continued)

$ZnOH^+$	-81190.[q]	-86990.[j]	15.[q]	10.[q]	-5.3[x]	1.1499	-4.9677	7.6896	-2.5735	15.0306	-0.9975	0.3260
ZnO	-67420.[q]	-78290.[j]	-2.[q]	-10.[q]	-21.9[x]	-1.2418	-10.8072	9.9819	-2.3321	0.0295	-5.0715	-0.0300
$HZnO_2^-$	-110720.[q]	-142370.[j]	-16.[q]	20.[q]	-13.4[x]	0.5623	-6.4047	8.2588	-2.5141	35.0874	1.0394	1.8669
ZnO_2^{-2}	-93290.[q]	-132100.[j]	-40.[q]	-15.[q]	-26.4[x]	-0.5559	-9.1347	9.3301	-2.4013	32.5837	-6.0900	3.8216
YOH^{+2}	-210000.[h]	-220900.[j]	-17.2[i]	-17.6[k]	2.1[x]	2.4985	-1.6806	6.4099	-2.7094	8.0136	-6.6196	1.3201
YO^+	-198100.[h]	-204600.[j]	-2.2[l]	-58.3[ab]	4.5[x]	2.5778	-1.4890	6.3393	-2.7173	-22.6289	-14.9102	0.5831
HYO_2	-241700.[h]	-254600.[j]	31.8[m]	-96.5[z]	19.7[x]	4.4506	3.0828	4.5443	-2.9063	-50.6646	-22.6916	-0.0300
YO_2^-	-227400.[h]	-243600.[j]	20.8[m]	-77.3[ae]	16.9[x]	4.5219	3.2579	4.4729	-2.9136	-27.0256	-18.7805	1.3145
$ZrOH^{+3}$	-190400.[h]	-212500.[j]	-71.6[l]	44.4[k]	-12.7[x]	0.9279	-5.5093	7.9015	-2.5511	56.7436	6.0097	2.6654
ZrO^{+2}	-187600.[h]	-204300.[j]	-53.4[q]	0.1[ab]	-3.6[x]	1.9014	-3.1364	6.9769	-2.6492	23.3712	-3.0141	1.8611
$HZrO_2^+$	-239700.[h]	-265300.[j]	-49.7[m]	89.3[z]	-0.7[x]	2.1106	-2.6299	6.7878	-2.6702	70.5343	15.1558	1.3060
ZrO_2	-233400.[h]	-263800.[j]	-43.7[m]	55.5[ae]	0.8[x]	1.8643	-3.2264	7.0119	-2.6455	38.4166	8.2708	-0.0300
$HZrO_3^-$	-281500.[h]	-333300.[j]	-32.7[m]	50.6[z]	7.9[x]	3.5625	0.9168	5.3901	-2.8168	55.3517	7.2726	2.1199
AgOH	-21900.[h]	-31800.[j]	17.2[l]	-10.6[v]	3.9[y]	2.2885	-2.1912	6.6063	-2.6883	-0.3221	-5.1937	-0.0300
AgO^-	-5500.[h]	-16300.[j]	13.9[m]	-31.3[v]	-5.7[x]	1.4640	-4.1994	7.3839	-2.6053	0.8786	-9.4103	1.4171
$CdOH^+$	-61500.[h]	-73400.[n]	-2.9[p,i]	12.3[v]	-13.3[x]	0.1473	-7.4141	8.6471	-2.4724	18.8886	-0.5290	0.5985
CdO	-47500.[h]	-59750.[j]	-4.2[l]	-10.7[v]	-13.9[x]	-0.1471	-8.1341	8.9312	-2.4426	-0.3806	-5.2141	-0.0300
$HCdO_2^-$	-86500.[h]	-117400.[j]	-10.9[l]	0.9[z]	-10.7[x]	0.9080	-5.5570	7.9176	-2.5492	23.2446	-2.8512	1.7965
CdO_2^{-2}	-67300.[h]	-101000.[j]	-20.3[i]	-59.9[aa]	-15.8[x]	0.7922	-5.8401	8.0303	-2.5375	3.4810	-15.2361	3.5190
$HfOH^{+3}$	-189000.[h]	-211800.[j]	-72.8[l]	45.8[k]	-12.9[x]	0.9047	-5.5670	7.9267	-2.5488	57.6774	6.2949	2.6777
HfO^{+2}	-186000.[h]	-200900.[j]	-46.2[q]	-8.1[ab]	-2.5[x]	2.0179	-2.8551	6.8743	-2.6609	17.6401	-4.6845	1.7607
$HHfO_2^+$	-237800.[h]	-264200.[j]	-51.0[m]	92.3[z]	-1.1[x]	2.0629	-2.7421	6.8221	-2.6655	72.4834	15.7669	1.3268
HfO_2	-231400.[h]	-262600.[j]	-45.1[m]	58.4[ae]	0.4[x]	1.8096	-3.3639	7.0739	-2.6398	40.1163	8.8615	-0.0300
$HHfO_3^-$	-279200.[h]	-331800.[j]	-34.3[m]	54.2[z]	7.3[x]	3.4908	0.7427	5.4561	-2.8096	57.7445	8.0059	2.1506
$HgOH^+$	-12700.[h]	-20400.[n]	16.7[p,i]	46.5[v]	-4.5[x]	1.2505	-4.7196	7.5872	-2.5838	36.1808	6.4374	0.2998
HgO	-8900.[h]	-19200.[j]	8.2[l]	-24.8[v]	-8.3[x]	0.6191	-6.2664	8.2051	-2.5198	-8.6440	-8.0863	-0.0300
$HHgO_2^-$	-45200.[h]	-73800.[j]	2.3[l]	-29.2[z]	-3.6[x]	1.8118	-3.3572	7.0689	-2.6401	3.7588	-8.9825	1.5962

a. cal mol^{-1}. b. cal mol^{-1} K^{-1}. c. cm^3 mol^{-1}. d. cal mol^{-1} bar^{-1}. e. cal K mol^{-1} bar^{-1}. f. cal K mol^{-1}. g. Glushko (1965, 1966, 1968, 1970, 1971, 1972, 1973, 1974, 1978, 1979, 1981, 1982). h. Calculated from log K for the hydrolysis reaction given by Baes and Mesmer (1976, 1981), together with values of ΔG_f° of the ions from Table 1, 4, or 5. i. Value selected in this study from those listed in Table 8. j. Calculated from ΔG_f° and S° in the table, together with S° of the element from Cox et al. (1989), ref. g., and/or ref. w. k. Estimated with Eqn. (63). l. Estimated from S° of the cation from Tables 1, 4, or 5, together with the correlations shown in Figs. (38-41). m. Estimated from S° of the cation from Tables 1, 4, or 5, using equations listed in Table 9. n. Calculated from ΔH_r° for the hydrolysis reactions given by Baes and Mesmer (1981), together with values of ΔH_f° of the ions from Tables 1, 4, or 5. p. Calculated from ΔG_f° and ΔH_f° in the table, together with values of S° for the ions from Tables 1, 4, or 5. q. Obtained in this study through regression of log K data (see text and Table 7). r. Calculated from hydrolysis constant reported by Smith and Martell (1989). s. Calculated from hydrolysis constant reported by Sillen and Martell (1971). t. Calculated from hydrolysis constant reported by Högfeldt (1982). u. Calculated from data reported by Bard et al. (1985). v. Estimated with Eqn. (60). w. Wagman et al. (1982). x. Estimated with Eqn. (12) using slopes and intercepts as given in Table 9. y. Estimated from V° of the cation using the correlation developed by Sverjensky et al. (1997). z. Estimated with Eqn. (61). aa. Estimated with Eqn. (62). ab. Estimated with Eqn. (64). ac. Calculated from the corresponding anion from reaction property given by Bjerrum et al. (1958). ad. Asano and Le Noble (1978). ae. Estimated with Eqn. (31). af. Estimated with Eqn. (12) using parameters for metal oxygen-bearing species with #O=2.

5. CONCLUDING REMARKS

The estimation methods described above result from theoretical research into methods which can be used to obtain standard state thermodynamic data for aqueous species involved in a wide variety of geochemical processes. One result is that it is now possible to include tetravalent cations in the type of correlation algorithms initially presented by Shock and Helgeson (1988). In addition, new correlations allow improved estimates for charged and neutral oxygen-bearing inorganic aqueous species. These new correlations, together with regression of the available high temperature data, provide a framework for an estimation procedure for standard state thermodynamic properties for hydroxide complexes of many aqueous cations. All of these data** can be used in speciation and mass-transfer calculations to obtain an improved understanding of the geochemical consequences of fluid-rock reactions. As examples, the results described above facilitate studies of the aqueous transport of many trace elements and are applied to the speciation of rare earth cations by Haas et al. (1995), to platinum-group element mobility by Sassani and Shock (1997a), and to titanium transport by Willis and Shock (1997). These data, together with results of coordinated research on metal-ligand com-

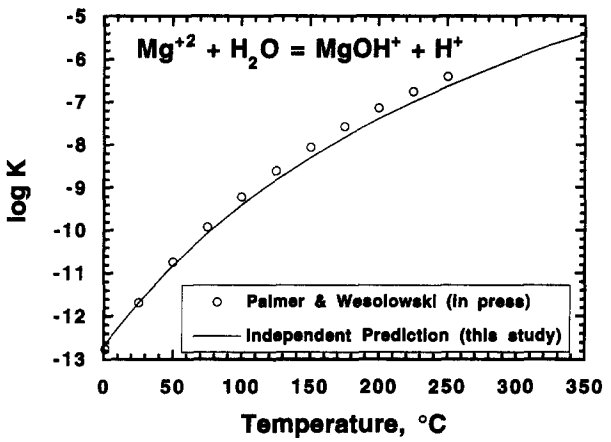

Fig. 42. Plot of equilibrium constants for reaction 67 as a function of temperature at P_{SAT} showing close agreement between recent experimental measurements and independent predictions made with data and parameters for $MgOH^+$ given in Table 10.

** A modified database for the program SUPCRT92 (Johnson et al., 1992) containing all of the data and parameters in Tables 1, 4, 5, and 10, together with other data and parameters from papers published from this laboratory, is available on the GEOPIG Home Page (http://zonvark.wustl.edu/geopig/).

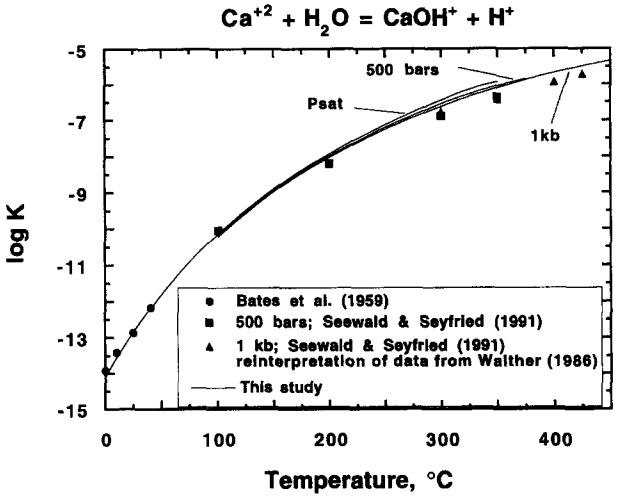

Fig. 43. Plot of equilibrium constants for reaction 68 as a function of temperature at P_{SAT}, 500 bars and 1 kb. The curves represent values predicted in this study using parameters for $CaOH^+$ from Table 10, and are independent of the experimental data shown as symbols at all temperatures and pressures other than 25°C and 1 bar.

plexes (Sverjensky et al., 1997) and linear free energy relations used to predict data at 25°C and 1 bar (Sverjensky and Molling, 1992; Sverjensky, 1992; Sassani and Shock, 1997b), are also instrumental in studies of aqueous speciation and the progress of fluid-rock reactions in geologic environments ranging from sedimentary basins (Shock and Koretsky, 1993, 1995; Helgeson et al., 1993; Shock, 1994) to the zone of contact between hydrothermal fluids and magmatic systems (Pasteris et al., 1995; Sassani and Shock, 1990; McCollom et al., 1993a,b; McCollom and Shock, 1997). The approach taken in this study will help to place calculations of geologic fluid speciation and geochemical mass-transfer by such fluids on a sound, quantitative, theoretical basis and should help to liberate the prevailing petrologic view that geologic fluids can be adequately characterized as H_2O/CO_2 mixtures. We expect many other applications of these data and encourage experimental studies which will test and ultimately lead to improvements in these predictive methods.

Acknowledgments—We wish to thank several colleagues for helpful discussions during the course of this study including Tom McCollom, Mitch Schulte, Jill Pasteris, J. K. Böhlke, Harold Helgeson, Vitalii Pokravskii, Eric Oelkers, James W. Johnson, William Murphy, Johnson Haas, Carla Koretsky, and Laura Wetzel. Rho plots used in this study were generated by Rebecca Lloyd with help from Tom McCollom, Jonathan Icenhower, Mitch Schulte, and Bill Moss. Considerable technical assistance was supplied by Rachel Lindvall, Jennifer Thieme, Patty DuBois, Bill Winston, Dee Becker, Carla Koretsky, Heidi Betz, Stephan Schmidt, Doug Larowe, Gavin Chan, Jenny Yoo, Barbara Winston, and Michelle Morgan, and is greatly appreciated. Careful reviews and comments by Don Palmer, Jim Johnson, Jeff Seewald, Greg Anderson, and Eric Oelkers were helpful in revising the manuscript. In addition, we want to thank Jamie Hovey, Jacques Schott, and Dave Wesolowski for generously sharing results of their experimental work in advance of publication. This research was funded by NSF grants EAR-8905018 and OCE-9220337, and DOE grant DE-FG02-92ER14297 to ELS, and NSF grants EAR-872251, EAR-9526623, and OCE-9200208, and DOE grant DEFG-0296ER-14616 to DAS. This is GEOPIG Contribution 34.

Editorial handling: E. H. Oelkers

REFERENCES

Amend J. P. and Helgeson H. C. (1997) Group additivity equations of state for calculating the standard molal thermodynamic properties of aqueous organic species at elevated temperatures and pressures. *Geochim. Cosmochim. Acta* **61,** 11–46.

Archer D. G. and Wang P. (1990) The dielectric constant of water and Debye-Huckel limiting slopes. *J. Phys. Chem. Ref. Data* **19,** 371–411.

Asano T. and Le Noble W. J. (1978) Activation and reaction volumes in solution. *Chem. Rev.* **78,** 407–489.

Baes C. F., Jr., and Mesmer R. E. (1976) *The Hydrolysis of Cations.* Wiley.

Baes C. F., Jr., and Mesmer R. E. (1981) The thermodynamics of cation hydrolysis. *Amer. J. Sci.* **281,** 935–962.

Bailey N., Carrington A., Lott K. A. K., and Symons M. C. R. (1960) Structure and reactivity of the oxyanions of transition metals. Part VIII. Acidities and spectra of protonated oxyanions. *J. Chem. Soc.,* 290–297.

Bard A. J., Parsons R., and Jordan J. (1985) Standard Potential in Aqueous Solution. In *IUPAC* (ed. A. J. Bard, R. Parsons, and J. Jordan), p. 843. Marcel Dekker.

Bates R. G., Bower V. E., Canham R. G., and Prue J. E. (1959) The dissociation constant of $CaOH^+$ from 0° to 40°C. *Trans. Faraday Soc.* **55,** 2062–2068.

Benson S. W. (1976) *Thermochemical Kinetics,* 2nd ed. Wiley.

Biedermann G. and Romano V. (1975) On the standard potential of the Cr(III)-Cr(II) couple in 1 M NaCl medium. *Acta Chem. Scand.* **A29,** 615–622.

Bjerrum J., Schwarzenbach G., and Sillén L. G. (1958) *Stability Constants of Metal-Ion Complexes with Solubility Products of Inorganic Substances. Part II: Inorganic Ligands.* The Chemical Soc., London.

Bolzan J. A. and Arvía A. J. (1962) Hydrolytic equilibria of metallic ions—I. The hydrolysis of Co(II) ion in $NaClO_4$ solution. *Electroch. Acta* **7,** 589–599.

Bourcier W. L., Knauss K. G., and Jackson K. J. (1993) Aluminum hydrolysis constants to 250°C from boehmite solubility measurements. *Geochim. Cosmochim. Acta* **57,** 747–762.

Castet S., Dandurand J. L., Schott J., and Gout R. (1992) Experimental study of aluminum hydrolysis and complexation with acetate and sodium ions in hydrothermal solutions. In *Proc. 7th Intl. Symp. on Water-Rock Interaction 2,* pp. 1013–1016. USGS.

Castet S., Dandurand J. L., Schott J., and Gout R. (1993) Boehmite solubility and aqueous aluminum speciation in hydrothermal solutions (90–350°C): Experimental study and modeling. *Geochim. Cosmochim. Acta* **57,** 4869–4884.

Chaberek S., Jr., Courtney R. C., and Martell A. E. (1952) Stability of metal chelates. II. β-Hydroxyethyliminodiacetic acid. *J. Amer. Chem. Soc.* **74,** 5057–5060.

Christensen J. J. and Izatt R. M. (1983) *Handbook of Metal Ligand Heats and Related Thermodynamic Quantities.* Marcel Dekker.

Collados M. P., Brito F., and Cadavieco R. D. (1967) Hidrolisis de cobato(II) en (Ba,Co) $(ClO_4)_2$ 1,5 M y 25°C. *Anales de Fisica Y Quimica,* 843–845.

Couturier Y., Michard G., and Sarazin G. (1984) Constantes de formation des complexes hydroxydés de l'aluminium en solution aqueuse de 20 a 70°C. *Geochim. Cosmochim. Acta* **48,** 649–659.

Cox J. D., Wagman D. D., and Medvedev V. A. (1989) *CODATA Key Values for Thermodynamics.* Hemisphere Pub. Corp.

Davies W. G. and Prue J. E. (1955) A spectrophotometric study of the equilibrium $Cr_2O_7^{2-} + H_2O \leftrightarrow 2HCrO_4^-$. *Trans. of the Faraday Soc.* **51,** 1045–1051.

Dellien I. (1977) The Gibbs energy of formation and the entropy of aqueous tungstate ion from the activity coefficients of sodium tungstate in aqueous solution. *J. Chem. Thermo.* **9,** 897–900.

Dellien I., Hall F. M., and Hepler L. G. (1976) Chromium, molybde-

num, and tungsten: thermodynamic properties, chemical equilibria, and standard potentials. *Chem. Rev.* **76,** 283–310.

Dickson A. G., Wesolowski D. J., Palmer D. A., and Mesmer R. E. (1990) Dissociation constant of bisulfate ion in aqueous sodium chloride solutions to 250°C. *J. Phys. Chem.* **94,** 7978–7985.

Dirkse T. P., Postmus C., Jr., and Vandenbosch R. (1954) A study of alkaline solutions of zinc oxide. *J. Amer. Chem. Soc.* **76,** 6022–6024.

Franck E. U., Rosenzweig S., and Christoforakos M. (1990) Calculation of the dielectric constant of water to 1000°C and very high pressures. *Ber. Bunsenges. Phys. Chem.* **94,** 199–203.

Frink C. R. and Peech M. (1963) The solubility of gibbsite in aqueous solutions and soil extracts. *Soil Science Society Proceedings* **26,** 346–347.

Fulton J. W. and Swinehart D. F. (1954) The equilibria of crystalline zinc hydroxide in dilute hydrochloric acid and sodium hydroxide at 25°C. The first and second acidic dissociation constants of zinc hydroxide. *J. Amer. Chem. Soc.* **76,** 864–867.

Garrett A. B., Vellenga S., and Fontana C. M. (1939) The solubility of red, yellow, and black lead oxides (2) and hydrated lead oxide in alkaline solutions. The character of the lead-bearing ion. *J. Amer. Chem. Soc.* **61,** 367–373.

Gayer K. H. and Garrett A. B. (1949) The equilibria of nickel hydroxide, $Ni(OH)_2$, in solutions of hydrochloric acid and sodium hydroxide at 25°C. *J. Amer. Chem. Soc.* **71,** 2973–2975.

Gayer K. H. and Woontner L. (1952) Hydrolysis of cobalt chloride and nickel chloride at 25°C. *J. Amer. Chem. Soc.* **74,** 1436–1437.

Gedansky L. M. and Hepler L. G. (1969) Thermochemistry of the aqueous manganus ion. *Canadian J. Chem.* **47,** 699–701.

Giasson G. and Tewari P. H. (1978) Hydrolysis of Co(II) at elevated temperatures. *Canadian J. Chem.* **56,** 435–440.

Gildseth W. M., Habenschuss A., and Spedding F. H. (1975) Densities and thermal expansion of some aqueous rare earth chloride solutions between 5° and 80°C. I. $LaCl_3$, $PrCl_3$, and $NdCl_3$. *J. Chem. Eng. Data* **20,** 292–309.

Glushko V. P. (1965) *Thermal Constants of Substances: Directory in Ten Issues.* Issue 1. Moscow, Academy of Sciences of the U.S.S.R., All-Union Institute of Scientific and Technical Information, Institute of High Temperatures.

Glushko V. P. (1966) *Thermal Constants of Substances: Directory in Ten Issues.* Issue 2. Moscow, Academy of Sciences of the U.S.S.R., All-Union Institute of Scientific and Technical Information, Institute of High Temperatures.

Glushko V. P. (1968) *Thermal Constants of Substances: Directory in Ten Issues.* Issue 3. Moscow, Academy of Sciences of the U.S.S.R., All-Union Institute of Scientific and Technical Information, Institute of High Temperatures.

Glushko V. P. (1970a) *Thermal Constants of Substances: Directory in Ten Issues.* Issue 4, Part 1. Moscow, Academy of Sciences of the U.S.S.R., All-Union Institute of Scientific and Technical Information, Institute of High Temperatures.

Glushko V. P. (1970b) *Thermal Constants of Substances: Directory in Ten Issues.* Issue 4, Part 2. Moscow, Academy of Sciences of the U.S.S.R., All-Union Institute of Scientific and Technical Information, Institute of High Temperatures.

Glushko V. P. (1971) *Thermal Constants of Substances: Directory in Ten Issues.* Issue 5. Moscow, Academy of Sciences of the U.S.S.R., All-Union Institute of Scientific and Technical Information, Institute of High Temperatures.

Glushko V. P. (1972) *Thermal Constants of Substances: Directory in Ten Issues.* Issue 6, Part 1. Moscow, Academy of Sciences of the U.S.S.R., All-Union Institute of Scientific and Technical Information, Institute of High Temperatures.

Glushko V. P. (1973) *Thermal Constants of Substances: Directory in Ten Issues.* Issue 6, Part 2. Moscow, Academy of Sciences of the U.S.S.R., All-Union Institute of Scientific and Technical Information, Institute of High Temperatures.

Glushko V. P. (1974) *Thermal Constants of Substances: Directory in Ten Issues.* Issue 7, Part 1–2. Moscow, Academy of Sciences of the U.S.S.R., All-Union Institute of Scientific and Technical Information, Institute of High Temperatures.

Glushko V. P. (1978) *Thermal Constants of Substances: Directory in Ten Issues.* Issue 8, Part 1–2. Moscow, Academy of Sciences of the U.S.S.R., All-Union Institute of Scientific and Technical Information, Institute of High Temperatures.

Glushko V. P. (1979) *Thermal Constants of Substances: Directory in Ten Issues.* Issue 9. Moscow, Academy of Sciences of the U.S.S.R., All-Union Institute of Scientific and Technical Information, Institute of High Temperatures.

Glushko V. P. (1981) *Thermal Constants of Substances: Directory in Ten Issues.* Issue 10, Part 1–2. Moscow, Academy of Sciences of the U.S.S.R., All-Union Institute of Scientific and Technical Information, Institute of High Temperatures.

Glushko V. P. (1982) *Thermal Constants of Substances: Directory in Ten Issues.* Issue 10, Part 3. Moscow, Academy of Sciences of the U.S.S.R., All-Union Institute of Scientific and Technical Information, Institute of High Temperatures.

Grenthe I., Fuger J., Lemire R., Muller A., Nguyen-Trung C., and Wanner H. (1992) *Chemical Thermodynamics of Uranium.* Nuclear Energy Agency.

Gubeli A. O. and Ste-Marie J. (1967) Stabilité des complexes hydroxo et produtits de solubilité des hydroxydes de métaux. I. Argent et zinc. *Canadian J. Chem.* **45,** 827–832.

Haar L., Gallagher J. S., and Kell G. S. (1984) *NBS/NRC Steam Tables: Thermodynamic and Transport Properties and Computer Programs for Vapor and Liquid States of Water in SI Units.* Hemisphere Publications.

Haas J. R. and Shock E. L. (1994) Predictions of rare earth element (REE) speciation in a simulated hydrothermal solution as a function of pressure, temperature, and fluid pH. *Eos, Trans. Amer. Geophys. Union* **75,** 361 (abstr.).

Haas J., Shock E. L., and Sassani D. C. (1995) Rare earth elements in hydrothermal systems: Estimates of standard partial molal thermodynamic properties of aqueous complexes of the REEs at high pressures and temperatures. *Geochim. Cosmochim. Acta* **59,** 4329–4350.

Helgeson H. C. (1969) Thermodynamics of hydrothermal systems at elevated temperatures and pressures. *Amer. J. Sci.* **267,** 729–804.

Helgeson H. C. (1992) Calculation of the thermodynamic properties and relative stabilities of aqueous acetic and chloroacetic acids, acetate and chloracetates, and acetyl and chloroacetyl chlorides at high and low temperatures and pressures. *Appl. Geochem.* **7,** 291–308.

Helgeson H. C. and Kirkham D. H. (1974a) Theoretical prediction of the thermodynamic behavior of aqueous electrolytes at high pressures and temperatures. I. Summary of the thermodynamic/electrostatic properties of the solvent. *Amer. J. Sci.* **274,** 1089–1198.

Helgeson H. C. and Kirkham D. H. (1974b) Theoretical prediction of the thermodynamic behavior of aqueous electrolytes at high pressures and temperatures. II. Debye-Hückel parameters for activity coefficients and relative partial molal properties. *Amer. J. Sci.* **274,** 1199–1261.

Helgeson H. C. and Kirkham D. H. (1976) Theoretical prediction of the thermodynamic behavior of aqueous electrolytes at high pressures and temperatures. III. Equation of state for aqueous species at infinite dilution. *Amer. J. Sci.* **276,** 97–240.

Helgeson H. C., Kirkham D. H., and Flowers G. C. (1981) Theoretical prediction of the thermodynamic behavior of aqueous electrolytes at high pressures and temperatures. IV. Calculation of activity coefficients, osmotic coefficients, and apparent molal and standard and relative partial molal properties to 5 kb and 600°C. *Amer. J. Sci.* **281,** 1241–1516.

Helgeson H. C., Knox A. M., Owens C. E., and Shock E. L. (1993) Petroleum, oil field waters and authigenic mineral assemblages: Are they in metastable equilibrium in hydrocarbon reservoirs? *Geochim. Cosmochim. Acta* **57,** 3295–3339.

Hemingway B. S. and Robie R. A. (1977) Enthalpies of formation of low albite ($NaAlSi_3O_8$), gibbsite ($Al(OH)_3$), and $NaAlO_2$; revised values for $\Delta H^\circ_{f,298}$ and $\Delta G^\circ_{f,298}$ of some aluminosilicate minerals. *J. Res. USGS* **5,** 413–429.

Herrington T. M., Pethybridge A. D., and Roffey M. G. (1985) Densities of hydrochloric, hydriodic, and perchloric acids from 25 to 75°C at 1 atm. *J. Chem. Eng. Data* **30,** 264–267.

Herrington T. M., Roffey M. G., and Smith D. P. (1986) Density of

aqueous electrolytes: $MnCl_2$, $CoCl_2$, $NiCl_2$, $ZnCl_2$, and $CdCl_2$ from 25 to 75°C at 1 atm. *J. Chem. Eng. Data* **31,** 221–225.

Hill P. G. (1990) A unified fundamental equation for the thermodynamic properties of H_2O. *J. Phys. Chem. Ref. Data* **19,** 1233–1274.

Hill J. O., Worsley I. G., and Hepler L. G. (1971) Thermochemistry and oxidation potentials of vanadium, niobium, and tantalum. *Chem. Rev.* **71,** 127–137.

Högfeldt E. (1982) *Stability Constants of Metal-Ion Complexes. Part A: Inorganic Ligands. IUPAC Chemical Data Series, No. 21.* Pergamon Press.

Hovey J. K. and Hepler L. G. (1989) Apparent and partial molar heat capacities and volumes of aqueous $HClO_4$ and HNO_3 from 10 to 55°C. *Canadian J. Chem.* **67,** 1489–1495.

Hovey J. K. and Hepler L. G. (1990) Apparent and partial molar heat capacities and volumes of CrO_4^{2-}(aq), $HCrO_4^-$(aq), and $Cr_2O_7^{2-}$(aq) at 25°C: Chemical relaxation and calculation of equilibrium constants for high temperatures. *J. Phys. Chem.* **94,** 7821–7830.

Hovey J. K., Hepler L. G., and Tremaine P. R. (1988) Apparent molar heat capacities and volumes of aqueous $HClO_4$, HNO_3, $(CH_3)_4NOH$ and K_2SO_4 at 298.15 K. *Thermochim. Acta* **126,** 245–253.

Hovey J. K., Nguyen-Trung C., and Tremaine P. R. (1989) Thermodynamics of aqueous uranyl ion: Apparent and partial molar heat capacities and volumes of aqueous uranyl perchlorate from 10 to 55°C. *Geochim. Cosmochim. Acta* **53,** 1503–1509.

Howard J. R., Nair V. S. K., and Nancollas G. H. (1958) Potentiometric and spectrophotometric studies of the equilibrium $HCrO_4^- \leftrightarrow 2H^+ + CrO_4^{2-}$. *Trans. Faraday Soc.* **54,** 1034–1037.

Johnson G. K. and Bauman J. E., Jr. (1978) Equilibrium constants for the aquated iron(II) cation. *Inorg. Chem.* **17,** 2774–2779.

Johnson J. W. and Norton D. (1991) Critical phenomena in hydrothermal systems: State, thermodynamic, electrostatic, and transport properties of H_2O in the critical region. *Amer. J. Sci.* **291,** 541–648.

Johnson J. W., Oelkers E. H., and Helgeson H. C. (1992) SUPCRT92: A software package for calculating the standard molal thermodynamic properties of minerals, gases, aqueous species, and reactions from 1 to 5000 bars and 0° to 1000°C. *Computers and Geosciences* **18,** 899–947.

Karpet'yants M. Kh., Vasilëv V. A., and Sanaev E. S. (1977) The heat capacities and volume properties of aqueous iron(II) and nickel chloride solutions at 25°C. *Russian J. Phys. Chem.* **51,** 1281–1283.

Khodakovskiy I. L. and Yelkin A. Y. (1975) Measurement of the solubility of zincite in aqueous NaOH at 100, 150, and 200°C. *Geochemistry Intl.,* 127–133.

Krumhansl J. L. (1976) Geochemistry of Tungsten. Ph.D. thesis, Stanford Univ.

Kuyunko N. S., Malinin S. D., and Khodakovskiy I. L. (1983) An experimental study of aluminum ion hydrolysis at 150, 200, and 250°C. *Geochemistry Intl.* **20,** 76–86.

Langmuir D. (1978) Uranium solution-mineral equilibria at low temperatures with applications to sedimentary ore deposits. *Geochim. Cosmochim. Acta* **42,** 547–569.

Larson J. W., Zeeb K. G., and Hepler L. G. (1982) Heat capacities and volumes of dissociation of phosphoric acid (1st, 2nd and 3rd) bicarbonate ion, and bisulfate ion in aqueous solution. *Canadian J. Chem.* **60,** 2141–2150.

Latimer W. M. (1952) *The Oxidation States of the Elements and their Potentials in Aqueous Solutions.* Prentice-Hall, New York.

Lemire R. J., Saluja P. P. S., and Campbell A. B. (1992) Aqueous partial molar heat capacities and volumes for $NaTcO_4$ and $NaReO_4$. *J. Sol. Chem.* **21,** 507–523.

Levelt Sengers J. M. H., Kamgar-Parsi B., Balfour F. W., and Sengers J. V. (1983) Thermodynamic properties of steam in the critical region. *J. Phys. Chem. Ref. Data* **12,** 1–28.

Li J. C. M. and Ritter D. M. (1953) Decomposition of nitrosyl disulfonate ion. IV. The reaction of sulfamate ion with nitrous acid. *J. Amer. Chem. Soc.* **75,** 5828–5830.

Linge H. G. and Jones A. L. (1968a) The equilibrium constant of the reaction $Cr_2O_7^{2-} + H_2O \leftrightarrow HCrO_4^-$ at 15° to 45°. *Australian J. Chem.* **21,** 1445–1449.

Linge H. G. and Jones A. L. (1968b) The acidity constant of the hydrogen chromate ion in the range 5–60° in water. *Australian J. Chem.* **21,** 2189–2198.

Lukkari U. O., Hakoila E. J., and Lukkari H. K. (1972) Studies on membrane electrodes, 1. Barium chromate-impregnated silicone rubber membrane. *Soumen Kemistilehti* **B45,** 182–185.

Martell A. E. and Smith R. M. (1982) *Critical Stability Constants Vol. 5: First Supplement.* Plenum Press.

Mathieson J. G. and Curthoys G. (1974) Apparent molal volumes of KCN, $K_2Zn(CN)_4$ and $K_2Cd(CN)_4$ in aqueous solutions at 15–45°C. *J. Chem. Soc.,* 1114–1126.

May H. M., Helmke P. A., and Jackson M. L. (1979) Gibbsite solubility and thermodynamic properties of hydroxy-aluminum ions in aqueous solution at 25°C. *Geochim. Cosmochim. Acta* **43,** 861–868.

McCollom T., Sassani D. C., and Shock E. L. (1993a) Mass transfer of rock-forming elements during contact metamorphism. In *GSA Abstr. Progr.* **25,** A-263 (abstr.).

McCollom T., Shock E. L., and Sassani D. C. (1993b) "Igneous" assemblages produced by aqueous alteration in the lower oceanic crust. *Eos, Trans. Amer. Geophys. Union* **74,** 666 (abstr.).

McCollom T. and Shock E. L. (1997) Hydrothermal circulation in the lower oceanic crust: constraints from thermodynamic reaction path models. *J. Geophys. Res.* (in press).

Mesmer R. E. (1971) Hydrolysis of Iron (2+) in dilute chloride at 25°. *Inorg. Chem.* **10,** 857–858.

Millero F. J. (1971) The molal volumes of electrolytes. *Chem. Rev.* **71,** 147–176.

Morozumi T. and Posey F. A. (1967) An application of the electrochemical pH-stat to study on the hydrolysis of metal ions. *Denki Kagaku* **35,** 633–638.

Morss L. R. (1976) Thermochemical properties of yttrium, lanthanum, and the lanthanide elements and ions. *Chem. Rev.* **76,** 827–841.

Morss L. R. and McCue M. C. (1976) Partial molal entropy and heat capacity of the aqueous thorium (IV) ion. Thermochemistry of thorium nitrate pentahydrate. *J. Chem. Eng. Data* **21,** 337–341.

Neuss J. D. and Rieman W., III (1934) The application of the glass electrode to a study of chromic acid. *J. Amer. Chem. Soc.* **56,** 2238–2243.

Oelkers E. H. and Helgeson H. C. (1988) Calculation of the thermodynamic and transport properties of aqueous species at high pressures and temperatures: dissociation constants for supercritical alkali metal halides at temperatures from 400° to 800°C and pressures from 500 to 4000 bars. *J. Phys. Chem.* **92,** 1631–1639.

O'Hare P. A. G. and Boerio J. (1975) Standard enthalpy of solution and formation of cesium chromate. Derived thermodynamic properties of the aqueous chromate, bichromate, and dichromate ions, alkali metal and alkaline earth chromates, and lead chromate. *J. Chem. Thermodynamics* **7,** 1195–1204.

Page F. M. (1953) The dissociation constants of thiosulphuric acid. *J. Chem. Soc.,* 1719–1724.

Palmer D. A. and Wesolowski D. J. (1992) Aluminum speciation and equilibria in aqueous solution: II. The solubility of gibbsite in acidic sodium chloride solutions from 30 to 70°C. *Geochim. Cosmochim. Acta* **56,** 1093–1111.

Palmer D. A. and Wesolowski D. J. (1993) Aluminum speciation and equilibria in aqueous solution: III. Potentiometric determination of the first hydrolysis constant of aluminum(III) in sodium chloride solutions to 125°C. *Geochim. Cosmochim. Acta* **57,** 2929–2938.

Palmer D. A., Wesolowski D., and Mesmer R. E. (1987) A potentiometric investigation of the hydrolysis of chromate (VI) ion in NaCl media to 175°C. *J. Soln. Chem.* **16,** 443–463.

Palmer D. A. and Wesolowski D. J. (1997) Potentiometric measurements of the first hydrolysis quotient of magnesium (II) to 250°C and 5 molal ionic strength (NaCl). *J. Soln. Chem.* (in press).

Pan P. and Tremaine P. R. (1994) Thermodynamics of aqueous zinc: Standard partial molar heat capacities and volumes of Zn^{+2}(aq) from 10 to 55°C. *Geochim. Cosmochim. Acta* **58,** 4867–4874.

Pasteris J. D., Harris T. N., and Sassani D. C. (1995) Interactions of mixed volatile-brine fluids in rocks of the southwestern footwall of the Duluth Complex, Minnesota: Evidence from aqueous fluid inclusions. *Amer. J. Sci.* **295,** 125–172.

Perrin D. D. (1962) The hydrolysis of metal ions. Part III. Zinc. *J. Chem. Soc.*, 4500–4502.

Perrin D. D. (1964) The hydrolysis of metal ions. Part IV. Nickel(II). *J. Chem. Soc.* 3644–3648.

Plyasunov A. V., Belonozhko A. B., Ivanov I. P., and Khodakovskiy I. L. (1988) Solubility of zinc oxide in alkaline solutions at 200–350°C under saturated steam pressure. *Geochem. Intl.* **25,** 77–85.

Pogue R. F. and Atkinson G. (1988) Apparent molal volumes and heat capacities of aqueous HCl and $HClO_4$ at 15–55°C. *J. Chem. Eng. Data* **33,** 495–499.

Pogue R. F. and Atkinson G. (1989a) Solution thermodynamics of first row transition elements. 2. apparent molal volumes of aqueous $MnCl_2$, $Mn(ClO_4)_2$, $CoCl_2$, $Co(ClO_4)_2$, $FeCl_2$, and $Fe(ClO_4)_2$, from 15 to 55°C. *J. Chem. Eng. Data* **34,** 227–232.

Pogue R. F. and Atkinson G. (1989b) Solution thermodynamics of first row transition elements. 3. apparent molal volumes of aqueous $ZnCl_2$ and $Zn(ClO_4)_2$ from 15 to 55°C and an examination of solute-solute and solute-solvent interactions. *J. Soln. Chem.* **18,** 249–263.

Randall M. and Spencer H. M. (1928) Solubility of lead monoxide and basic lead carbonate in alkaline solutions. *J. Amer. Chem. Soc.* **50,** 1572–1583.

Rard J. A. and Miller D. G. (1984) Densities and apparent molal volumes of aqueous manganese, cadmium and zinc chlorides at 25°C. *J. Chem. Eng. Data* **29,** 151–156.

Reichle R. A., McCurdy K. G., and Helper L. G. (1975) Zinc hydroxide: Solubility product and hydroxy-complex stability constants from 12.5–75°C. *Canadian J. Chem.* **53,** 3841–3845.

Sanjuan B. and Michard G. (1987) Aluminum hydroxide solubility in aqueous solutions containing fluoride ions at 50°C. *Geochim. Cosmochim. Acta* **51,** 1823–1831.

Sassani D. C. and Shock E. L. (1990) Speciation and solubility of palladium in aqueous magmatic hydrothermal solutions. *Geology* **18,** 925–928.

Sassani D. C. and Shock E. L. (1992) Estimation of standard partial molal entropies of aqueous ions at 25°C and 1 bar. *Geochim. Cosmochim. Acta* **56,** 3895–3908.

Sassani D. C. and Shock E. L. (1994) Errata to Sassani & Shock (1992). *Geochim. Cosmochim. Acta* **58,** 2756–2758.

Sassani D. C. and Shock E. L. (1997a) Solubility and transport of platinum-group elements in supercritical fluids: Thermodynamic properties of Ru, Rh, Pd, and Pt solids, ions and complexes to 5 kbar and 1000°C. (in prep.)

Sassani D. C. and Shock E. L. (1997b) Estimation of standard Gibbs free energies of reaction for aqueous complexes of metal cations and monovalent ligands at 25°C and 1 bar. (in prep).

Sassani D. C., Betz H., and Shock E. L. (1993a) Predicted speciation of uranyl-chloride and- fluoride complexes and variations in uraninite solubility in heated pore fluids. *Eos, Trans. Amer. Geophys. Union* **74,** 328 (abstr.).

Sassani D. C., Betz H., and Shock E. L. (1993b) Predicted effects of temperature, oxygen fugacity, pH and solution composition on the speciation of aqueous uranium and the solubility of uraninite. *GSA Abstr. Progr.* **25,** 100 (abstr.).

Schulte M. D. and Shock E. L. (1993) Aldehydes in hydrothermal solution: Standard partial molal thermodynamic properties and relative stabilities at high temperatures and pressures. *Geochim. Cosmochim. Acta* **57,** 3835–3846.

Schofield R. K. and Taylor A. W. (1954) The hydrolysis of aluminium salt solutions. *J. Chem. Soc.*, 4445–4448.

Seewald J. S. and Seyfried W. E., Jr. (1991) Experimental determination of portlandite solubility in H_2O and acetate solutions at 100–350°C and 500 bars: constraints on calcium hydroxide and calcium acetate complex stability. *Geochim. Cosmochim. Acta* **55,** 659–669.

Shankar J. and De Souza B. C. (1963) Hydrolysis of Co^{2+}_{aq} and Ni^{2+}_{aq} ions. *Australian J. Chem.* **16,** 1119–1122.

Shock E. L. (1992) Stability of peptides in high temperature aqueous solutions. *Geochim. Cosmochim. Acta* **56,** 3481–3491.

Shock E. L. (1993) Hydrothermal dehydration of aqueous organic compounds. *Geochim. Cosmochim. Acta* **57,** 3341–3349.

Shock E. L. (1994) Application of thermodynamic calculations to geochemical processes involving organic acids. In *The Role of Organic Acids in Geochemical Processes* (ed. M. Lewan and E. Pittman), pp. 270–318. Springer-Verlag.

Shock E. L. (1995) Organic acids in hydrothermal solutions: Standard molal thermodynamic properties of carboxylic acids, and estimates of dissociation constants at high temperatures and pressures. *Amer. J. Sci.* **295,** 496–580.

Shock E. L. and Helgeson H. C. (1988) Calculation of the thermodynamic and transport properties of aqueous species at high pressures and temperatures: Correlation algorithms for ionic species and equation of state predictions to 5 kb and 1000°C. *Geochim. Cosmochim. Acta* **53,** 2009–2036.

Shock E. L. and Helgeson H. C. (1989) Erratum to E. L. Shock and H. C. Helgeson (1988). *Geochim. Cosmochim. Acta* **53,** 215.

Shock E. L. and Helgeson H. C. (1990) Calculation of the thermodynamic and transport properties of aqueous species at high pressures and temperatures: Standard partial molal properties of organic species. *Geochim. Cosmochim. Acta* **54,** 915–945.

Shock E. L. and Koretsky C. M. (1993) Metal-organic complexes in geochemical processes: Calculation of standard partial molal thermodynamic properties of aqueous acetate complexes at high pressures and temperatures. *Geochim. Cosmochim. Acta* **57,** 4899–4922.

Shock E. L. and Koretsky C. M. (1995) Metal-organic complexes in geochemical processes: Estimation of standard partial molal thermodynamic properties of aqueous complexes between metal cations and monovalent organic acid ligands at high pressures and temperatures. *Geochim. Cosmochim. Acta* **59,** 1497–1532.

Shock E. L. and McKinnon W. B. (1993) Hydrothermal processing of cometary volatiles—Application to Triton. *Icarus* **106,** 464–477.

Shock E. L., Helgeson H. C., and Sverjensky D. A. (1989) Calculation of the thermodynamic and transport properties of aqueous species at high pressures and temperatures: Standard partial molal properties of inorganic neutral species. *Geochim. Cosmochim. Acta* **53,** 2157–2183.

Shock E. L., Oelkers E. H., Johnson J. W., Sverjensky D. A., and Helgeson H. C. (1992) Calculation of the thermodynamic properties of aqueous species at high pressures and temperatures: Effective electrostatic radii, dissociation constants, and standard partial molal properties to 1000°C and 5 kbar. *J. Chem. Soc. Faraday Trans.* **88,** 803–826.

Shock E. L., Sassani D. C., and Betz H. (1997a) Actinide ions in aqueous solution: Summary of standard state properties and estimates at high temperatures and pressures. *Appl. Geochem.* (submitted).

Shock E. L., Sassani D. C., and Betz H. (1997b) Uranium in geologic fluids: Estimates of oxidation potentials and hydrolysis constants at high temperatures and pressures. *Geochim. Cosmochim. Acta* (in prep.).

Sillén L. G. and Martell A. E. (1964) *Stability Constants of Metal-Ion Complexes.* The Chem. Soc.

Sillén L. G. and Martell A. E. (1971) *Stability Constants of Metal-Ion Complexes: Supplement No. 1.* The Chem. Soc.

Smith R. M. and Martell A. E. (1976) *Critical Stability Constants. Vol. 4: Inorganic Complexes.* Plenum Press.

Smith R. M. and Martell A. E. (1989) *Critical Stability Constants. Vol. 6: Second Supplement.* Plenum Press.

Spedding F. H., Pikal M. J., and Ayers B. O. (1966) Apparent molal volumes of some aqueous rare earth chloride and nitrate solutions at 25°C. *J. Phys. Chem.* **70,** 2440–2449.

Spedding F. H., Saeger V. W., Gray K. A., Boneau P. K., Brown M. A., DeKock C. W., Baker J. L., Shiers L. E., Weber H. O., and Habenschuss A. (1975a) Densities and apparent molal volumes of some rare earth solutions at 25°C. I. Rare earth chlorides. *J. Chem. Eng. Data* **20,** 72–81.

Spedding F. H., Shiers L. E., Brown M. A., Derer J. L., Swanson D. L., and Habenschuss A. (1975b) Densities and apparent molal volumes of some rare earth solutions at 25°C. II. Rare earth chlorides. *J. Chem. Eng. Data* **20,** 81–88.

Spedding F. H., Baker J. L., and Walters J. P. (1975c) Apparent and partial molal heat capacities of aqueous rare earth perchlorate solutions at 25°C. *J. Chem. Eng. Data* **20,** 189–195.

Spedding F. H., Walters J. P., and Baker J. L. (1975d) Apparent and partial molal heat capacities of some aqueous rare earth chlorate solutions at 25°C. *J. Chem. Eng. Data* **20,** 438–443.

Spedding F. H., Baker J. L., and Walters J. P. (1979) Apparent and partial molal heat capacities of aqueous rare earth nitrate solutions at 25°C. *J. Chem. Eng. Data* **24,** 293–305.

Spitzer J. J., Singh P. P., McCurdy K. G., and Hepler L. G. (1978a) Apparent molar heat capacities and volumes of aqueous electrolytes: $CaCl_2$, $Cd(NO_3)_2$, $CoCl_2$, $Mg(ClO_4)_2$, $Cu(ClO_4)_2$, and $NiCl_2$. *J. Soln. Chem.* **7,** 81–86.

Spitzer J. J., Singh P. P., Olofsson I. V., and Hepler L. G. (1978b) Apparent molar heat capacities and volumes of aqueous electrolytes at 25°C: $Cd(ClO_4)_2$, $Ca(ClO_4)_2$, $Co(ClO_4)_2$, $Mn(ClO_4)_2$, $Ni(ClO_4)_2$, and $Zn(ClO_4)_2$. *J. Soln. Chem.* **7,** 623–629.

Spitzer J. J., Olofsson I. V., Singh P. P., and Hepler L. G. (1979b) Apparent molar heat capacities and volumes of aqueous electrolytes at 25°C: $NaIO_3$, $KMnO_4$, and $MnCl_2$. *Thermochem. Acta* **28,** 155–160.

Spitzer J. J., Olofsson I. V., Singh P. P., and Hepler L. G. (1979c) Apparent molar heat capacities and volumes of aqueous electrolytes at 25°C: $Cr(NO_3)_3$, $LaCl_3$, $K_3Fe(CN)_6$, and $K_4Fe(CN)_6$. *Canadian J. Chem.* **57,** 2798–2803.

Sverjensky D. A. (1992) Linear free energy relations for predicting dissolution rates of solids. *Nature* **358,** 310–313.

Sverjensky D. A. and Molling P. A. (1992) A linear free energy relationship for crystalline solids and aqueous ions. *Nature* **356,** 231–234.

Sverjensky D. A., Shock E. L., and Helgeson H. C. (1997) Prediction of the thermodynamic properties of aqueous metal complexes to 1000°C and 5 kb. *Geochim. Cosmochim. Acta* (in press).

Swaddle T. W. and Mak M. K. S. (1983) The partial molar volumes of aqueous metal cations: their prediction and relation to volumes of activation for water exchange. *Canadian J. Chem.* **61,** 473–480.

Sweeton F. H. and Baes C. F., Jr. (1970) The solubility of magnetite and hydrolysis of ferrous ion in aqueous solutions at elevated temperatures. *J. Chem. Thermodynamics* **2,** 479–500.

Tanger J. C., IV and Helgeson H. C. (1988) Calculation of the thermodynamic and transport properties of aqueous species at high pressures and temperatures. Revised equations of state for the standard partial molal properties of ions and electrolytes. *Amer. J. Sci.* **288,** 19–98.

Tong J. Y.-P. and King E. L. (1953) A spectrophotometric investigation of the equilibria existing in acidic solutions of chromium (VI). *J. Amer. Chem. Soc.* **75,** 6180–6186.

Tremaine P. R. and LeBlanc J. C. (1980a) The solubility of nickel oxide and hydrolysis of Ni^{2+} in water to 573K. *J. Chem. Thermodynamics* **12,** 521–538.

Tremaine P. R. and LeBlanc J. C. (1980b) The solubility of magnetite and the hydrolysis and oxidation of Fe^{2+} in water to 300°C. *J. Soln. Chem.* **9,** 415–442.

Tugarinov I. A., Ganeyev I. A., and Khodakovskiy I. L. (1975) Experimental determination of hydrolysis constants of lead ions in aqueous solutions at temperatures up to 300°C. *Geochemistry Intl.* **12,** 47–55.

van Gaans P. F. M., Oonk H. A. J., and Somsen G. (1990) Thermodynamics of aqueous gallium chloride. Apparent molar volumes and heat capacities at 25°C. *J. Soln. Chem.* **19,** 831–854.

Volokhov Y. A., Pavlov L. N., Eremin N. I., and Mironov V. E. (1971) Hydrolysis of aluminum salts. *J. Appl. Chem. USSR* **44,** 243–246.

Wagman D. D., Evans W. H., Parker V. B., Schumm R. H., Halow I., Bailey S. M., Churney K. L., and Nuttall R. L. (1982) *The NBS Tables of Chemical Thermodynamic Properties—Selected Values for Inorganic and C_1 and C_2 Organic Substances in SI Units. J. Phys. Chem. Ref. Data 11, Supplement No. 2.*

Walther J. V. (1986) Experimental determination of portlandite and brucite solubilities in supercritical H_2O. *Geochim. Cosmochim. Acta* **50,** 733–739.

Wasserman E., Wood B., and Brodholt J. (1995) The static dielectric constant of water at pressures up to 20 kbar and temperatures to 1273 K: experiment, simulations, and empirical equations. *Geochim. Cosmochim. Acta* **59,** 1–6.

Wesolowski D. J. (1992) Aluminum speciation and equilibria in aqueous solution: I. The solubility of gibbsite in the system Na-K-Cl-OH-$Al(OH)_4$ from 0–100°C. *Geochim. Cosmochim. Acta* **56,** 1065–1092.

Wesolowski D. J. and Palmer D. A. (1994) Aluminum speciation and equilibria in aqueous solution: V. Gibbsite solubility at 50°C and pH 3–9 in 0.1 molal NaCl solutions (a general model for aluminum speciation; analytical methods). *Geochim. Cosmochim. Acta* **58,** 2947–2969.

Wesolowski D. J., Drummond S. E., Mesmer R. E., and Ohmoto H. (1984) Hydrolysis equilibria of tungsten (VI) in aqueous sodium chloride solutions to 300°C. *Inorg. Chem.* **23,** 1120–1132.

Willis M. A. and Shock E. L. (1997) Titanium speciation in hydrothermal fluids: Calculation of standard state properties of aqueous ions and complexes, and mineral solubilities at high temperatures and pressures. (in prep.)

Yatsimirskii K. B. and Prik K. E. (1964) Kinetics of the catalytic oxidation of iodide ion by hydrogen peroxide in the presence of tungsten(VI). *Russ. J. Inorg. Chem.* **9,** 995–999.

Ziemniak S. E., Jones M. E., and Combs K. E. S. (1992) Zinc(II) oxide solubility and phase behavior in aqueous sodium phosphate solutions at elevated temperatures. *J. Soln. Chem.* **21,** 1153–1176.

APPENDIX

Standard State Conventions

The standard state employed in this study for gases is unit fugacity of the hypothetical ideal gas at any temperature and 1 bar. The standard state for H_2O calls for unit activity of the pure solvent at any pressure and temperature, and that for minerals corresponds to unit activity for the pure solid at any pressure and temperature. Any standard partial molal property of the kth aqueous electrolyte ($\bar{\Xi}^\circ_k$) is related to the corresponding absolute standard partial molal properties of its constituent ions by

$$\bar{\Xi}^\circ_k = \sum_j \upsilon_{j,k}\, \bar{\Xi}^{\circ_{abs}}_j \qquad \text{(A1)}$$

where the subscripts k and j refer to the electrolyte and ion, respectively, and $\upsilon_{j,k}$ stands for the number of moles of the jth ion in one mole of the kth electrolyte. The conventional standard partial molal properties of the jth ion are defined by

$$\bar{\Xi}^\circ_j \equiv \bar{\Xi}^{\circ_{abs}}_j - Z_j \bar{\Xi}^{\circ_{H^+ abs}} \qquad \text{(A2)}$$

where $\bar{\Xi}^{\circ_{H^+ abs}}$ refers to the absolute standard partial molal property of the hydrogen ion, and Z_j stands for the charge of the jth ion. As a consequence, all conventional standard partial molal properties of H^+ are equal to 0.0 at all pressures and temperatures. It follows from Eqns. A1 and A2 and the requirement for electrical neutrality of an aqueous electrolyte that

$$\bar{\Xi}^\circ_k = \sum_j \upsilon_{j,k} \bar{\Xi}^\circ_j \qquad \text{(A3)}$$

Summary of the Revised-HKF Equation of State

The standard partial molal properties of aqueous species are expressed in the revised-HKF equation of state in terms of structural and solvation contributions. A general statement of this summation can be expressed

$$\bar{\Xi}^\circ_j = \Delta\bar{\Xi}^\circ_n + \Delta\bar{\Xi}^\circ_s \qquad \text{(A4)}$$

where the subscripts n and s refer to the nonsolvation (or structural) and solvation contributions, respectively. The revised-HKF equations for the standard partial molal volume, $\bar{V}^\circ$, and heat capacity, $\bar{C}^\circ_P$, are given by (Tanger and Helgeson, 1988)

$$\bar{V}^\circ = \Delta\bar{V}^\circ_n + \Delta\bar{V}^\circ_s = \sigma + \frac{\xi}{T-\theta} - \omega Q + \left(\frac{1}{\epsilon} - 1\right)\left(\frac{\partial\omega}{\partial P}\right)_T = a_1 + \frac{a_2}{\Psi + P} + \left(a_3 + \frac{a_4}{\Psi + P}\right)\left(\frac{1}{T-\theta}\right) - \omega Q + \left(\frac{1}{\epsilon} - 1\right)\left(\frac{\partial\omega}{\partial P}\right)_T \quad \text{(A5)}$$

$$\bar{C}^\circ_P = \Delta\bar{C}^\circ_{P,n} + \Delta\bar{C}^\circ_{P,s} = c_1 + \frac{c_2}{(T-\theta)^2} - \left(\frac{2T}{(T-\theta)^3}\right)\left(a_3(P - Pr) + a_4 \ln\left(\frac{\Psi + P}{\Psi + Pr}\right)\right) + \omega TX + 2TY\left(\frac{\partial\omega}{\partial T}\right)_P - T\left(\frac{1}{\epsilon} - 1\right)\left(\frac{\partial^2\omega}{\partial T^2}\right)_P \quad \text{(A6)}$$

where ξ, σ, a_1, a_2, a_3, a_4, c_1, c_2, and ω represent species-dependent equation-of-state parameters, Ψ and θ designate solvent-dependent parameters equal to 2600 bars and 228 K for H_2O, T and P stand for temperature and pressure, Pr signifies the reference pressure of 1 bar, and Q, Y, and X indicate the Born functions defined by

$$Q \equiv \frac{1}{\epsilon}\left(\frac{\partial \ln \epsilon}{\partial P}\right)_T \quad \text{(A7)}$$

$$Y \equiv \frac{1}{\epsilon}\left(\frac{\partial \ln \epsilon}{\partial T}\right)_P \quad \text{(A8)}$$

$$X \equiv \left(\frac{\partial Y}{\partial T}\right)_P = \frac{1}{\epsilon}\left[\left(\frac{\partial^2 \ln \epsilon}{\partial T^2}\right)_P - \left(\frac{\partial \ln \epsilon}{\partial T}\right)^2_P\right] \quad \text{(A9)}$$

where ϵ stands for the dielectric constant of H_2O. The following identities are consistent with Eqns. A5 and A6

$$\Delta\bar{V}^\circ_s = -\omega Q + \left(\frac{1}{\epsilon} - 1\right)\left(\frac{\partial\omega}{\partial T}\right)_T \quad \text{(A10)}$$

$$\Delta\bar{V}^\circ_n = \sigma + \frac{\xi}{T-\theta} \quad \text{(A11)}$$

$$\sigma = a_1 + \frac{a_2}{\Psi + P} \quad \text{(A12)}$$

$$\xi = a_3 + \frac{a_4}{\Psi + P} \quad \text{(A13)}$$

$$\Delta\bar{C}^\circ_{P,s} = \omega TX + 2TY\left(\frac{\partial\omega}{\partial T}\right)_P - T\left(\frac{1}{\epsilon} - 1\right)\left(\frac{\partial^2\omega}{\partial T^2}\right)_P \quad \text{(A14)}$$

$$\Delta\bar{C}^\circ_{P,n} = c_1 + \frac{c_2}{(T-\theta)^2} - \left(\frac{2T}{(T-\theta)^3}\right)\left(a_3(P - Pr) + a_4 \ln\left(\frac{\Psi + P}{\Psi + Pr}\right)\right) \quad \text{(A15)}$$

which reduces for $P = Pr$ to

$$\Delta\bar{C}^\circ_{P,n} = c_1 + \frac{c_2}{(T-\theta)^2} \quad \text{(A16)}$$

Eqn. A16 can be used at P_{SAT} and temperatures of ~200°C without introducing substantial error (Shock and Helgeson, 1988, 1990; Shock et al., 1989; Shock, 1995). Integration of Eqn. A6 with respect to temperature yields

$$\bar{S}^\circ = \bar{S}^\circ_{Pr,Tr} + c_1 \ln(T/Tr) - \frac{c_2}{\theta}\left[\left(\frac{1}{T-\theta}\right) - \left(\frac{1}{Tr-\theta}\right) + \frac{1}{\theta}\ln\left(\frac{Tr(T-\theta)}{T(Tr-\theta)}\right)\right] + \left(\frac{1}{T-\theta}\right)^2\left(a_3(P - Pr) + a_4 \ln\left(\frac{\Psi + P}{\Psi + Pr}\right)\right) + \omega Y - \left(\frac{1}{\epsilon} - 1\right)\left(\frac{\partial\omega}{\partial T}\right)_P - \omega_{Pr,Tr}Y_{Pr,Tr} \quad \text{(A17)}$$

where T_r indicates the reference temperature of 298.15 K.

The apparent standard partial molal Gibbs free energy and enthalpy of formation are given by (Benson, 1976; Helgeson et al., 1981; Tanger and Helgeson, 1988)

$$\Delta\bar{G}^\circ_{P,T} \equiv \Delta\bar{G}^\circ_f + (\bar{G}^\circ_{P,T} - \bar{G}^\circ_{Pr,Tr}) \quad \text{(A18)}$$

$$\Delta\bar{H}^\circ_{P,T} \equiv \Delta\bar{H}^\circ_f + (\bar{H}^\circ_{P,T} - \bar{H}^\circ_{Pr,Tr}) \quad \text{(A19)}$$

where $\Delta\bar{G}^\circ_f$ and $\Delta\bar{H}^\circ_f$ stand for the conventional standard partial molal Gibbs free energy and enthalpy of formation of the species from the elements at the reference conditions of 1 bar and 298.15 K, respectively, and the parenthetical terms represent the difference between the standard partial molal Gibbs free energy and enthalpy of formation at the reference conditions and those at the temperature and pressure of interest. It follows from Eqns. A5, A6, A18, and A19 together with

$$\bar{H}^\circ_{P,T} - \bar{H}^\circ_{Pr,Tr} = \int_{Tr}^{T}\bar{C}^\circ_{Pr}dT + \int_{Pr}^{P}\left(\bar{V}^\circ - T\left(\frac{\partial\bar{V}^\circ}{\partial T}\right)_P\right)_T dP \quad \text{(A20)}$$

$$\bar{G}^\circ_{P,T} - \bar{G}^\circ_{Pr,Tr} = -\bar{S}^\circ_{Pr,Tr}(T - Tr) + \int_{Tr}^{T}\bar{C}^\circ_{Pr}dT - T\int_{Tr}^{T}\bar{C}^\circ_{Pr}d\ln T + \int_{Pr}^{P}\bar{V}^\circ_T dP \quad \text{(A21)}$$

and the partial isobaric temperature derivative of Eqn. A5, that we can write

$$\Delta\bar{H}^\circ_{P,T} = \Delta\bar{H}^\circ_f + c_1(T - Tr) - c_2\left[\left(\frac{1}{T-\theta}\right) - \left(\frac{1}{Tr-\theta}\right)\right] + a_1(P - Pr) + a_2\ln\left(\frac{\Psi + P}{\Psi + Pr}\right) + \left(\frac{2T-\theta}{(T-\theta)^2}\right)\left(a_3(P - Pr) + a_4\ln\left(\frac{\Psi + P}{\Psi + Pr}\right)\right) + \omega\left(\frac{1}{\epsilon} - 1\right) + \omega TY - T\left(\frac{1}{\epsilon} - 1\right)\left(\frac{\partial\omega}{\partial T}\right)_P - \omega_{Pr,Tr}\left(\frac{1}{\epsilon_{Pr,Tr}} - 1\right) - \omega_{Pr,Tr}TrY_{Pr,Tr} \quad \text{(A22)}$$

and

$$\Delta\bar{G}^\circ_{P,T} = \Delta\bar{G}^\circ_f - \bar{S}^\circ_{Pr,Tr}(T - Tr) - c_1\left(T\ln\left(\frac{T}{Tr}\right) - T + Tr\right) - c_2\left(\left[\left(\frac{1}{T-\theta}\right) - \left(\frac{1}{Tr-\theta}\right)\right]\left(\frac{\theta - T}{\theta}\right) - \frac{T}{\theta^2}\ln\left(\frac{Tr(T-\theta)}{T(Tr-\theta)}\right)\right) + a_1(P - Pr) + a_2\ln\left(\frac{\Psi + P}{\Psi + Pr}\right) + \left(\frac{1}{T-\theta}\right)\left[a_3(P - Pr) + a_4\ln\left(\frac{\Psi + P}{\Psi + Pr}\right)\right] + \omega\left(\frac{1}{\epsilon} - 1\right) - \omega_{Pr,Tr}\left(\frac{1}{\epsilon_{Pr,Tr}} - 1\right) - \omega_{Pr,Tr}Y_{Pr,Tr}(T - Tr) \quad \text{(A23)}$$

The conventional Born coefficient (ω) which appears in Eqns. A5, A6, A10, A14, A17, A22, and A23 is defined for the jth ionic species by

$$\omega \equiv \omega^{abs}_j - Z_j\omega^{abs}_{H^+} \quad \text{(A24)}$$

where ω_H^{abs} denotes the absolute Born coefficient of the hydrogen ion, which is taken to be 0.5387×10^5 cal mol^{-1} at 25°C and 1 bar (Helgeson and Kirkham, 1976), and

$$\omega_j^{abs} = \frac{\eta Z_j^2}{r_{e,j}} \tag{A25}$$

where $\eta = 1.66027 \times 10^5$ (Å, cal, mol^{-1}), and $r_{e,j}$ designates the effective electrostatic radius of the jth aqueous ion given by (Tanger and Helgeson, 1988; Shock et al., 1992; Sassani and Shock, 1992, 1994)

$$r_{e,j} = r_{x,j} + |z_j|(k_z + \mathbf{g}) \tag{A26}$$

where $r_{x,j}$ stands for the crystallographic radius of the ion, k_z represents a constant equal to 0.0 for anions and 0.94 for cations, and **g** denotes a temperature and pressure dependent solvent function. Values of the **g** function have been regressed from standard partial molal volume and heat capacity data for the electrolyte NaCl (Tanger and Helgeson, 1988) and from supercritical equilibrium constants (Shock et al., 1992) for the reaction

$$NaCl^\circ = Na^+ + Cl^- \tag{A27}$$

where NaCl° represents the neutral, associated complex species. Available expressions for the **g** function allow calculation of conventional Born coefficients and their partial derivatives to 1000°C and 5 kb (Shock et al., 1992).

In the case of neutral aqueous species, the solvation terms in the revised-HKF equations of state can be expressed in terms of the effective Born coefficient (ω_e). Regression of experimental data is consistent with the assumption that the effective Born coefficients of neutral aqueous species are independent of temperature and pressure (Shock et al., 1989, 1992; Shock and Helgeson, 1990; Sverjensky et al., 1997; Shock, 1995). It follows that the revised-HKF expressions for the solvation contributions to the standard partial molal volumes and heat capacities are given by

$$\Delta\bar{V}^\circ_s = -\omega_e Q \tag{A28}$$

$$\Delta\bar{C}^\circ_{P,s} = \omega_e TX \tag{A29}$$

As a consequence, the revised HKF expressions for the standard partial molal properties of neutral aqueous species can be expressed as (Shock et al., 1989)

$$\bar{V}^\circ = a_1 + \frac{a_2}{\Psi + P} + \left(a_3 + \frac{a_4}{\Psi + P}\right)\left(\frac{1}{T - \theta}\right) - \omega_e Q \tag{A30}$$

$$\bar{C}^\circ_P = c_1 + \frac{c_2}{(T - \theta)^2} - \left(\frac{2T}{(T - \theta)^3}\right) \times \left(a_3(P - Pr) + a_4 \ln\left(\frac{\Psi + P}{\Psi + Pr}\right)\right) + \omega_e TX \tag{A31}$$

$$\bar{S}^\circ = \bar{S}^\circ_{Pr,Tr} + c_1 \ln(T/Tr) - \frac{c_2}{\theta}\left[\left(\frac{1}{T - \theta}\right) - \left(\frac{1}{Tr - \theta}\right) + \frac{1}{\theta}\ln\left(\frac{Tr(T - \theta)}{T(Tr - \theta)}\right)\right] + \left(\frac{1}{T - \theta}\right)^2 \times \left(a_3(P - Pr) + a_4 \ln\left(\frac{\Psi + P}{\Psi + Pr}\right)\right) + \omega_e(Y - Y_{Pr,Tr}) \tag{A32}$$

$$\Delta\bar{H}^\circ_{P,T} = \Delta\bar{H}^\circ_f + c_1(T - Tr) - c_2\left[\left(\frac{1}{T - \theta}\right) - \left(\frac{1}{Tr - \theta}\right)\right] + a_1(P - Pr) + a_2 \ln\left(\frac{\Psi + P}{\Psi + Pr}\right) + \left(\frac{2T - \theta}{(T - \theta)^2}\right) \times \left(a_3(P - Pr) + a_4 \ln\left(\frac{\Psi + P}{\Psi + Pr}\right)\right) + \omega_e\left(TY - TrY_{Pr,Tr} + \left(\frac{1}{\epsilon} - 1\right) - \left(\frac{1}{\epsilon_{Pr,Tr}} - 1\right)\right) \tag{A33}$$

$$\Delta\bar{G}^\circ_{P,T} = \Delta\bar{G}^\circ_f - \bar{S}^\circ_{Pr,Tr}(T - Tr) - c_1\left(T \ln\left(\frac{T}{Tr}\right) - T + Tr\right) - c_2\left(\left[\left(\frac{1}{T - \theta}\right) - \left(\frac{1}{Tr - \theta}\right)\right]\left(\frac{\theta - T}{\theta}\right) - \frac{T}{\theta^2}\ln\left(\frac{Tr(T - \theta)}{T(Tr - \theta)}\right)\right) + a_1(P - Pr) + a_2 \ln\left(\frac{\Psi + P}{\Psi + Pr}\right) + \left(\frac{1}{T - \theta}\right)\left[a_3(P - Pr) + a_4 \ln\left(\frac{\Psi + P}{\Psi + Pr}\right)\right] + \omega_e\left(Y_{Pr,Tr}(T - Tr) + \left(\frac{1}{\epsilon} - 1\right) - \left(\frac{1}{\epsilon_{Pr,Tr}} - 1\right)\right) \tag{A34}$$